Delineating the Role of Organic Cation Transporters in Ocular Toxicity of Systemic Drugs

THESIS

Submitted in partial fulfilment
of the requirements for the degree of
DOCTOR OF PHILOSOPHY

By

Manisha Malani
ID No.: 2019PHXF0065H

Under the Supervision of
Prof. Nirmal J

BIRLA INSTITUTE OF TECHNOLOGY AND SCIENCE, PILANI
2024

BIRLA INSTITUTE OF TECHNOLOGY AND SCIENCE, PILANI

CERTIFICATE

This is to certify that the thesis titled **"Delineating the Role of Organic Cation Transporters in Ocular Toxicity of Systemic Drugs",** submitted by **Ms. Manisha Malani** ID No **2019PHXF0065H** for award of Ph.D. of the Institute embodies original work done by her under my supervision.

Signature of the Supervisor:

Name in capital letters: Prof. NIRMAL J

Designation: Associate Professor

Date: 22nd March 2024

BIRLA INSTITUTE OF TECHNOLOGY AND SCIENCE, PILANI

DECLARATION

I, **Manisha Malani** bearing ID No. **2019PHXF0065H**, hereby declare that the thesis titled, "**Delineating the Role of Organic Cation Transporters in Ocular Toxicity of Systemic Drugs**" is original research work and have been composed solely by myself under the supervision of Prof. Nirmal J. The similarity report of the submitted thesis was found to be 5%, using anti-plagiarism software (DrillBit). Any relevant material taken from the open literature has been referred and cited as per established ethical norms and practices.

The matter embodied in this Thesis has not been submitted by me for the award of any other degree of any other University/Institute. If anything found guilty or copied from the other sources, I am the sole responsible for the same and I abide for any action taken by Birla Institute of Technology and Science Pilani University authorities.

Signature of the candidate:

Name in capital letters: MANISHA MALANI

Place: Hyderabad

Date: 22nd March 2024

Acknowledgments

For the successful completion of my thesis, the words may not be sufficient for the immense sacrifices and help received from the universe in one way or another. Though it may not be possible to mention everyone here, I would like to appreciate all the help received directly or indirectly from every individual.

I could not have undertaken this journey without the guidance of my mentor, Prof. Nirmal J. I will always be in debt to him for teaching me the true meaning of science. "Science is not about the positive or negative results, but it is to find the reasons behind the results." He supported me as a guide and always stood by me as a family. His intellectual and spiritual thoughts never let me feel frustrated with unexpected outcomes. It has been an incredible journey with him. He helped groom me academically and also helped me improve my personality. He is a great scientist and a very down-to-earth individual. His approach to solving problems has improved my critical thinking. His enthusiasm for science is infectious. His guidance has made me punctual and organized, which has allowed me to perform my research in a structured manner. His constant efforts to instill science in us through various means, be it informal discussion or videos, has always been motivational. His approach to solving common yet complex problems is appreciable. Words are not enough to thank him for all the learnings he gave us. I cherish and feel lucky to complete the doctoral degree under his guidance.

Dedicated

"Dig deeper the sand-well, more water flows
Read deeper, more wisdom grows"

Kural 399 by Thiruvalluvar (200 BC)

To

My guru, family & friends

Abstract

Several systemic drugs, including intravenous injection and oral formulations used for acute and chronic treatments, accumulate at the off-target sites and are known to cause ocular toxicities leading to vision loss. However, the entry mechanism of systemic drugs into the eye despite the ocular barriers is unclear. Membrane transporters in the ocular barriers facilitate the selective entry of endogenous molecules across the tight junctions, hence we hypothesize the transporters may falsely recognize the drugs as substrates and facilitate their translocation. The functional role of transporters has been reported in the blood-aqueous and blood-retinal barrier, but it is under-explored in the blood tear barrier.

Unfortunately, more than 40% of the marketed drugs are cations at physiological pH, which cannot cross the biological membranes. We hypothesize that the systemic drug that are substrates for organic cation transporters 1 (OCT1) (highly expressed isoform in the eye) enters the anterior eye segment through the lacrimal gland by tear secretion. The understanding of transporters in the lacrimal gland could lead to the development of non-therapeutic interventions, such as excipients to inhibit OCT1 transporters in the lacrimal gland, while not blocking the therapeutic effect of systemic drugs.

Artificial intelligence models based on supervised learning algorithms and computational studies such as molecular dynamics and metadynamics simulations were performed to understand the interaction between systemic drugs and OCT1 transporter. Further, to confirm these predictions, in vivo topical tear kinetics were performed in New Zealand white rabbits for the predicted substrates in the presence and absence of OCT1 blockers (Atropine

and Quinidine). To understand the functional role of OCT1 in the lacrimal gland, expression studies were performed using reverse-transcriptase polymerase chain reaction, western blotting, and immunohistochemistry. The selected predicted OCT1 substrate was administered intravenously in presence and absence of topical OCT1 blockers to delineate the functional role of OCT1 in the lacrimal gland. Further, to understand the potential of excipients to block the OCT1 transporter, in vitro uptake studies were performed in transiently hOCT1 transfected Human Embryonic Kidney (HEK) 293 cells. The selected excipient was used for in vivo studies that could block intravenously administered OCT1 substrate entry into the tear.

The developed AI model showed an accuracy of about 85% and predicted n=125 novel drug-OCT1 interactions, which were not reported earlier. Molecular dynamics simulations evaluated the binding stability and molecular interactions of drug-OCT1, whereas metadynamics simulation visualized the transport of substrates across the OCT1. The predictions demonstrate that the sulfur-containing drugs could be an additional factor facilitating the transport of OCT1 substrates. Further, Piroxicam, Pregabalin, Glipizide, Busulfan, and Cyclophosphamide were selected from OCT1-predicted substrates based on their clinical relevance and physicochemical properties for in vivo validation. Earlier studies have reported the functioning of the OCT1 pump from tear to aqueous humor, which infers that when OCT1 is blocked, the substrate concentration is increased in the tear. The in vivo topical tear kinetics showed that the tear concentration was higher in the blocker-treated group (at least 2-fold higher) than in the control group, indicating the predicted molecules are OCT1 substrates.

Further, the gene and protein expression of OCT1 was confirmed in the rabbit lacrimal gland, and the transporter was localized in the terminal acinar cells as indicated by immunohistochemistry. Cyclophosphamide was chosen among the predicted OCT1 substrates to evaluate the functional role of OCT1 in the lacrimal gland. The $AUC_{(0-2h)}$ of Cyclophosphamide was found to be 1.7-fold less in the atropine pre-treated group and 2.4-fold less in the quinidine pre-treated group when compared to the control group. The tear kinetics of intravenously administered OCT1 substrate reveals that the OCT1 in the lacrimal gland is positioned from the basal to the apical side, i.e., from blood to the tear side. The in vitro uptake studies revealed that Tween 20 and Poloxamer 407 could block the OCT1 transporter with IC_{50} values 2.26 ± 0.82 μM and 1.41 ± 0.0.23 mM, respectively. Further, in vivo studies indicated a higher tear concentration of substrate (Cyclophosphamide) in the control group compared to the excipient-treated group (Tween 20 and Poloxamer 407).

The presence and active role of OCT1 in the lacrimal gland confirms our hypothesis that transporters allow systemic drugs causing ocular toxicity to enter the anterior segment of the eye and excipients can be used locally to block the uptake transporters, preventing systemic drug entry into the eye thereby reducing ocular toxicity. However, the effect of blocking the transporters for the transport of endogenous molecules needs to be further elucidated.

Table of Contents

Contents	Page Number

List of Tables

List of Figures

List of Abbreviations and Symbols

MPP	1-methyl-4-phenylpyridinium
POPC	1-palmitoyl-2-oleoyl-sn-glycero-3-phosphocholine
MTT	3-(4,5-dimethylthiazol-2-yl)-2,5-diphenyl-2H-tetrazolium bromide
DAPI	4',6-diamidino-2-phenylindole
SN-38	7-ethyl-10-hydroxy-camptothecin
API	Active pharmaceutical ingredient
ATP	Adenosine triphosphate
ANN	Advanced neural network
ALA	Alanine
α	Alpha
Å	Angstrom
AUC	Area under the curve
ARG	Arginine
AI	Artificial intelligence
ASN	Asparagine
ASP	Aspartic acid
ABC	ATP binding cassette
β	Beta
BAB	Blood-aqueous barrier
BTB	Blood-tear barrier
BRB	Blood-retinal barrier
BSA	Bovine serum albumin
BCRP	Breast cancer resistance protein
CMC	Carboxymethyl cellulose
CVS	Cardiovascular system
CNS	Central nervous system
cDNA	Complementary DNA
CS	Computer simulations
NPγT	Constant number of molecules, pressure, surface tension, and temperature
CTR1	Copper transporter 1
R^2	Correlation coefficient
CYS	Cysteine
°C	Degree Celsius
DHEAS	Dehydroepiandrosterone
DNA	Deoxyribonucleic acid
DMSO	Dimethyl sulfoxide
TPGS	D-α-tocopheryl polyethylene glycol 1000 succinate
ESI	Electrospray ionization
E. coli	*Escherichia coli*

EDTA	Ethylene diamine tetra acetic acid
EMA	European Medicines Agency
e.g	Exempli gratia (for example)
XP	Extra precision docking
XG	Extreme gradient boosting
FAERS	FDA adverse event reporting system
GRAS	Generally regarded as safe
GHS	Globally harmonized system of classification and labelling of chemicals
GLUT-1	Glucose transporter 1
GLU	Glutamic acid
GLN	Glutamine
GSH	Glutathione
GLY	Glycine
g/mol	Gram per mole
g	Gravitational force
HPLC	High performance liquid chromatography
HRP	Horseradish peroxidase
h	Hour
HEK-293	Human embryonic kidney 293
hERG	Human ether-a-go-go-related gene
hOCT1	Human organic cation transporter 1
h-bond	Hydrogen bond
HCQ	Hydroxychloroquine
IDU	Idoxuridine
ISTD	Internal standard
ITC	International Transporter Consortium
IOP	Intraocular pressure
IV	Intravenous
ILE	Isoleucine
K	Kelvin
kcal/mol	Kilocalorie per mole
kD	Kilodalton
kg	Kilogram
KNN	K-nearest neighbor
LEU	Leucine
LCMS-MS	Liquid chromatography-mass spectrometry
L/min	Liter per minute
LSD	Lysergic acid diethylamide
LYS	Lysine
ML	Machine learning
C_{max}	Maximum concentration

V_{max}	Maximum velocity
MRT	Mean residence time
MET	Methionine
K_m	Michaelis constant
µg	Microgram
µg/µl	Microgram per microliter
µg/ml	Microgram per milliliter
µl	Microliter
µm	Micrometer
µM	Micromolar
µM/ml	Micromole per milliliter
µmol/ml*h	Micromole per milliliter hour
mg/kg	Milligram per kilogram
mg/ml	Milligram per milliliter
ml	Milliliter
ml/min	Milliliter per minute
mm	Millimeter
mM	Millimolar
mins	Minutes
MEK	Mitogen-activated protein kinase kinase
M	Molar
MD	Molecular dynamics
MCT6	Monocarboxylate transporter 6
MATE	Multidrug and toxic compound extrusion
MDR	Multidrug resistance transporter
MRP	Multidrug resistance-associated protein
MuDRA	Multiple descriptor read across
ng/ml	Nanogram per milliliter
nm	Nanometer
nmol/ml	Nanomole per milliliter
ns	Nanoseconds
NS	Non-substrate
OCTN	Novel organic cation transporter
OPLS4	Optimized potential for liquid simulations 4
OAT	Organic anion transporter
OATPs	Organic anion transporting polypeptides
OCT	Organic cation transporter
OC	Organic cations
OPM	Orientations of proteins in membranes
PEPT	Peptide transporter
%	Percentage

P-gp	P-glycoprotein
PMSF	Phenyl methyl sulfonyl fluoride
PHE	Phenylalanine
Φ	Phi
PBS	Phosphate buffered saline
ps	Picoseconds
PVA	Polyvinyl alcohol
PVP	Polyvinyl pyrrolidone
PVDF	Polyvinylidene difluoride
PRO	Proline
PDB	Protein data bank
Ψ	Psi
QSAR	Quantitative-structure activity relationship
RIPA	Radioimmunoprecipitation assay
BRAF	Rapidly accelerated fibrosarcoma B-type
RT-PCR	Reverse transcription polymerase chain reaction
RNA	Ribonucleic acid
RMSD	Root mean square deviation
RMSF	Root mean square fluctuation
rpm	Rotations per minute
SER	Serine
SMILES	Simplified molecular input line entry system
SLC	Solute carrier
SEM	Standard error mean
S	Substrate
SVM	Support vector machine
TEA	Tetraethylammonium
OECD	The organization for economic co-operation and development
THR	Threonine
T4	Thyroxine
TPSA	Topological polar surface area
T3	Triiodothyronine
TBST	Tris-buffered saline with 0.1% tween® 20
TRP	Tryptophan
TYR	Tyrosine
UN	United Nations
USFDA	United States Food and Drug Administration
VAL	Valine
VSGB	Variable dielectric surface generalized born

Chapter 1

Introduction

Introduction

1.1 Systemic drugs induced ocular toxicity

The lifespan of patients suffering from chronic diseases has increased worldwide due to advancements in drug discovery and medical technologies (Ebeling et al. 2020). On one hand, medicines improve the patient's therapeutic outcome; on the other, they also cause severe adverse effects. Many systemic drugs (intravenous injection and oral formulations) such as anticancer, antibiotics, cardiovascular drugs, central nervous system drugs, and anti-arrhythmic drugs used to treat chronic illnesses have been reported to accumulate in the eye and cause toxicity such as dry eye syndrome, conjunctivitis, edema, cataracts, optic neuropathy, and retinopathy leading to reversible or irreversible vision loss and blindness (**Figure 1.1**) (Fraunfelder and Fraunfelder 2021).
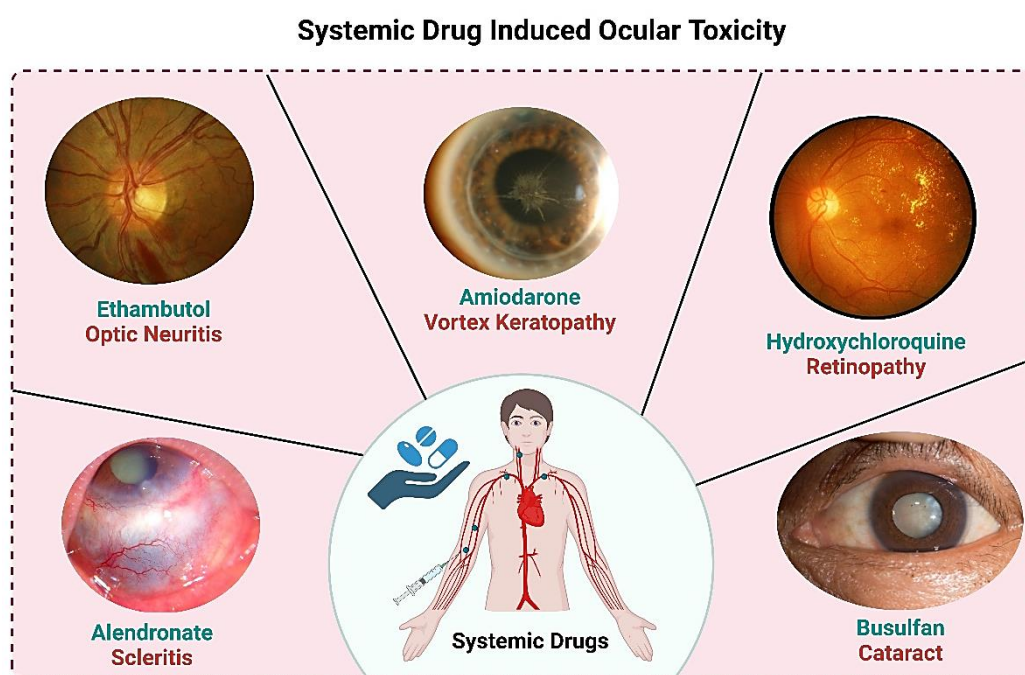
Figure 1.1: Systemic drugs causing ocular toxicity. Drugs consumed for long-term are known to accumulate at non-target site which causes toxicity. Cyclophosphamide (anticancer drug) causes lacrimal duct stenosis, Amiodarone (antiarrhythmic) caused vortex keratopathy, Hydroxychloroquine (antirheumatic) causes retinopathy, Alendronate (bisphosphonates) causes scleritis and Busulfan (anticancer drug) causes cataract (Fraunfelder and Fraunfelder 2021).

Introduction

The current treatment strategies primarily focus on treating life-threatening diseases but not the associated risks. The benefits of using the drugs to treat chronic diseases or the lack of alternate therapies often justify the associated risk of ocular toxicities; thereby, patients usually have no choice and end up continuing their medication, which can potentially impact their quality of life (compromised Vision) (Brock et al. 2013). Unfortunately, ocular toxicity was considered as an underestimated consequence of systemic drugs compared to other life-threatening side effects. However, "Vision is considered the most important among senses that most people fear of losing. It is often considered as the key enabling sense for a person to work and function independently" (Awwad et al. 2017). Unfortunately, ophthalmologists also have a limited role in improving patients' lives under chronic drug treatment; hence, patients are helpless. However, the ocular toxicity associated with systemic drugs has recently been gaining attention. It is highly recommended for cooperative work between physicians, ophthalmologists, and basic researchers in order to identify and prevent the incidence of vision loss due to daily medications at the earlier stages (Bhatti and Salama 2018).

One well-known example of drug-induced ocular toxicity is Hydroxychloroquine (HCQ) induced retinopathy in autoimmune patients. An irreversible retinopathy develops that can progress even after cessation of therapy, with a prevalence of 7.5% in patients on HCQ therapy for more than five years. Therefore, the only choice left is to regularly monitor all patients with HCQ in the clinic (Yusuf et al. 2017). Ethambutol, an anti-mycobacterial drug used to treat tubercular infections, is known to cause dose and duration-dependent optic neuritis (Saxena et al. 2021). Anticancer drugs such as busulfan, tamoxifen, and methotrexate are known to cause subcapsular cataracts (Ali et al. 2022; Noureddin et al. 1999). Amiodarone, an anti-arrhythmic drug, is known to induce vortex keratopathy, causing whorls and linear

opacities in the cornea (Alshehri and Joury 2020). Even with the increasing evidence of systemic drug-induced ocular toxicity, it is unclear how these drugs enter the eye and cause toxicity. Systemically administered drug molecules can selectively bind and accumulate in ocular tissues such as conjunctiva, cornea, lens, choroid, or retina, which causes toxicity (Mason 1977). In addition, the rich vasculature of the eye allows increased blood circulation, making it more susceptible to entry of systemic drugs into the eye (KONERU et al. 1986).

1.2 Eye

The eye is a well-protected organ due to various ocular barriers in the anterior and posterior segments of the eye, such as the tear film, corneal, blood-tear, blood-aqueous, and blood-retinal barrier (**Figure 1.2**). Moreover, tear turnover, blinking latency, and nasolacrimal drainage lead to rapid drug clearance from the eye (Kels et al. 2015). Most of these barriers are formed by tight junctions between epithelial cells. However, for normal eye functioning, nutrients, vitamins, hormones, neurotransmitters, and other endogenous molecules must cross these barriers to supplement the eye with nourishment (Kubo et al. 2014a; Nirmal, Sirohiwal, et al. 2013a; Nirmal et al. 2010; Velpandian, Nirmal, Sirohiwal, et al. 2012).

1.3 Membrane transporters

Membrane transporters are known to facilitate the movement of molecules across the biological membranes, which is also responsible for the entry of endogenous molecules into the eye (Dhananjay et al. 2013; Kato et al. 2008). These transporters can be unidirectional or bidirectional and are responsible for the molecules' influx and efflux. Due to the evolutionary conservation of transporters, slight changes in the structure of substrates are not differentiated, leading to false recognition of the xenobiotics, including drug molecules as

their substrates, and facilitating their transport across the ocular barriers (Shu et al. 2003).

These transporters can lead to toxicity when drug molecules act as a competitor to their

endogenous substrate (Gao et al. 2015; Taylor-Wells and Meredith 2014). The study of

transporters in toxicology has gained much attention, followed by understanding the uptake

of Cisplatin into kidney cells mediated by Organic Cation Transporter (OCT) 2 transporter

(Nigam 2015), specifically in the proximal tubule of the kidney and cochlea hair cells (Cridge

2018). Also, increasing evidence shows that the role of membrane transporters in drug

accumulation at the non-target site leads to toxicity, which was also highlighted in a scientific

session, "Transporters and Toxicity," at the International Transporter Consortium (ITC)

Workshop IV in 2021 (Hafey et al. 2022).
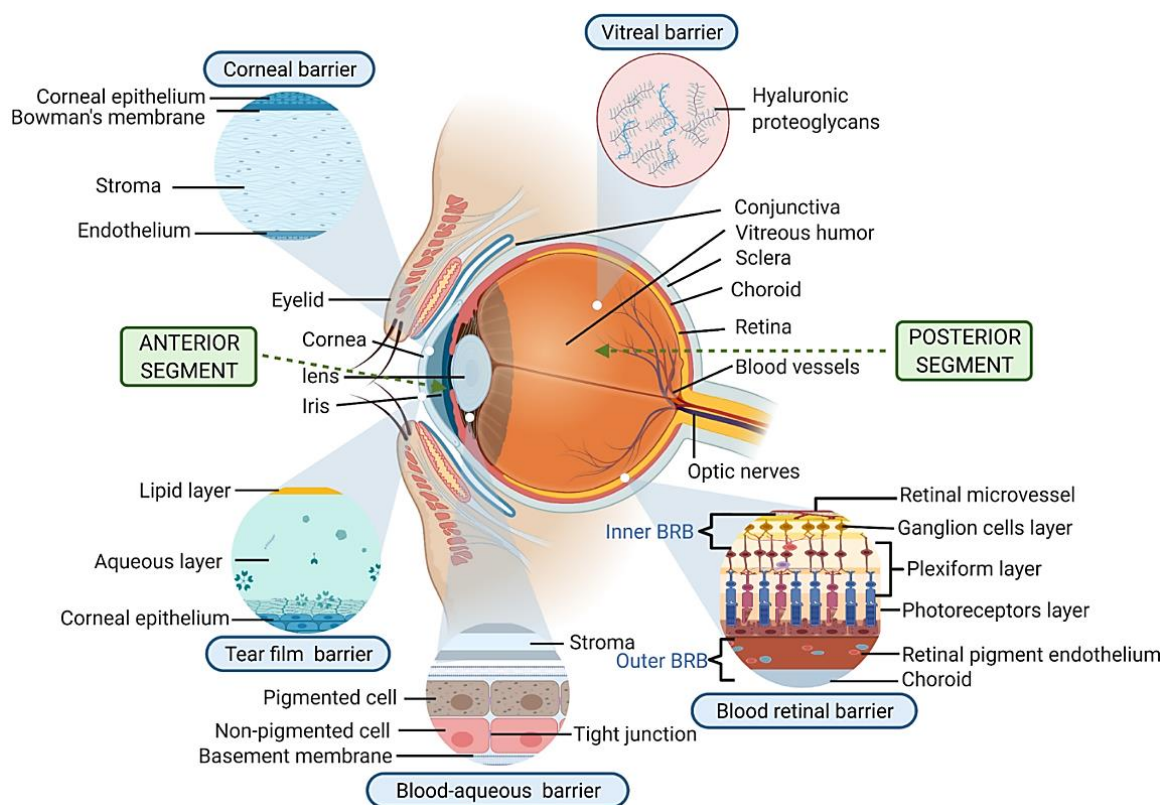
Figure 1.2: Eye anatomy and ocular barriers. Eye is divided into anterior and posterior segment. Anterior segment comprises of conjunctiva, cornea, lens, iris-ciliary body and aqueous humor; whereas posterior segment comprises of vitreous humor, retina, choroid, retinal pigment epithelium and sclera. Eye is surrounded by various ocular barriers such as tear film barrier, corneal barrier, blood-aqueous barrier, vitreal barrier and blood-retinal barrier (Adrianto et al. 2022).

1.4 Organic cation transporters in the eye

Ocular transporters are majorly present in various ocular barriers to mediate the influx of peptides, vitamins, amino acids, and other nutrients into the eye and the efflux of xenobiotics and metabolic waste from the eye. The most widely studied ocular influx transporters include OCT, organic anion transporters (OAT), monocarboxylate transporters, peptide transporters, and organic anion-transporting polypeptide families (Dhananjay et al. 2013). OCT1 is a membrane protein with 12 transmembrane helices comprising 556 amino acids (**Figure 1.3**). OCT1 is electrogenic and polyspecific, responsible for translocating hydrophobic and hydrophilic drugs with high substrate overlapping (Gründemann et al. 1994; Zhang et al. 1997). OCT1 has several intracellular sites for phosphorylation, indicating the regulation is mainly by protein kinases (Ciarimboli 2020).
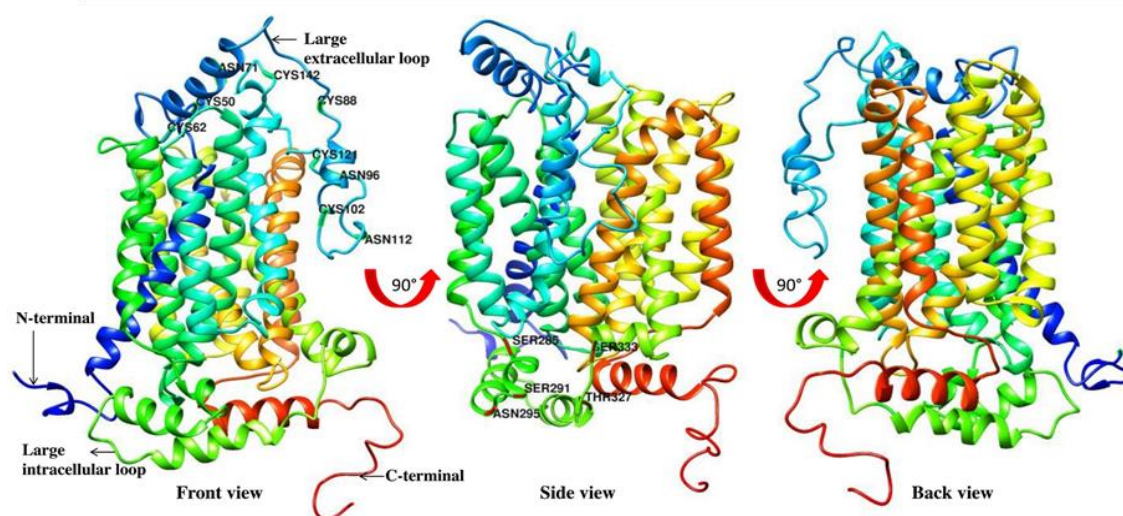
Figure 1.3: Structure of Organic Cation Transporter 1. OCT1 contains 556 amino acids in 12 transmembrane helices with N-terminal and C-terminals located intracellularly. It consists of a large extracellular loop and an intracellular loop. The intracellular loops of OCT1 possess several protein kinase C phosphorylation sites along with protein kinase A, and tyrosine kinase sites (Dakal et al. 2017).

To date, no clear evidence links the ocular transporters and the systemic drug-induced ocular toxicity. Organic Cation Transporters (OCT)/Novel Organic Cation Transporters (OCTN) such as OCT1, OCT2, OCT3, OCTN1, and OCTN2 are reported to be expressed in various ocular

tissues such as cornea (Garrett et al. 2008), conjunctiva (Garrett et al. 2008), iris-ciliary body, and retina (Zhang et al. 2008). OCT/OCTN, belonging to the solute carrier family, are well-studied for facilitating the uptake of cationic drugs. Almost 40% of the clinically used drugs are organic cations (OC), indicating a higher possibility of cationic drug interaction with OCT/OCTN transporters (Neuhoff et al. 2003). Several systemic drugs, which are known substrates of OCT/OCTN, cause ocular toxicities due to their accumulation in the eye upon their chronic usage.

1.5 Lacrimal gland

In the anterior segment of the eye, tear, and aqueous humor enrich and supply the nutritional demand of the eye (Lee and Pelis 2016). The tear is the primary nourishment source for the ocular surface; therefore, endogenous molecules are continuously secreted from blood to the tear. Therefore, the drug entry onto the ocular surface could be majorly attributed to lacrimal secretion. Tear consists of water, electrolytes, lipids, carbohydrates, proteins, enzymes, and other endogenous molecules. The lacrimal gland secretes more than 95% of the tear; the remaining tear is produced by goblet cells and accessory glands (Schirmer 1903; Van Haeringen 1981b). The lacrimal gland plays a multifaceted role in maintaining the homeostasis environment for the ocular surface. It is an exocrine gland sharing similarities with the salivary glands and consists of acinar cells, which are responsible for significant tear secretion, whereas the ductal cells facilitate the movement of tears on the ocular surface by producing a few components in the tear (Schechter et al. 2010b). The tight junctions between the acinar and ductal cells of the lacrimal gland form a blood tear barrier, which prevents the free passage of molecules across the barrier. The ionic composition of the tear resembles the ultra-filtrate of plasma, indicating the transport of endogenous molecules from the blood to

the tear via membrane transporters (Alexander et al. 1972). Therefore, we hypothesize that the membrane transporters present in the lacrimal gland could be one of the potential routes for the entry of systemic drugs into the anterior eye segment.

The functional importance of OCT1 has been demonstrated earlier in the corneal and retinal uptake of its substrates from the blood (Nirmal, Singh, et al. 2013b; Nirmal, Sirohiwal, et al. 2013b). Interestingly, earlier studies had also reported the secretion of tetraethylammonium (TEA) (OCT 1 substrate) in the tear when administered intravenously, and the same was inhibited when OCT inhibitor was administered topically – suggesting lacrimal gland as a portal from blood to tear (Velpandian, Nirmal, Sirohiwal, et al. 2012). Based on these findings, we hypothesize that by tear secretion, OCT drug substrates can reach the precorneal area through OCT1 transporters in the lacrimal gland. Once it reaches the precorneal area, it accumulates in various ocular tissues and causes ocular toxicity.

Chapter 2

Literature Review

2.1 Drug and toxicity

Toxicity is defined as the ability of any substance to cause adverse effects that can alter the normal physiological process due to its exposure. Based on the longevity of adverse effects, toxicity can be broadly categorized as acute toxicity and chronic toxicity. Exposure to substances can also be acute (single dose) or chronic (multiple exposures) (Raies and Bajic 2016). Various factors, such as the nature of the substance, including its structural and physicochemical properties or the route of exposure, dose of exposure, its interaction with endogenous molecules, and other biological properties, determine the toxicity of the substance (Pérez Santín et al. 2021). Drugs are a boon to human health but can also be a curse if not used precisely. Many drugs used today are associated with minor or significant adverse effects.

All the drugs undergo a laborious process for their safety and efficacy during the drug development process under pre-clinical and clinical trials. After thorough screening, several regulatory bodies, including the United States Food and Drug Administration (USFDA) and European Medicines Agency (EMA), approve the drugs for human use; however, specific adverse effects emerge only after long-term use in a heterogeneous population. Therefore, the safety of the drugs for long-term usage is observed as part of Phase 4 clinical trials (Pharmacovigilance). The FDA Adverse Event Reporting System (FAERS) recorded more than 10 million Adverse Event reports, of which more than 5 million were associated with chronic conditions and around 1.1 million were associated with death (**Figure 2.1**) (FDA 2023). Though many of these drugs are known to cause adverse effects during the pharmacovigilance phase, they are not withdrawn from the market due to their high benefit vs risk ratio (Curtin and Schulz 2011).

Reports received by Report Seriousness
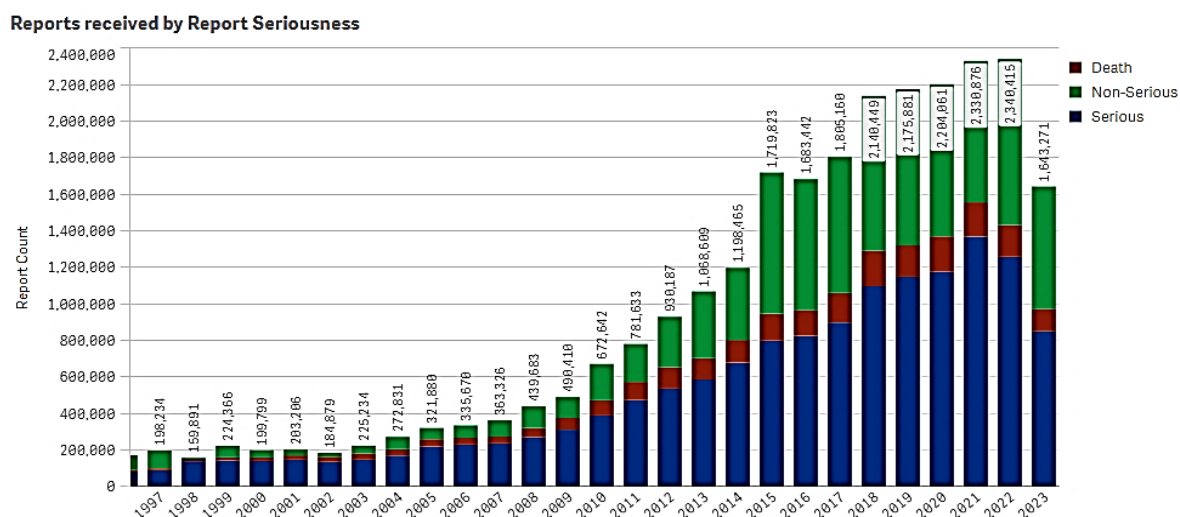
Figure 2.1: Adverse event reported by the FDA Adverse Event Reporting system (FAERS) from 1997-2023. The reported events are classified based on the seriousness of the report. "Serious" indicates that the outcome was documented in the report as hospitalization, life-threatening, disability, congenital anomaly, required intervention and/or other outcomes. "Death" indicates that the outcome was documented as death. The outcomes not documented as death and serious were labelled as "Non-serious". Data obtained from USFDA website (FDA 2023).

2.2 Regulatory Guidelines

To overcome the unseen toxicities associated with the molecules, several regulatory agencies have developed guidelines for a detailed toxicological study in the initial phase of drug development. The Organization for Economic Co-operation and Development (OECD) is where governments can collaborate to share knowledge, experience, and solutions to common obstacles. It regulates global standards of agriculture, tax, and the safety of chemicals. OECD also focuses on issues that directly affect human life. It relates different socioeconomic policies of various countries to improve the quality of life ("Organisation for Economic Co-operation and Development, About OECD iLibrary" ; OECD. 1994). Guidelines given by the OECD for the testing of chemicals are an exclusive tool for evaluating the plausible effects of chemicals on the environment and human health. It is recognized globally as a standard method for safety testing of chemicals. These guidelines are used by experts in academia, industry, regulatory agencies, animal and environmental welfare organizations,

and governmental agencies involved in testing and evaluating chemicals ("Organisation for Economic Co-operation and Development, About OECD iLibrary" ; OECD. 1994).

OECD guidelines consist of about 150 most significant agreed testing methods globally, used by independent laboratories, industry, and government to recognize and characterize the potential dangers of chemicals. They are a collection of tools primarily focused on safety evaluation, consequent registration, and evaluation of the chemical product. In addition, they can be also used as a screening tool for developing novel chemicals in toxicology research (Development ; OECD. 1994). OECD Guidelines for the Testing of Chemicals are broadly categorized into five sections

Section 1: Physical Chemical properties (Development).

Section 2: Effects on Biotic Systems (Development).

Section 3: Environmental Fate and Behaviour (Development).

Section 4: Health effects (Development).

Section 5: Other Test Guidelines (Development).

Each section consists of numerous tests with detailed protocols for different screenings (Development). The guidelines for studying the effect of chemicals and drugs on the health of individuals by in vitro and in vivo models are mentioned in section 4, comprising a total of 80 tests, each with different criteria (Development). Several tests are required to evaluate various types of toxicity, including dermal toxicity, skin sensitization, ocular toxicity, genotoxicity, reproductive and developmental toxicity. These guidelines give detailed protocol regarding the use of animals, their handling, dosing of drugs in case of acute and

chronic studies, and evaluating parameters. They also assist in screening molecules during the initial drug discovery phase and suggest animal replacement, reuse, and refinement. To minimize the use of animals, the European Chemical Agency has also proposed five basic principles in the regulatory context for using computational techniques, including a defined end-point, defined domain of applicability, definite algorithm, suitable measures for robustness, prediction, reliability of the developed model, and interpretation of mechanism if possible (Pérez Santín et al. 2021). Even pharmacovigilance is in continuous effort to employ in silico studies to minimize the use of animals and also due to their higher accuracy and reproducibility – making use of enormous databases available for the development of artificial intelligence, deep learning, and neural network models (Basile et al. 2019).

2.3 OECD guidelines and ocular toxicity

In vitro, ex vivo, organ culture, and in vivo methods are used to establish the ocular safety of the molecules/drugs. The OECD proposes various guidelines to evaluate the ocular toxicity of new chemical entities or molecules (**Table 2.1**), categorizing the molecules as UN GHS Category 1, 2, or No category. UN GHS "Category 1" includes the molecules causing severe ocular damage with irreversible effects, whereas "Category 2" includes the molecules causing ocular irritation; however, the effect is fully reversible. "No category" includes the molecules that are non-irritant.

Literature Review

Table 2.1: Organization for Economic Co-operation and Development (OECD) Guidelines for testing chemicals for ocular toxicity.

Test Guideline No.	Type	Test Name
405	In-vivo	In Vivo Eye Irritation/Serious Eye Damage
437	Ex-vivo	Bovine Corneal Opacity And Permeability Test Method For Identifying i) Chemicals Inducing Serious Eye Damage And ii) Chemicals Not Requiring Classification For Eye Irritation Or Serious Eye Damage
438	Ex-vivo	Isolated chicken eye test method for identifying i) chemicals inducing serious eye damage and ii) chemicals not requiring classification for eye irritation or serious eye damage
460	In-vitro	Fluorescein Leakage Test Method for Identifying Ocular Corrosives and Severe Irritants
491	In-vitro	Short Time Exposure In Vitro Test Method for Identifying i) Chemicals Inducing Serious Eye Damage and ii) Chemicals Not Requiring Classification for Eye Irritation or Serious Eye Damage
492	In-vitro	In vitro Macromolecular Test Method for Identifying i) Chemicals Inducing Serious Eye Damage and ii) Chemicals not Requiring Classification for Eye Irritation or Serious Eye Damage
494	In-vitro	Vitrigel®-Eye Irritancy Test Method for Identifying Chemicals Not Requiring Classification and Labelling for Eye Irritation or Serious Eye Damage
496	In-vitro	In vitro Macromolecular Test Method for Identifying i) Chemicals Inducing Serious Eye Damage and ii) Chemicals not Requiring Classification for Eye Irritation or Serious Eye Damage

2.4 Systemic drug-induced ocular toxicity

Systemic drugs that are administered to patients undergoing chronic therapy (for example cardiovascular, hypertension, and rheumatoid arthritis) enter the eye (off-target site) and cause severe ocular toxicity (Garg and Yadav 2019). Numerous drugs are known to cause ocular toxicity after their systemic administration, including but not limited to salbutamol, tamsulosin, amitriptyline, amiodarone, losartan, atorvastatin, tamoxifen, imatinib, aspirin, and dexamethasone (Dogan and Esmaeli 2009; Gokulgandhi et al. 2012; Moorthy and Valluri 1999; Vijayakumar et al. 2011). These drugs are known to cause various ocular complications in both the anterior and posterior segment of the eye, to highlight a few – conjunctivitis, dry eye, uveitis, lacrimation, inflammation of eyelids, allergic conditions, diplopia, optic neuritis, retinopathy, all leading to vision impairment (**Table 2.2**) (Constable et al. 2022a; Moorthy and Valluri 1999). Even upon discontinuing the medications, these damages can be irreversible, such as maculopathy and keratopathy caused by amiodarone (Bratulescu et al. 2005). Another classic example includes irreversible eye damage – retinopathy caused by hydroxychloroquine; the severity of ocular toxicity depends on the dose and duration of hydroxychloroquine (Jui-Hung Kao 2022; Melles and Marmor 2014). Also, several cases have reported irreversible lacrimal duct stenosis in women consuming cyclophosphamide, methotrexate, and fluorouracil for early-stage breast cancer (Stevens and Spooner 2001). Another case report found that bisphosphonates (alendronate) could cause scleritis, and the symptoms were reversed upon discontinuing its use (Leung et al. 2005). A retrospective cohort study showed that several anticancer agents (BRAF inhibitors, MEK inhibitors, Immune checkpoint inhibitors, therapeutic antibodies) could cause ocular toxicities such as inflammatory uveitis, dry eye, and central serous retinopathy (Vishnevskia-Dai et al. 2021).

Literature Review

Table 2.2: Systemic drugs causing ocular toxicity.

Systemic Drugs	Ocular Toxicity	References
Hydroxychloroquine	Macular degeneration, Retinopathy.	
Ethambutol	Retrobulbar optic neuritis, diplopia, mydriasis.	(Castells et al. 2002; Constable et al. 2022a; Jui-Hung Kao 2022; Li et al. 2008; Liu et al. 2018; Melles and Marmor 2014; Moorthy and Valluri 1999; Mukhtar and Jhanji 2022; Prakash et al. 2019; Richa and Yazbek 2010; Santaella and Fraunfelder 2007)
Cytarabine	Ocular pain, blurred vision, corneal toxicity, photophobia.	
Gabapentin	Mydriasis, secondary angle closure glaucoma, uveitis.	
Paclitaxel	Open-angle glaucoma.	
Oxybutynin chloride	Dry eye, increased risk of angle closure glaucoma.	
Amitriptyline	Cycloplegia, dry eye, increased IOP, glaucoma.	
Diphenhydramine	Dry eye, Increase of IOP, pupil-block glaucoma.	
Cidofovir	Uveitis and hypotony.	

The patient's pre-existing medical conditions make it difficult to diagnosis the drugs associated ocular toxicity and decide the initiation of treatment of ocular toxicity (Vishnevskia-Dai et al. 2021). Also, such toxicities vary among patients, making it even more challenging for physicians to provide timely intervention (Shin et al. 2020; Yuan et al. 2019). Many studies suggest a regular ophthalmic examination of patients (management among experts from different specializations) consuming anti-neoplastic, Central Nervous System (CNS) drugs, cardiovascular drugs, anti-arthritis drugs, and any other drug used for a chronic

period (Ali et al. 2022). Most patients have no alternative other than discontinuing systemic therapy to reduce/avoid ocular toxicity to protect their vision (Hollander and Aldave 2004).

The ocular toxicity caused by systemic drugs depend on various factors, including the nature of the drug, the amount of drug consumed, the route of administration, drug metabolism, and the pathological status of the drug. Many host (ocular) factors also play a crucial role in determining the extent of toxicity of systemic drugs, especially barrier integrity (Moorthy and Valluri 1999). Drugs reach the anterior segment of the eye through tear film, aqueous humor, uveal circulation, or limbal vasculature. In addition, the choroid, sclera, and ciliary body have fenestrated capillaries that allow the entry of small drug molecules into the eye (Garg and Yadav 2019). Lipophilic molecules can diffuse freely from systemic circulation into the eye and might get accumulated or cleared over time. If the drug is accumulated, drug interaction with ocular tissues is prolonged, which can cause toxicity (Vijayakumar et al. 2011). Retention of the drug in the ocular tissues often define the extent of toxicity. Hence, understanding the drug entry mechanism into off-target tissues, such as ocular tissues, could provide new insights to intervene in ocular toxicity due to systemic drugs (Moorthy and Valluri 1999).

2.5 Toxicity due to drug-transporter interactions

Membrane proteins known as "Transporter" are known to facilitate the influx or efflux of substrates (endogenous or drug substances) across biological membranes (Kato et al. 2008). Drug regulatory agencies, including the US FDA and the EMA, have recognized the clinical significance of transporters for drug safety. The human genome sequencing project has identified 850 genes encoding for transporters in establishing the barrier function of cells, such as P-Glycoprotein (P-gp), multidrug resistance-associated proteins (MRPs), and organic

cation transporters (OCTs), organic anion transporter proteins (OATPs), and other transporters (Venter et al. 2001). Drug resistance is directly related to the expression of transporters in various organs, which limits the success of drug usage for various diseases (Khuri and Deshmukh 2018). These transporters can cause toxicity when drug molecules are falsely recognized as substrates similar to their endogenous substrates (Gao et al. 2015; Hafey et al. 2022; Taylor-Wells and Meredith 2014).

Several studies confirmed the crucial role of transporters in the accumulation of drugs at off-target sites which leads to toxicity (**Figure 2.2**). One well-known example of transporter-induced toxicity is cisplatin-induced nephrotoxicity caused due to off-target accumulation through OCT. Another study explored the penetration of antimuscarinic agents (P-gp substrates) into the CNS which are used in treating overactive bladder into the CNS (Muderrisoglu et al. 2019). Also, reports suggest the role of transporters in the ocular toxicity of systemic drugs. In vitro and in vivo studies have shown that taurine transporter plays a crucial role in retinal toxicity caused by accumulation of systemic vigabatrin in the retina (Police et al. 2020b).
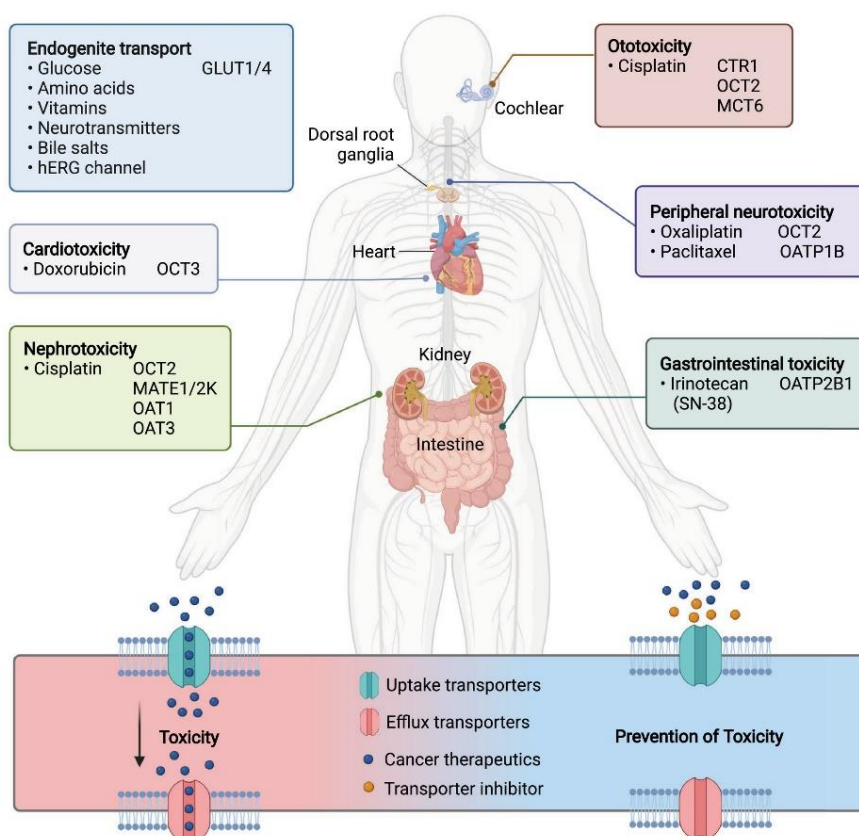
Figure 2.2: Role of transporters in toxicity. Both uptake and efflux transporters are present ubiquitous in the body. Transporters could be one of the major factors that regulates the metabolism of drug, leading to altered pharmacokinetics, toxicity and pharmacology of the drug. The translocation of drug through transporters at off-target site could lead to the accumulation of drugs which causes toxicity (Hafey et al. 2022).

2.6 Ocular barriers and transporters

The eye is considered a well-protected organ due to the presence of various static and dynamic barriers – Blood-tear Barrier (BTB), Blood-Aqueous Barrier (BAB), and Blood-Retinal Barrier (BRB). BTB is formed by tight junctions of acinar cells, whereas in the anterior segment, BAB is formed by tight junctions of epithelial cells in the iris-ciliary body. In the posterior segment of the eye, BRB is formed by tight junctions of retinal pigment epithelium and endothelial cells (Kubo et al. 2014a; Nirmal, Sirohiwal, et al. 2013a; Nirmal et al. 2010; Velpandian, Nirmal, Sirohiwal, et al. 2012). Several transporters are reported to be expressed

in ocular tissues which are crucial for these barrier functions (Zhang et al. 2008). Transporters belonging to more than 11 families have been reported to be expressed in corneal epithelium and blood retinal barrier. Multiple uptake transporters belonging to solute carrier (SLC) family such as glucose transporter (GLUT), taurine transporter, amino acid transporter, nucleoside transporter, folate transporter, organic anion and organic cation transporters mediate the translocation of endogenous molecules from blood to ocular tissues across various barriers (Liu and Liu 2019; Mannermaa et al. 2006). These transporters can also regulate the drug metabolism which can further impact the pharmacokinetics, toxicity and efficacy of drug.

2.7 Lacrimal gland

The ocular surface of the eye gets nourishment from the tear and aqueous humor. The lacrimal gland produces tears, known to be ultra-filtrate of the plasma, indicating the selective movement of molecules from the blood to the tear (Alexander et al. 1972; Schechter et al. 2010b). It comprises of acinar cells, which are pyramidal-shaped and encircled with myoepithelial cells in the basal lamina, whereas microvilli characterize the luminal surfaces. Acinar cells secrete tears into the ductal segments, consisting of cuboidal epithelium underlined with myoepithelial cells in the basal lamina, similar to acinar cells. The first ductal segments form intralobular ducts, which converge to form interlobular (Multiple acini), intralobar (Multiple lobes), interlobar (Multiple lobes), and central excretory duct (**Figure 2.3**) (Schechter et al. 2010b). The acinar cells pose tight junctions as a barrier for entry of endogenous molecules and xenobiotics from blood to tears. However, to enrich the nutritional demand, a continuous supply of nutrients, vitamins, hormones, neurotransmitters, and other endogenous molecules is provided from blood to the tear (**Table 2.3**) (Dey and Mitra 2005). Endogenous molecules are transported through the

membrane transporters in the lacrimal gland. Due to the evolutionary conservation of transporters, slight changes in the structure of substrates are not differentiated, leading to false recognition of the xenobiotics, including drug molecules as their substrates, thus facilitating their transport.
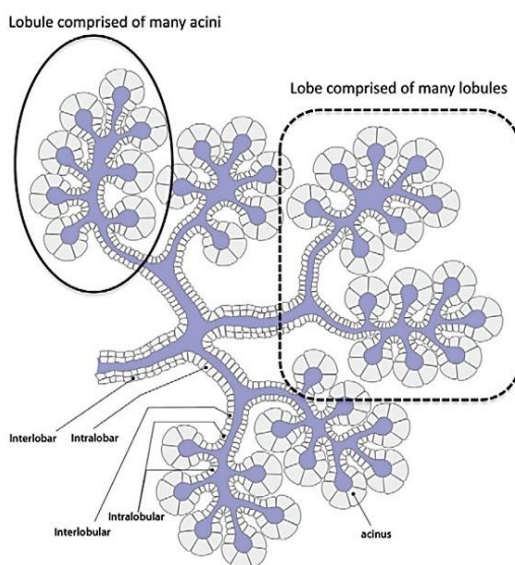
Figure 2.3: Classification of lacrimal gland. Acinar cells are the secretory cells of lacrimal gland which drains into intercalated or intralobular ducts. The different intralobular ducts then converges to form interlobular duct followed by intralobar and interlobar duct opening to main excretory duct (Schechter et al. 2010b).

Table 2.3: Endogenous molecules in tear as substrates of various transporters. OCT: Organic Cation Transporter, OCTN: Novel Organic Cation Transporter, OAT: Organic Anion Transporter, OATP: Organic Anion Type Protein Transporter, PEPT: Peptide transporter, MRP: Multidrug resistance protein, BCRP: Breast Cancer Research Protein, MDR: Multidrug resistance transporter, SLC: Solute carrier, ABC: ATP binding cassette, DHEAS: Dehydroepiandrosterone-sulfate, T3: Triiodothyronine, T4: Thyroxine, GSH: Growth Stimulating Hormone.

S.No	Endogenous substrate	Transporters	References
1	Choline	OCT1 (SLC22A1), OCT2 (SLC22A2), OCT3 (SLC22A3)	(Chhadva et
2	Acetylcholine	OCT1 (SLC22A1), OCT3 (SLC22A3), OCTN1 (SLC22A4)	al. 2015;
3	Dopamine	OCT1 (SLC22A1), OCT2 (SLC22A2), OCT3 (SLC22A3)	Dartt 2009;
4	Norepinephrine	OCT1 (SLC22A1), OCT2 (SLC22A2), OCT3 (SLC22A3)	Lee et al.

5	Creatinine	OCT1 (SLC22A1), OCT2 (SLC22A2), OCT3 (SLC22A3), OAT2 (SLC22A7)	2015; Trope and Rumley 1984; Van Haeringen 1981b)
6	Serotonin	OCT1 (SLC22A1), OCT2 (SLC22A2), OCT3 (SLC22A3)	
7	Prostaglandin E2	OCT1 (SLC22A1), OCT2 (SLC22A2), OAT1 (SLC22A6), OATP1A2 (SLCO1A2), OAT2 (SLC22A7), MRP1 (ABCC1)	
8	Prostaglandin F2α	OCT1 (SLC22A1), OCT2 (SLC22A2), OAT1 (SLC22A6), OAT2 (SLC22A7), MRP1 (ABCC1)	
9	Biotin	OCT2 (SLC22A2)	
10	Histamine	OCT2 (SLC22A2), OCT3 (SLC22A3)	
11	Catecholamines	OCT2 (SLC22A2)	
12	Putrescine	OCT2 (SLC22A2)	
13	Epinephrine	OCT2 (SLC22A2), OCT3 (SLC22A3)	
14	L-carnitine	OCT3 (SLC22A3)	
15	Guanidine	OCT3 (SLC22A3)	
16	Corticosterone	OCT3 (SLC22A3)	
17	Progesterone	OCT3 (SLC22A3)	
18	Testosterone	OCT3 (SLC22A3)	
19	Ergothioneine	OCTN1 (SLC22A4)	
20	Carnitine	OCTN1 (SLC22A4), OCTN2 (SLC22A5)	
21	Di- and tripeptides	PEPT1 (SLC15A1), PEPT2 (SLC15A2)	
22	Uric acid	OAT1 (SLC22A6), OAT2 (SLC22A7), OAT3 (SLC22A8), BCRP (ABCG2)	
23	Folates	OAT1 (SLC22A6)	
24	DHEAS	OAT2 (SLC22A7), OATP1A2 (SLCO1A2), MRP1 (ABCC1)	
25	Conjugated sex steroids	OATP1A2 (SLCO1A2)	
26	T3	OATP1A2 (SLCO1A2)	
27	T4	OATP1A2 (SLCO1A2)	

28	Linear and cyclic peptides	OATP1A2 (SLCO1A2)	
29	Cholecystokinin	OATP1B3 (SLCO1B3), MRP2 (ABCC2)	
30	Steroid hormones	OATP1B3 (SLCO1B3), OATP2B1 (SLCO2B1), MDR1/Pgp (ABCB1)	
31	Lipids	MDR1/Pgp (ABCB1)	
32	Leukotrienes	MRP1 (ABCC1), MRP2 (ABCC2), MRP3 (ABCC3)	
33	GSH	MRP1 (ABCC1)	
34	Sphingosine 1-phosphate glucuronide conjugates of 17β-estradiol	MRP1 (ABCC1)	
35	Ethinylestradiol-3-O-glucuronide	MRP2 (ABCC2)	
36	Estrone 3-sulfate	MRP2 (ABCC2), BCRP (ABCG2)	
37	Estradiol-17β-glucuronide	MRP3 (ABCC3)	
38	Porphyrins	BCRP (ABCG2)	

2.8 Organic Cation Transporters in Eye

Systemic medications may accumulate in the eye due to membrane transporters in the ocular barriers (Abdollahi et al. 2004; Hornof et al. 2005). Reports indicate that transporters are expressed and have vital functions at BAB, BRB, and the lacrimal gland to supply nutrients from the blood to the eye (Nirmal, Sirohiwal, et al. 2013b; Nirmal et al. 2010; Velpandian, Nirmal, Arora, et al. 2012; Velpandian, Nirmal, Sirohiwal, et al. 2012). Many endogenous amines (Organic cations) such as dopamine, epinephrine, serotonin, and histamine are secreted to the tear from the blood through lacrimal secretion and BAB. Organic Cation transport system is present in the corneal and conjunctival epithelial cells to reabsorb these endogenous amines from the tear fluid (Martin and Brennan 1993, 1994; Nirmal et al. 2010;

Van Haeringen 1981a; Velpandian, Nirmal, Sirohiwal, et al. 2012). Organic Cation Transporters (OCT)/Novel Organic Cation Transporters (OCTN) like OCT1, OCT3, OCTN1, and OCTN2 are reported to be expressed in various ocular tissues like cornea (Garrett et al. 2008), conjunctiva (Garrett et al. 2008), iris-ciliary body, retina (Zhang et al. 2008) and lacrimal gland (Velpandian, Nirmal, Sirohiwal, et al. 2012) (**Figure 2.4**).
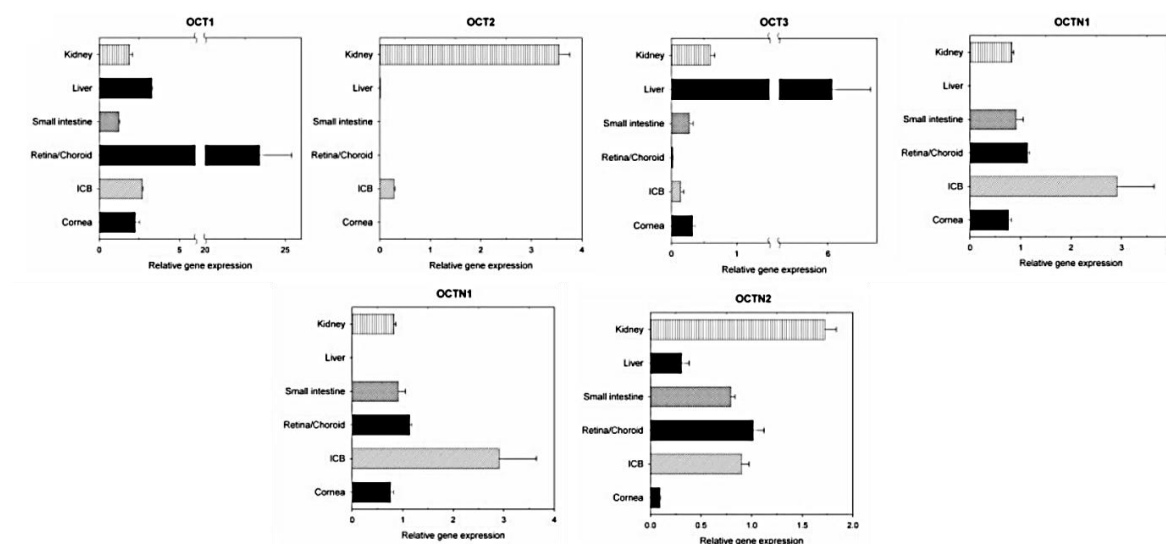
Figure 2.4: Relative gene expression of organic cation transporters in the various ocular tissues (Zhang et al. 2008).

However, OCT1 is reported to be highly expressed isoform in the ocular tissues (Zhang et al. 2008). Many ocular drugs are substrates or inhibitors of these transporters (Huang et al. 2005; Mannermaa et al. 2006; Nirmal, Singh, et al. 2013a; Nirmal, Sirohiwal, et al. 2013b). Many of the drugs approved by the FDA exist as cations at physiological pH, which might interact (as substrate/inhibitor) with OCT/OCTN, thereby gaining access inside the eye, which could lead to adverse effects like ocular toxicity (**Table 2.4**) (Baidya et al. 2020).

Table 2.4: Systemic OCT/OCTN drug substrates causing ocular toxicity.

Drug	Cation transporters	Ocular toxicity	References
Verapamil	OCTN2	Periorbital edema, lacrimation, conjunctival chemosis, erythema,	(Shimizu et al. 2015; Vijayakumar et al. 2011)
Ethambutol	OCT1, OCT2, OCTN1, OCTN2	Retrobulbar optic neuritis, green-red color vision, diplopia, mydriasis	(Pan et al. 2013; Vijayakumar et al. 2011)
Paclitaxel	OCTN2	Open angle glaucoma	(Console et al. 2020; Vijayakumar et al. 2011)
Oxybutynin chloride	OCT1, OCT2, OCT3	Dry eye, increased risk of angle closure glaucoma	(Vijayakumar et al. 2011; Wenge et al. 2011)
Amitriptyline	OCT1, OCT2	Cycloplegia, dry eye, diplopia, increased IOP, toxic amblyopia, pupil-block glaucoma	(Jouan et al. 2014; Vijayakumar et al. 2011)
Progestogens	OCT1, OCT3	Dry eye, loss of vision, decreased tolerance to contact lenses,	(Hayer-Zillgen et al. 2002; Vijayakumar et al. 2011)
Diphenhydramine	OCT1, OCT2, OCT3	Dry eye, Increase of IOP, pupil-block glaucoma	(Boxberger et al. 2014; Vijayakumar et al. 2011)

OCT/OCTN is responsible for the significant uptake of organic cations at physiological pH from plasma to the eye across the BRB, BAB, and lacrimal glands (Nirmal, Singh, et al. 2013a;

Nirmal, Sirohiwal, et al. 2013b; Nirmal et al. 2010; Nirmal et al. 2012). A study reported that the lacrimal gland could act as a gateway for the entry of OCT substrates (Tetraethylammonium) into tears when administered intravenously, which was inhibited in the presence of OCT blockers (Atropine, Quinidine) (Velpandian, Nirmal, Sirohiwal, et al. 2012). OCT1 is also reported to be functionally active in corneal epithelium from tear to aqueous humor side, as indicated by a study where the TEA concentration in aqueous humor decreased in presence of topical blockers (**Figure 2.5A**). The uptake of tetraethylammonium from systemic circulation was also inhibited through OCT in BRB when quinidine (OCT inhibitor) was pre-administered intravenously (**Figure 2.5B**) (Nirmal, Sirohiwal, et al. 2013b). Another study suggests that the direction of OCT in BRB is from blood-to-vitreous rather than in the vitreous-to-blood route, indicating that the OCT facilitates the entry of systemic drugs into the eye. Moreover, the poor elimination of intravitreally injected drugs could lead to accumulation which causes ocular toxicity (Nirmal et al. 2012).

Drug-transporter interactions can cause toxicity based on the transporter expression in specific cells, which could lead to high drug accumulation, such as metformin and cisplatin-induced kidney toxicity (Ciarimboli 2011). Substrate-transporter interaction can be exploited to determine interventions for blocking drug uptake in off-target cells to minimize specific cell toxicity. Therefore, the role of transporters in drug absorption and clearance mechanisms must be understood to determine drug concentration at both target and off-target sites to predict the drug's pharmacokinetics and toxicity. However, the conventional in vitro and in vivo methods are not feasible to screen hundreds of molecules for their interactions with various transporters, thereby modern techniques such as artificial intelligence (AI) methods

can be used as a high-throughput screening tool to predict the drug-transporter interactions and the associated toxicities.
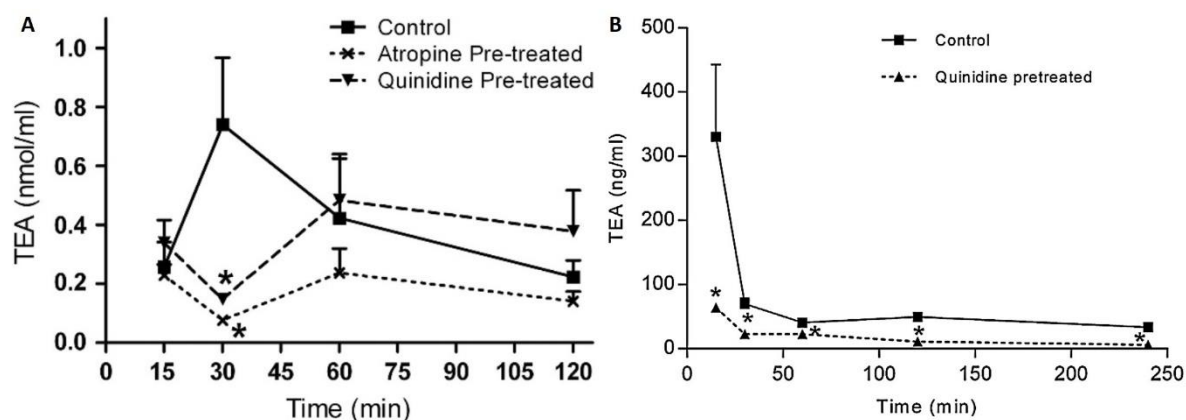
Figure 2.5: Functional role of OCT1 in eye. A. Transcorneal kinetics of topically administered tetraethyl ammonium (TEA), OCT1 substrate in presence and absence of OCT1 blockers (Atropine and Quinidine) administered topically. The uptake of TEA decreased in the presence of OCT1 blockers indicating the direction of OCT1 pump from tear to aqueous humor. B. Vitreal kinetics of intravenously administered TEA in presence and absence of OCT1 blocker (Quinidine) administered intravenously. The TEA uptake decreased in the presence of OCT1 blocker indicating the direction of OCT1 pump from blood to vitreous humor (Nirmal, Singh, et al. 2013a; Nirmal, Sirohiwal, et al. 2013a).

2.9 AI in toxicity prediction

The intracellular concentration of the drug is determined by understanding the equilibrium of influx and efflux transporters. Combining various computational methods, statistical analysis, and experimental confirmation can be an efficient tool to solve complex drug-transporter interactions (Zeino et al. 2014). The significant time and cost required for experimental testing make AI an emerging tool to build predictive computational models for determining the potential substrate binding with transporters (Diao et al. 2010; Moaddel et al. 2007). Many modeling approaches are being proposed to understand the specificity of transporters with various drugs in the human body.

Literature Review

Machine learning (ML) techniques or models can be broadly classified into three categories – Supervised, Unsupervised, and Reinforcement learning. In supervised learning, the input dataset is labeled, i.e., correct values are provided for the data, and based on these input values, the algorithm shows a labeled output. It classifies the objects in a pool using a set of characteristics while excluding annotations. In unsupervised learning, the input dataset in not labelled i.e., the algorithm finds a pattern in the given input data in the form of groups or clusters. It groups all the objects within an area so that likeness is established and once the groupings are made they are categorized into plausible groups. Whereas in reinforcement learning the algorithm works on reward and action phenomenon in an environment. The algorithm has an environment where it sequentially solves the task and modifies its actions based on the experience to get a reward and maximize the performance (Sarker 2021). In simple terms, a reinforcement-enabled system can learn from the consequences of prior interactions with the environment and monitor how these results impact future interactions. Neural networks are even more advanced algorithms biologically inspired based on the nervous system. An artificial neural network (ANN) comprises complex neurons connected by weighted links. ANN models are classified as static, dynamic, and statistical ANN. It usually consists of three layers – an input, output, and hidden layer (Malekian and Chitsaz 2021).

AI-based machine learning models are also developing rapidly to understand the toxicity caused by various chemicals, drugs, and other molecules (Khuri and Deshmukh 2018). Computational methods are essential as thousands of drug features can be computed, analyzed, filtered, and selected based on algorithms. Moreover, it is beyond the scope of humans to study these features individually for all the existing and emerging drug molecules (Khuri and Deshmukh 2018). AI-based models can predict toxicities of molecules based on

their physicochemical properties such as topological surface area, LogP or LogD values, presence of various functional groups, molecular weight, molecular volume, aromatic rings, and also based on the structure of molecules, which helps in determining its interaction and binding efficacy with various biomolecules in body. Both chemical and biological properties of molecules are also considered while developing a model, such as the structure of molecules, dose and time response, pharmacokinetics, and pharmacodynamics data (Wu and Wang 2018). Various techniques such as pharmacophores, Quantitative-Structure Activity Relationship (QSAR), similarity finders, i.e., common fingerprints, machine learning models, molecular modeling, and other network analysis tools are developed to build an efficient computational model (Ekins et al. 2007).

Earlier models were constructed based on a single parameter, such as chemical structure or biological property. However, as the field is diverging, new models using a combination of structural and biochemical parameters are developed to predict a better outcome with high accuracy (Wu and Wang 2018). Apart from multifeatured input data, more advanced models are computed by combining perturbations and machine learning, which integrates biological and chemical data to predict toxicity against diverse living organisms (V Kleandrova et al. 2015). The toxicity estimations as accurate predictions using in silico methods range between 85% to 90%, as it out-turns that the available literature and biological data showing the experimental proofs are limited. Also, the selection of properties (descriptors) used for input data is limited. Hence, it is crucial to understand the workings of these models to identify the significant characteristics or the descriptors to be used for developing a model that gives a reliable output with reproducibility (Hutter 2018).

QSAR models have been developed for studying the toxicological properties of various drugs based on their structure and physiochemical properties. It involves the use of data mining to calculate molecular descriptors and also to identify relationships within these features (Helma and Kazius 2006). QSAR models are built to predict the ocular toxicity of compounds; however, the dataset used for their construction was small (Abraham et al. 1998; Cronin et al. 1994; SUGAI et al. 1991). Another approach to test eye irritants and corrosive chemicals was developed by QSAR and Multiple Descriptor Read Across (MuDRA) models using different descriptors. The dataset was obtained from the European Chemical Agency, and the chemicals were classified as eye irritant or non-irritant and eye corrosive or non-corrosive. Ensemble decision tree and MuDRA, an instance-based learning process, were used to develop the model and predict the activity of molecules to be ocular irritant or corrosive (Silva et al. 2021).

In addition, a machine learning model was applied where diverse data of eye corrosive (n = 2299) and eye irritant (n = 5220) molecules was collected from various databases and literature. These molecules were represented with nine molecular fingerprints, and six machine learning algorithms were used to develop binary classification models with five-fold cross-validation to predict ocular toxicity. The sensitivity and specificity of the developed model for eye corrosive were 94.9% and 96.2%, respectively, whereas, for eye irritant molecules, it was found to be 96.9% and 82.7%, respectively. The high sensitivity and specificity of the developed model ensure the reliability and robustness of the model in predicting the activity of molecules causing ocular toxicity (Wang et al. 2017).

AI also helps predict the drug's role as a substrate or inhibitor for a transporter by studying their interactions (Khuri and Deshmukh 2018). An AI study reported that 85% of newly tested substances screened through machine learning were confirmed as OCT1 substrates. It can also help in understanding the molecular mechanisms of transporters (Jensen et al. 2021b). Rapid meta-analysis using AI to study the ocular toxicity of hydroxychloroquine has proved to be time efficient, whereas traditional meta-analysis takes years to produce these observations (Michelson et al. 2020). Therefore, AI and computational models can be an efficient alternative to experimental studies for toxicity prediction and understanding drug-transporter interactions.

2.10 Non-therapeutic blocking of transporters

Pharmaceutical excipients are considered as non-therapeutic agents since they do not pose any pharmacological activity. Most pharmaceutical excipients are considered safe as per the GRAS (Generally Regarded as Safe) database, which is documented based on FDA-approved products (FDA). However, emerging data have demonstrated that excipients can interact with specific transporters and thus affect the absorption and bioavailability of drugs (Soodvilai et al. 2017a). Many studies have examined the effects of excipients on efflux transporters apically located in the gastrointestinal tract, such as P-gp, MRPs, and breast cancer resistance protein (BCRP) (Thakkar 2015). Vitamin E, TPGS (D-α-tocopheryl polyethylene glycol 1000 succinate), inhibits the efflux process of the P-gp transporter, which actively exports drugs out of cells in a concentration-dependent manner and thus increases the absorption of P-gp substrates (Dintaman and Silverman 1999). Surfactants, including Tween 20, Tween 80, Solutol HS 15, and Brij 58, also inhibit P-gp activity (Gurjar et al. 2018). Furthermore, Cremophor® EL inhibits BCRP and MRP2 receptors (Hanke et al. 2010; Yamagata et al. 2007).

Literature Review

Tween 20, Tween 60, and Tween 80 have shown inhibitory effects for OCT1 and OCT2 transporters in renal proximal tubular cell lines (Soodvilai et al. 2017b). Though there is evidence about the interaction of excipients with various uptake transporters such as OATP1/OCT and efflux transporters such as P-gp and MRP, to date, the role of pharmaceutical excipients in altering the drug-transporters interaction in the eye has not been evaluated (Engel et al. 2012; Ma et al. 2021).

Chapter 3

Lacunae and Objectives

Lacunae and Objectives

Lacunae

Systemic drugs used for chronic periods accumulate in off-target tissues such as the eye and cause toxicity. However, the entry mechanism of systemic drugs into the eye, despite various blood-ocular barriers, is unexplored. No systematic studies have been conducted to evaluate the entry of various systemic drugs inside the eye through transporters. Since 40 % of marketed drugs are cationic in nature at physiological pH, the interaction of systemic drugs with organic cation transporter (OCT) is a crucial question to be answered for understanding the mechanism of systemic drug entry into the eye. Also, to date, the role of pharmaceutical excipients in altering the transporters in the eye has not been evaluated, though there is evidence about the interaction of excipients with various uptake transporters and efflux transporters.

Hypothesis

In the proposed thesis work, we hypothesize that the systemic drugs that are cations gain access to the anterior eye segment via OCT in the lacrimal gland. This likely leads to ocular entry of systemic drugs, which causes ocular toxicity upon long-term exposure. Delineating the mechanism of drug entry into the eye could also enable the development of non-therapeutic interventions (using pharmaceutical excipients) to reduce the risk of systemic drug-induced toxicity in the eye by locally inhibiting (eye drops) the uptake transporters without inhibiting systemic pharmacological action of drugs (**Figure 3.1**). To test out hypothesis, the following objectives were structured under which various studies were conducted (**Figure 3.2**).

Lacunae and Objectives

<u>Objectives</u>

Objective 1

- Preparation of dataset and development of different screening models for Organic Cation Transporter (OCT) substrate using Artificial Intelligence based models (**Chapter 4**).

Objective 2

- Evaluation of drug substrate interaction with OCT transporters in the in vivo model (**Chapter 5**).

Objective 3

- Investigation of non-therapeutic inhibitors (Pharmaceutical excipients) to inhibit the uptake of drug substrates by OCT transporters using in vitro and in vivo models (**Chapter 6**).

We used artificial intelligence and computer simulations to predict the substrates for OCT1 among systemic drugs causing ocular toxicity (Objective 1). The predictions were validated in vivo by tear kinetics of topically administered predicted substrate (with more affinity to OCT1) in the presence and absence of topical OCT1 blocker (Objective 2). Further, the molecules confirmed as OCT1 substrate were administered intravenously, and tear kinetics were performed in the presence and absence of an OCT1 blocker (topical) to understand the functional importance of OCT1 in the lacrimal gland (Objective 2). Once we understood the interaction between OCT1 substrates and their transporters, the next question was how to stop their entry into the eye. For this purpose, pharmaceutical excipients reported to interact

with various transporters were screened for its application as an inhibitor of OCT1 using in

vitro and in vivo studies (Objective 3).
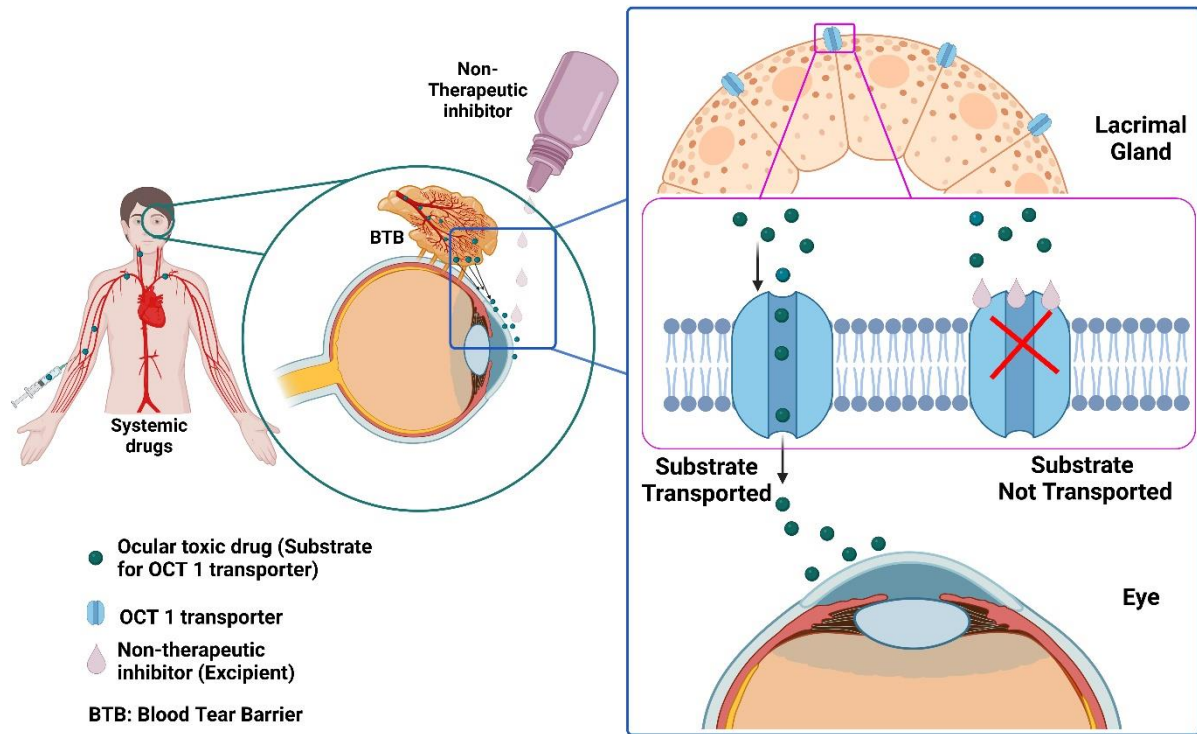
Figure 3.1: Hypothesis of the proposed work. Systemic/oral drugs (organic cations) enter the anterior eye segment through OCT1 transporters in the lacrimal gland and cause ocular toxicity. Excipients can be used as non-therapeutic inhibitors to block the entry of drugs into the eye by blocking the transporters.
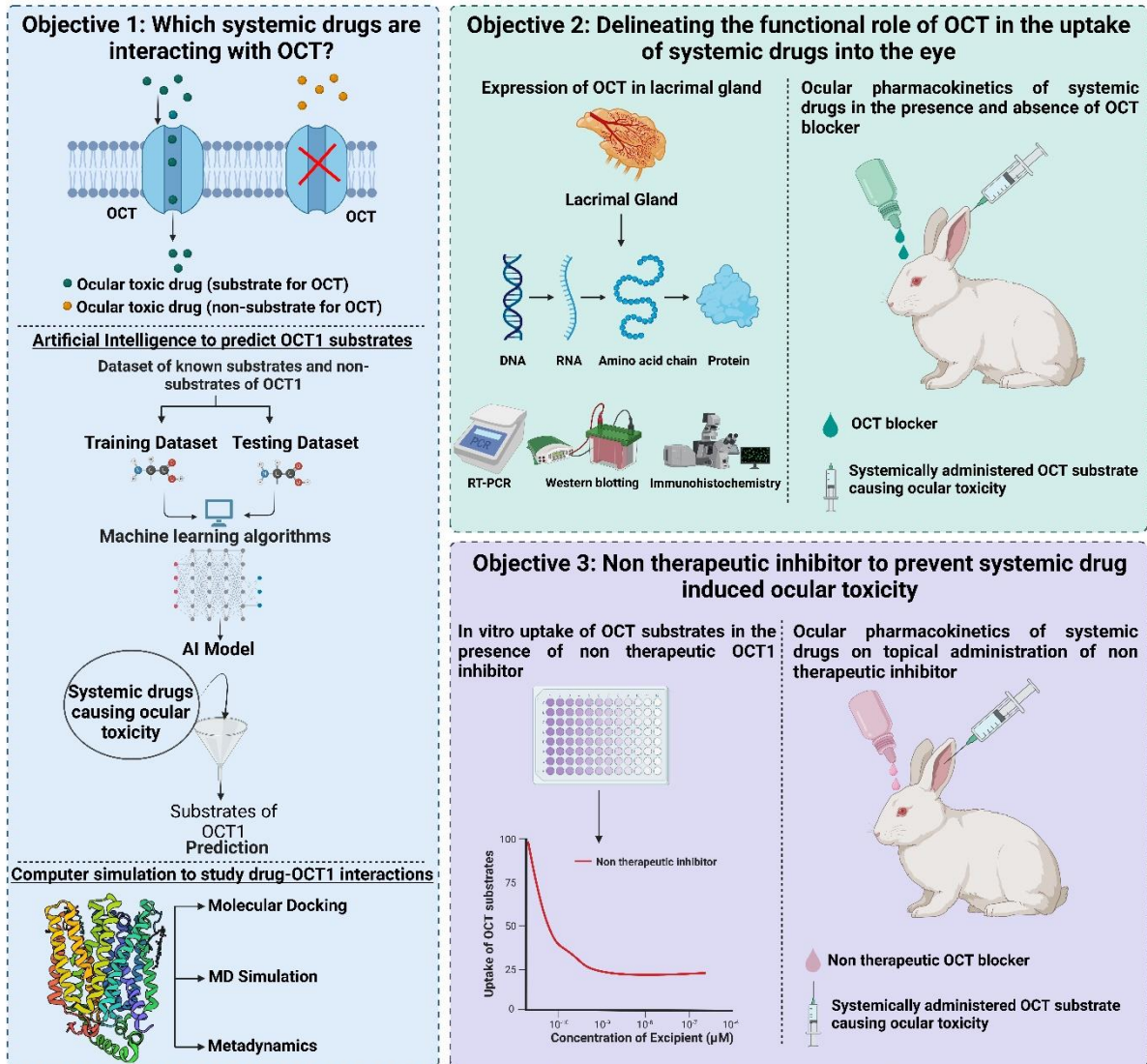
Figure 3.2: Overall workflow of proposed work. In Objective 1, artificial intelligence and computer simulations were used to understand the drug OCT1 interactions and predict the OCT1 substrates among systemic drugs causing ocular toxicity. In Objective 2, the predicted substrates were validated in vivo, and the expression and functional role of OCT1 in the lacrimal gland was evaluated to delineate systemic drugs' entry mechanism into the anterior eye segment. In Objective 3, the application of excipient as OCT1 blocker was evaluated in vitro and in vivo.

Chapter 4

Preparation of dataset and development of different screening models for Organic Cation Transporter (OCT) substrate using Artificial Intelligence based models

Artificial Intelligence in predicting drug Organic cation transporter interactions
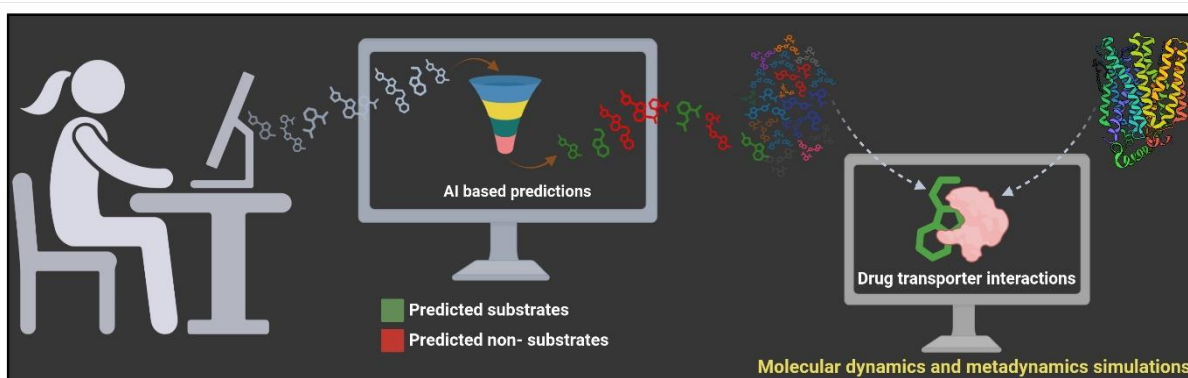
4.1 Introduction

Medicines can be a boon or bane to humanity based on their consumption. The changing lifestyle and environment have made us highly dependent on medicines. Unfortunately, these drugs also cause unwanted adverse effects despite their benefits (Coleman and Pontefract 2016; FDA 2018). Systemic drugs (oral, intravenous, intramuscular, sub-cutaneous) consumed by patients for arthritis, cancer, cardiovascular and other diseases are known to cause visual disturbances such as conjunctivitis, dry eye, uveitis, lacrimation, retinopathy, diplopia, and optic neuritis, all leading to vision impairment (Ali et al. 2022; Castells et al. 2002; Constable et al. 2022a; Li et al. 2008; Liu et al. 2018; Moorthy and Valluri 1999; Mukhtar and Jhanji 2022; Prakash et al. 2019; Richa and Yazbek 2010; Santaella and Fraunfelder 2007; Tehrani et al. 2008). Some of these ocular toxicities are reversible but may also lead to irreversible vision loss.

The benefits of the drugs to treat chronic diseases or the lack of other therapies often justify the associated risk of ocular toxicities; thereby, patients usually end up continuing their systemic medication (Brock et al. 2013; Vishnevskia-Dai et al. 2021). However, patients suffering with irreversible vision loss are left with no alternative but to stop their treatment. Also, such toxicities vary among patients, making it even more challenging for physicians to provide timely intervention (Shin et al. 2020; Yuan et al. 2019). Many studies indicate a regular ophthalmic examination of patients (management among experts from different specializations) consuming anti-neoplastic, central nervous system (CNS), cardiovascular (CVS), anti-arthritis drugs, and any other drug used for a chronic period (Ali et al. 2022).

Artificial Intelligence in predicting drug Organic cation transporter interactions

Systemic drugs selectively bind and accumulate in ocular tissues (off-target) such as the conjunctiva, cornea, lens, choroid, or retina despite the ocular barriers – causing ocular toxicity. We hypothesize that the transporters present in the ocular barriers for transporting endogenous molecules such as nutrients, vitamins, and neurotransmitters could falsely recognize the systemic drugs and enable their entry into the eye (Kubo et al. 2014b; Nirmal, Sirohiwal, et al. 2013a; Nirmal J 2010). In the last few decades, there has been increasing evidence of the role of membrane transporters in drug accumulation at the off-target site leading to toxicity, such as taurine transporter for vigabatrin uptake in the eye, and organic cation transporter (OCT) 2 for cisplatin uptake in the kidney (Filipski et al. 2009; Police et al. 2020a). It has also been highlighted as a scientific session, "Transporters and Toxicity," at the International Transporter Consortium (ITC) Workshop IV in 2021 (Hafey et al. 2022). Various ocular tissues show the expression of organic cation transporter in retina (Zhang et al. 2008), iris-ciliary body, the cornea (Garrett et al. 2008), conjunctiva (Garrett et al. 2008), and lacrimal gland (Velpandian, Nirmal, Sirohiwal, et al. 2012). It is also highly expressed in the liver, followed by the kidney and small intestine (Zhang et al. 2008). Around 40% of commonly prescribed drugs are organic cations at physiological pH, most acting as substrates or inhibitors for these transporters (Neuhoff et al. 2003). Cationic molecules need organic cation transporters (OCT) to translocate across the ocular barriers, of which OCT1 is the highly expressed isoform in ocular tissues (Zhang et al. 2008). Therefore, we aim to identify the potential substrates of OCT1 among the systemic drugs causing ocular toxicity to understand their entry into the eye despite the ocular barriers.

Screening thousands of drugs for their interaction with OCT1 using conventional invitro and invivo models is complex. However, artificial intelligence methods such as machine learning

and computer simulations can aid in better understanding about drug-transporter interactions and drug toxicity with high reproducibility and reliability (Jain and Ecker 2019; Jensen et al. 2021b; Khuri and Deshmukh 2018; Liu et al. 2016; Pu et al. 2019; Vamathevan et al. 2019). In silico predictions of drug toxicity have also been approved by The Organisation for Economic Co-operation and Development (OECD) and other regulatory boards (OECD 2020, 2021). Artificial intelligence methods were used earlier to predict the potential OCT1 substrates among Food and Drug Administration (FDA) approved drugs from 2014 to 2019 (Baidya et al. 2020; Hendrickx et al. 2013; Jensen et al. 2021a). However, the potential OCT1 substrates among the systemic drugs causing ocular toxicity were not scrutinized earlier. Therefore, in the present study, we used computer simulations to understand the drug-OCT1 interactions. Artificial intelligence models were developed based on the structural and physicochemical properties as well as the biological activity (OCT1 uptake ratio) to predict the substrate or non-substrates of OCT1. Molecular dynamics (MD) simulations were used to evaluate the drug-OCT1 binding stability and interactions at the atomic level, whereas metadynamics simulations were used to visualise drug movement across the transporter (OCT1).

4.2 Materials and Methods
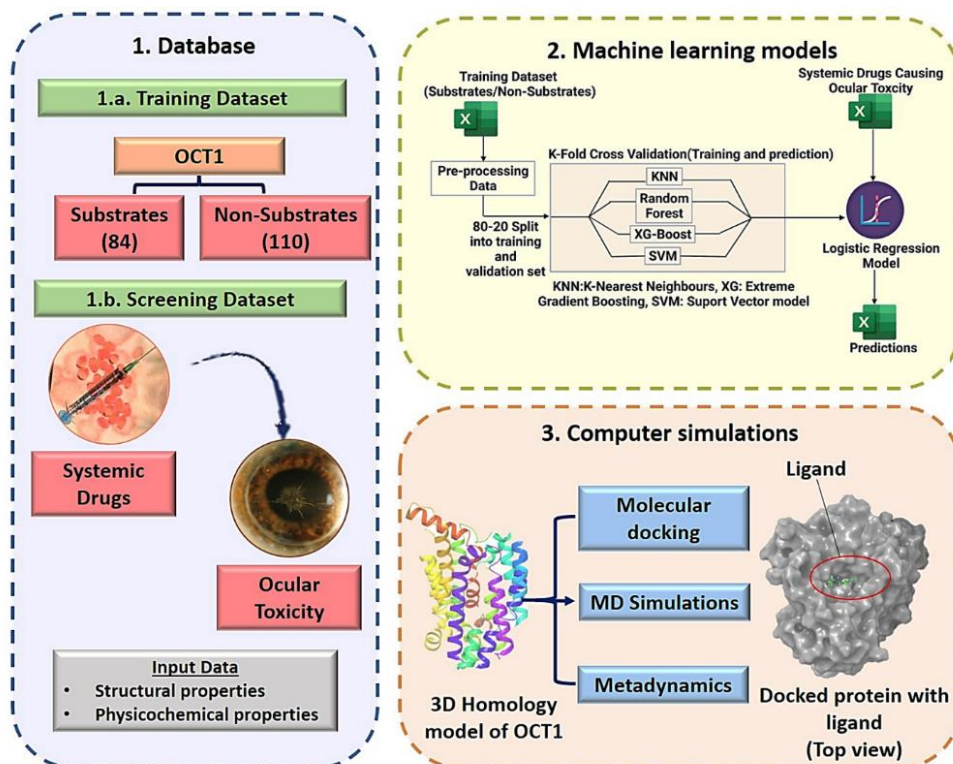
Figure: Workflow of chapter 4 (Objective 1).

4.2.1 Dataset preparation

To develop the machine learning model for the human OCT1 (hOCT1) training dataset was prepared based on Human Embryonic Kidney (HEK-293) in vitro experimental data to determine the uptake of drugs by hOCT1 (Hendrickx et al. 2013). The drugs with an uptake ratio greater than 1.3 were considered substrates for hOCT1. The training dataset comprised 110 substrates and 84 non-substrates, as reported earlier by our group (Baidya et al. 2020). The screening dataset consisted of 620 systemic drugs causing ocular toxicity collected from various literature sources, FDA, European Medicines Agency (EMA) labels, and other online sources (Bindiganavile et al. 2021; Constable et al. 2022b; Davies et al. 1983; Fraunfelder and Fraunfelder 2021; Gherghel 2020; Liang et al. 1996; Tehrani et al. 2008), which on data

curation and removal of duplicates, reduced to 424 drugs (Manisha 2023) (Ashburn and Thor ; Frederick T. Fraunfelder 2020). For both training and screening datasets, drug features were calculated based on the constitution, topology, charge, and molecular properties using the Biotriangle webserver (http://biotriangle.scbdd.com/chemical/index/). The data pre-processing using the Knime analytics platform (version 4.6.1) removed the features with less than 0.07 variance. Linear correlation was performed for all column pairs (two-tailed) followed by correlation analysis with 0.7 as the correlation threshold which reduced the dimensionality of the features.

4.2.2 Machine learning model development

Machine learning models were developed based on supervised learning algorithms and advanced neural network (ANN) using Python (Ver 3.6). The predictive models were obtained by running the parameters over various supervised machine learning algorithms such as k-Nearest neighbors, Random Forest, a particular class of decision tree C4.5, XG Boost, Support Vector Machines, and Naive Bayes probabilistic techniques. Additionally, k-fold cross-validation (k=5) was applied to accurately estimate the model's predictive performance. For the implementation of supervised learning models, the Sklearn library was used where substrates were denoted as one, and non-substrates as zero in the curated dataset.

The predictions of the test set from six base models were used as the input data for the logistic regression model to obtain consensus predictions. In addition, ANN was also used to predict the interactions between the drug and hOCT1. It is a particular type of algorithm which consists of three layers, namely, the input layer, hidden layer and output layer. In our model implementation, the input layer consisted of seven neurons, considering one neuron for each

input feature. The two hidden layers consisted of six neurons, each using a rectifier activation function. The output layer had one neuron, which used the sigmoid activation function to get the final predictions.

The performance of the developed model was assessed based on several metrics such as accuracy, precision, recall, and root mean square error. The screening dataset (systemic drugs causing ocular toxicity) was run through the developed model, and the molecules were predicted either as substrate or non-substrate for hOCT1.

4.2.3 Structural modeling of hOCT1 and ligands

4.2.3.1 Homology modeling and preparation of hOCT1 structure

Computer simulation studies were performed for hOCT1 using Schrödinger's Maestro suite (Maestro Version 12.9.123, MMshare Version 5.5.123, Release 2021-3, Platform Linux-x86_64). Homology modelling was performed using Prime module. Preparation of the OCT1 homology model was initiated by obtaining a gene sequence of hOCT1 (SLC22A1) from UniProt (https://www.uniprot.org/) database and running through Blast P algorithm to find its identical homolog (template) sequence. Human glucose transporter 1 (GLUT-1) in complex with bound inhibitor (2~{S})-3-(4-fluorophenyl)-2-(2-(3-hydroxyphenyl)ethanoylamino)-~{N}-((1~{S})-1-phenylethyl)propenamide) (PDB ID-5EQG) was selected as a template, and the model was developed using an energy-based homology modelling.

Since the sequence identity was less than 40% for the target and template protein, the non-template loop regions of homolog were refined with the Prime loop refinement tool. Variable dielectric surface generalized born solvation model (VSGB) was used as solvation model and

optimized potential for liquid simulations 4 (OPLS4) was used as the force field. Since hOCT1 is a membrane protein, the structural model was oriented according to the orientations of proteins in membranes (OPM) (Lomize et al. 2006). The loop regions of the protein structure containing less than five amino acid residues were refined using the default loop sampling method, six to eleven amino acid residues using the extended loop sampling method, and more than eleven amino acid residues were refined using the ultra-extended loop sampling method.

To perform molecular docking, MD simulations and metadynamics, the protein was prepared using Protein Preparation wizard of Schrödinger's Maestro suite to perform molecular docking, MD simulations, and metadynamics. The protein structure was prepared by assigning bond orders, adding missing hydrogen atoms, creating zero-order bonds to metals, creating disulphide bonds, pre-processing, and removing water molecules beyond 5 Å from the Het group. Further hydrogen bonds were assigned using PROPKA at pH 7.4 and energy was minimized for the protein structure. The accuracy of the developed model was evaluated using a protein reliability report and Ramachandran plot, which describes the plot of the torsional angle between phi (ϕ) and psi (ψ) amino acids in the protein and thereby gives information on the allowed and disallowed conformations of the developed homolog structure(Ramachandran and Sasisekharan 1968).

4.2.3.2 Preparation of ligand molecules

Ligand preparation was performed using LigPrep module of Schrödinger's Maestro suite. For ligand (known substrates/non-substrates of hOCT1 and systemic drugs causing ocular toxicity) preparation, 3D structures of all the ligand molecules were imported from PubChem.

The ligand structures were then prepared at a pH of 7.4 ± 0.2 in the OPLS4 force field of the protein. The prepared ligands were used for molecular docking studies.

4.2.4 Molecular Docking

Molecular docking was performed using Glide module of Schrödinger's Maestro suite. Molecular docking was performed to obtain the protein (hOCT1) ligand complex. A receptor grid was generated around the protein structure to define a search space for the docking calculations. A grid size of 30 Å was created around the bound ligand to cover the entire protein space, which was further docked with various prepared ligand molecules using the glide dock function with default parameters unless otherwise mentioned. Extra precision docking (XP) was performed for prepared ligand. The known substrates for OCT1, tetraethyl ammonium (TEA), and 1-methyl-4-phenylpyridinium (MPP) were used as the standards to optimize and validate the model's binding sites.

4.2.5 Molecular dynamic simulations

Molecular dynamic simulations were performed using Desmond module of Schrödinger's Maestro suite. We used MD simulations to visualize the interaction and binding stability of the protein and ligand complex (Hollingsworth and Dror 2018). The protein (hOCT1) and ligand molecules were placed in a system containing TIP3P water molecules, and the membrane region contained 1-palmitoyl-2-oleoyl-sn-glycerol-3-phosphocholine (POPC) molecules in a simulation box with buffer size of 10*10*10 Å. The system was neutralized by adding a calculated number of ions to account for electrostatic neutrality(Gapsys and de Groot 2020; Hub et al. 2014).

The prepared system was subjected to 100 ns MD simulations under the constant number of molecules, pressure, surface tension, and temperature (NPγT). Protein root mean square deviation (RMSD), ligand RMSD, protein root mean square fluctuation (RMSF) and protein-ligand interactions were analyzed at the end of MD simulations.

4.2.6 Metadynamics

Metadynamics was performed using Desmond module of Schrödinger's Maestro suite. The translocation of substrates was enhanced by performing metadynamics to visualize the movement of ligands along the protein molecule (hOCT1). MD simulations were performed for 10 ns to equilibrate and relax the system before metadynamics simulation. The distance between the center of mass of the protein molecule and the center of mass of the ligand was used as the collective variable for the metadynamics simulations. A wall-length limit of 35 Å was used to prevent the distancing of ligand molecule from the protein. Since hOCT1 is embedded in the membrane, NPγT ensemble class was used to maintain the constant number of molecules, pressure, surface tension, and temperature. Gaussian height was set at 0.03 kcal/mol with a width of 0.05 Å and applied at intervals of 0.09 ps. The total simulation time for metadynamics was set as 40 ns with a recording interval of trajectory at 40 ps. The temperature was set to 300 K with a pressure of 1 bar and surface tension of 0 bar*Å. The time and wall length were optimized for visualizing the transport process based on the trial and error method. The system's free energy was plotted as the function of the distance moved by the ligand molecule from its initial position during the metadynamics simulation. These energy profile diagrams were used to classify the ligand molecules as substrates or non-substrates of hOCT1.

4.3 Results

4.3.1 Dataset preparation

An initial 96 features were reduced by variance filter and correlation analysis. Based on their relevance in substrate translocation, few features were selected such as topological surface area (TPSA) and the number of acceptor groups (**Table 4.1**). Based on the distribution pattern of features among substrate and non-substrate of hOCT1, logP, hydrophilic index, and the number of sulfur atoms are considered as significant contributors, followed by TPSA and the number of h-bond donors in the molecules (**Figure 4.1**). Most of the molecules found beyond the range of threshold values had a higher probability of being non-substrate. A total of 424 systemic drugs causing ocular toxicity were collected in our database and further categorized based on their therapeutic use (**Figure 4.2**).
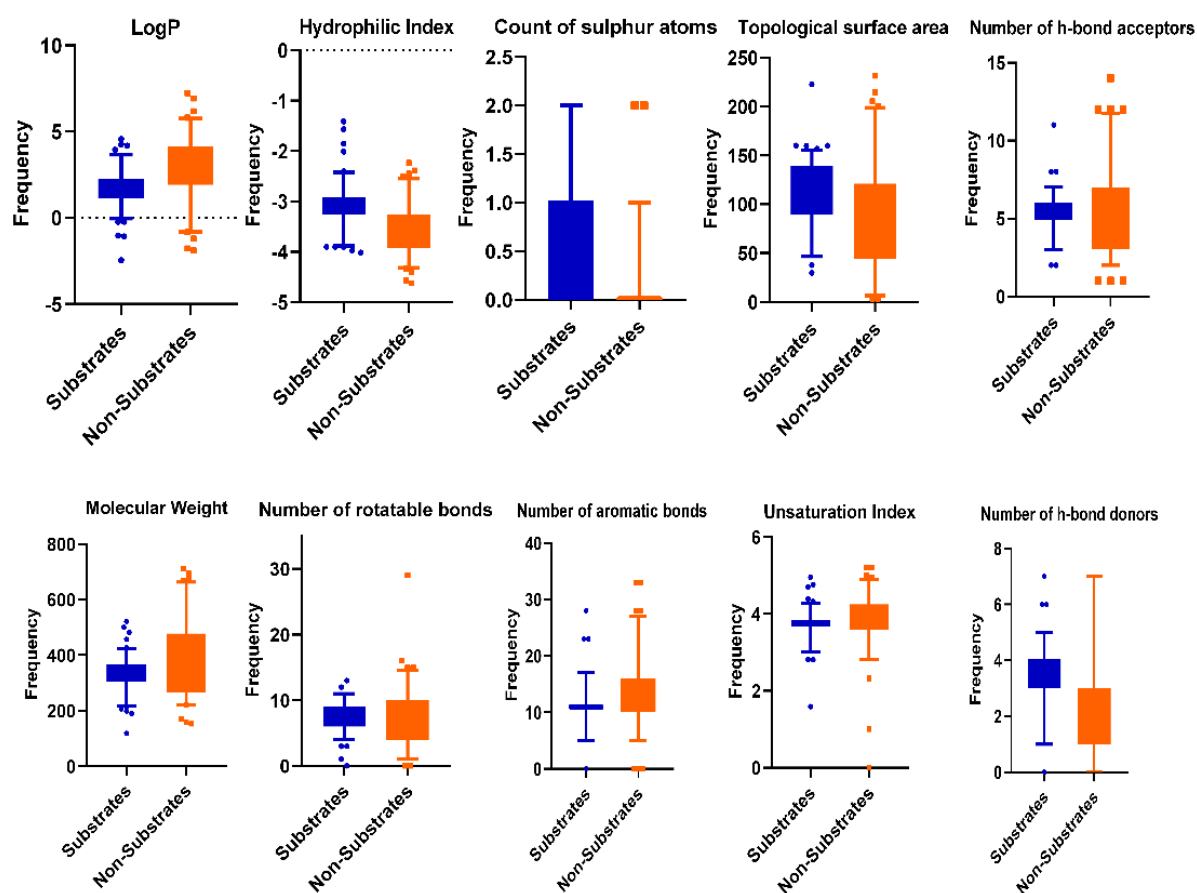
Figure 4.1: Structural, molecular and physicochemical features of substrates (blue) and non-substrates (orange) of organic cation transporter 1 (OCT1). The distribution pattern of structural, physiological and molecular features among substrate and non-substrate of OCT1 demonstrates that log P, hydrophilic index, and the number of sulfur atoms are significant contributors for classification of substrates, followed by topological polar surface area (TPSA) and the number of h-bond donors in the molecules.

Table 4.1: Training dataset for machine learning models consisting of known substrates and non-substrates of Organic cation transporter 1 with selected features. 0 – Non-substrate (NS), 1 – Substrate (S), A) Count of sulphur, B) number of aromatic bonds, C) number of h-bond donor, D) number of h-bond acceptors, E) number of rotatable bonds, F) Molecular weight, G) Topological polar surface area, H) Hydrophilic index, I) LogP, J) Unsaturation index

S.No.	SMILE	S/NS	A	B	C	D	E	F	G	H	I	J
1	CNC1CCN(Cc2cc(O)ccc2-c2cccc(-n3c(=O)n(C4CCC(NC(=O)c5cn6cc(F)ccc6n5)CC4)c(=O)c4cc(F)cnc43)c2)CC1	0	0	33	3	11	9	694.48	138.79	-4.263	4.94	5.209
2	COCCN1CCC(Oc2ccccc2-c2cc(C(N)=O)c(NC(N)=O)s2)C1	1	1	11	3	6	9	380.3	119.91	-3.262	2.104	3.807
3	Cc1c(-c2ccnn2-c2ccc(C#N)cc2)nc(CCCN)c(=O)n1-c1cccc(C(F)(F)F)c1	1	0	23	1	7	7	457.31	102.52	-3.664	4.175	4.7
4	CS(=O)(=O)N1CC=C(c2cc(C(N)=O)c(NC(N)=O)s2)CC1	1	2	5	3	5	5	328.29	135.59	-2.432	0.386	3.459
5	COc1ccc(CC(C)NCC(O)c2ccc(O)c(NC=O)c2)cc1	1	0	12	4	5	9	320.21	90.82	-3.529	2.223	3.807

#	SMILES											
6	Clc1cccc(Cl)c1N=C1NCCN1	0	0	6	2	1	1	221.02	36.42	-2.448	2.174	3
7	CNCC(O)COc1ccccc1-c1cc(C(N)=O)c(NC(N)=O)s1	1	1	11	5	6	9	344.26	139.7	-2.972	0.964	3.807
8	N#Cc1ccc(OC2CCNC2)c(-c2cc(C(N)=O)c(NC(N)=O)s2)c1	1	1	11	4	6	6	354.28	143.26	-3.073	1.617	3.907
9	NCC1OB(O)c2c1ccc2OCCCO	0	0	6	3	5	5	220.93	84.94	-2.645	-0.835	2.807
10	CCNC(=O)C1[CH][CH]C(n2cnc3cncnc32)O1	0	0	10	1	6	4	246.16	81.93	-2.683	0.268	3.585
11	CC(Cc1ccc(O)cc1)NCC(O)c1cc(O)cc(O)c1	1	0	12	5	5	6	282.19	92.95	-3.446	2.058	3.7
12	NCCCOc1ccccc1-c1nc(C(N)=O)c(NC(N)=O)s1	1	1	11	4	6	8	318.25	146.35	-2.753	1.127	3.807
13	CC(C)NC(=O)Nc1nc(C(N)=O)c(NC(N)=O)s1	1	1	5	5	5	7	272.20	152.23	-2.012	0.262	3.17
14	CCC1OC(=O)C(C)C(OC2CC(C)(OC)C(O)C(C)O2)C(C)C(OC2OC(C)CC(N(C)C)C2	0	0	0	5	14	7	676.42	180.08	-4.166	1.901	1

	O)C(C)(O)CC(C)CN(C)C(C)C(O)C1(C)O											
15	CNC(=C[N+](=O)[O-])NCCSCc1ccc(CN(C)C)o1	1	1	5	2	7	10	292.23	83.58	-2.719	1.459	3
16	NC(=O)COc1cccc(-c2cc(C(N)=O)c(NC(N)=O)s2)c1	1	1	11	4	5	7	320.24	150.53	-2.753	0.869	3.907
17	CC(C)(c1ccccn1)C(N)c1ccccc1F	0	0	12	1	2	3	227.17	38.91	-3.475	3.198	3.7
18	CN(C)CCCN1c2cccc2CCc2ccc(Cl)cc21	0	0	12	0	2	4	291.67	6.48	-3.851	4.528	3.7
19	NC(=O)Nc1sc(-c2ccccc2OC2CNC2)cc1C(N)=O	1	1	11	4	5	6	316.25	119.47	-2.95	1.355	3.807
20	C[N+]1(C)CCCC(OC(=O)C(O)(c2ccccc2)c2ccccc2)C1	1	0	12	1	3	5	314.23	46.53	-3.901	2.705	3.807
21	CC(C)(C)NCC(O)c1ccc(O)c(CO)c1	1	0	6	4	4	5	218.14	72.72	-3.126	1.306	2.807
22	NC(=O)Nc1sc(-c2ccccc2OCC(O)CNCCO)cc1C(N)=O	1	1	11	6	7	11	372.27	159.93	-2.994	0.326	3.807
23	CNC1(c2ccccc2Cl)CCCCC1=O	0	0	6	1	2	2	221.60	29.1	-3.25	2.898	3
24	N=C(N)NC(=O)c1nc(Cl)c(N)nc1N	1	0	6	5	6	3	221.56	156.79	-1.563	-1.082	3.17

25	NC(=O)Nc1sc(-c2ccccc2OCC(O)CNC2CCC2)cc1C(N)=O	1	1	11	5	6	10	380.3	139.7	-3.262	1.886	3.807
26	C=CCOc1ccccc1OCC(O)CNC(C)C	0	0	6	2	4	9	242.16	50.72	-3.354	1.989	3
27	O=C(NC1CCC(n2c(=O)c3cc(F)cnc3n(-c3cccc(-c4ccc(O)cc4CN4CCNCC4)c3)c2=O)CC1)c1cn2cc(F)ccc2n1	0	0	33	3	11	8	670.46	138.79	-4.166	4.165	5.209
28	NC(=O)Nc1sc(-c2ccccc2OC2CCNC2)nc1C(N)=O	1	1	11	4	6	6	330.26	132.36	-2.866	1.14	3.807
29	CN(C)C(=O)COC(=O)Cc1ccc(OC(=O)c2ccc(NC(=N)N)cc2)cc1	1	0	12	3	6	11	376.24	134.81	-3.35	1.385	4.087
30	CCc1cc2c(cc1CC)CC(NCC(O)c1ccc(O)c3(Cunha-Vaz)c(=O)ccc13)C2	1	0	17	4	4	6	364.27	85.35	-4.02	2.667	4.248
31	CC1(C)CN(CC(=O)N2CCCC2)C(C(=O)Nc2cc(Cl)cc3c4ccncc4(Cunha-Vaz)c32)CO1	0	0	15	2	5	6	441.74	90.56	-3.669	2.928	4.17

32	O=C(Nc1cc(Cl)cc2c3ccncc3(Cunha-Vaz)c21)c1cccnc1	0	0	21	2	3	3	311.66	70.67	-3.344	3.535	4.524
33	C[N+]12CCC(CC1)C(OC(=O)C(O)(c1ccccc1)c1ccccc1)C2	1	0	12	1	3	5	326.24	46.53	-3.977	2.705	3.807
34	CC(C)(C)OC(=O)N1CCC(COc2ccccc2-c2cc(C(N)=O)c(NC(N)=O)s2)C1	0	1	11	3	6	10	432.33	136.98	-3.438	3.64	3.907
35	COc1ccc(CC2NCC(O)C2OC(C)=O)cc1	0	0	6	2	5	5	246.15	67.79	-3.13	0.502	3
36	C[N+]1(C)CCC(Oc2cccc2-c2cc(C(N)=O)c(NC(N)=O)s2)C1	1	1	11	3	4	6	352.29	107.44	-3.254	2.232	3.807
37	NC(=O)Nc1sc(-c2ccccc2OC2CCC(N)CC2)cc1C(N)=O	1	1	11	4	5	6	352.29	133.46	-3.254	2.653	3.807
38	CC(C)(C)OC(=O)N1CCC(COc2ccccc2-c2cc(C(N)=O)c(NC(N)=O)s2)C1	0	1	11	3	6	10	432.33	136.98	-3.438	3.64	3.907
39	CN(C)C(=N)NC(=N)N	1	0	0	4	2	3	118.07	88.99	-1.409	-1.034	1.585
40	CNc1nccc(-c2cc3cc(C(=O)NC(CN(c4ccccc4)c4cccc	1	0	28	4	7	10	482.35	136.13	-3.867	3.601	4.954

	n4)C(=O)O)ccc3(Cunha-Vaz)2)n1											
41	O=c1c2cc(F)cnc2n(C2CCSCC2)c(=O)n1C1CCC(NCc2cn3ccccc3n2)CC1	0	1	21	1	9	5	479.39	86.22	-3.734	3.687	4.585
42	O=C(NCCNCC(O)COc1ccc(O)cc1)N1CCOCC1	1	0	6	4	6	10	314.19	103.29	-3.057	-0.237	3
43	CC1CCN(CC(=O)NC2CCC(n3c(=O)c4cc(F)cnc4n(C4CCSCC4)c3=O)CC2)CC1	0	1	11	1	8	6	481.38	89.23	-3.734	3.097	3.907
44	CCNC(=O)C1OC(n2cnc3c2nc(C(=O)NCNC(=O)Nc2ccncc2)nc3N)C(O)C1O	0	0	16	7	12	12	488.29	231.53	-2.957	-1.89	4.322
45	COCC(=O)OC1(CCN(C)CCCc2nc3ccccc3(Cunha-Vaz)2)CCc2cc(F)ccc2C1C(C)C	0	0	16	1	5	12	457.33	67.45	-4.165	4.789	4.17
46	CC(C)NC(C)COc1ccccc1-c1cc(C(N)=O)c(NC(N)=O)s1	1	1	11	4	5	9	352.29	119.47	-3.254	2.77	3.807

47	Nc1nc(N)c2nc(-c3ccccc3)c(N)nc2n1	1	0	17	3	7	1	242.18	129.62	-2.683	0.833	4.17
48	CC(C)NCC(O)COc1ccc(CC(N)=O)cc1	1	0	6	3	4	8	244.16	84.58	-3.13	0.452	3
49	COc1cc(OC)c(C(=O)CCCN2CCCC2)c(OC)c1	0	0	6	0	5	8	282.19	48	-3.446	2.771	3
50	C[N+]1(C)CCCC(c2cc(-c3c(O)cccc3OCC3CC3)nc3c2COC(=O)N3)C1	1	0	12	2	5	5	394.28	80.68	-3.836	4.259	3.807
51	C[N+]1(C)CCCC(c2cc(-c3c(O)cccc3OCC3CC3)nc(N)c2C#N)C1	1	0	12	2	5	5	364.27	92.16	-3.853	3.651	3.807
52	N#Cc1ccc(-n2nccc2-c2cc(C(N)=O)c(=O)n(-c3cccc(C(F)(F)F)c3)c2CN)cc1	0	0	23	2	7	6	461.29	132.72	-3.517	3.138	4.755
53	NC(=O)Nc1cc(-c2ccccc2O)sc1C(N)=O	1	1	11	4	4	4	266.21	118.44	-2.683	1.71	3.807

54	CN=C(NC#N)NCCSCc1nc(Cunha-Vaz)c1C	1	1	5	3	4	7	236.21	88.89	-2.404	0.115	3
55	NCC1OB(O)c2cccccc21	0	0	6	2	3	1	152.90	55.48	-2.39	-0.596	2.807
56	COc1cc2nc(N3CCN(C(=O)C4CCCO4)CC3)nc(N)c2cc1OC	1	0	11	1	8	5	362.24	103.04	-3.262	1.057	3.7
57	NCCOc1ccc(-c2cc(C(N)=O)c(NC(N)=O)s2)cc1	1	1	11	4	5	7	304.24	133.46	-2.838	1.342	3.807
58	CCN1CC2(OC(=O)c3ccccc3NC(C)=O)CC(OC)C34C5CC6C(OC)C5(O)C(O)(CC6OC)C(CC32)C14	0	0	6	3	9	9	540.35	126.79	-4.108	2.222	3.17
59	OCCN1CCN(CCCN2c3ccccc3Sc3ccc(C(F)(F)F)cc32)CC1	0	1	12	1	5	7	411.32	29.95	-3.598	4.308	3.7
60	CN1CCN(C2=Nc3cc(Cl)ccc3Nc3ccccc32)CC1	0	0	12	1	4	1	307.67	30.87	-3.54	3.723	3.807
61	CCOCCNCC(O)COc1ccccc1-c1cc(C(N)=O)c(NC(N)=O)s1	1	1	11	5	7	13	396.29	148.93	-3.183	1.37	3.807
62	CN1CCC(COc2ccccc2-	1	1	11	3	5	7	352.29	110.68	-3.254	2.335	3.807

	c2cc(C(N)=O)c(NC(N)=O)s2)C1											
63	CC(C)(C)OC(=O)N1CC=C(c2cc(C(N)=O)c(NC(N)=O)s2)CC1	0	1	5	3	5	7	344.26	127.75	-2.972	2.362	3.322
64	Cc1c(-c2ccnn2-c2ccc(C#N)cc2)cc(C(=O)NCCCN(C)C)c(=O)n1-c1cccc(C(F)(F)F)c1	1	0	23	1	7	10	521.35	95.95	-3.858	4.571	4.755
65	CCNCC(O)COc1ccccc1-c1cc(C(N)=O)c(NC(N)=O)s1	1	1	11	5	6	10	356.27	139.7	-3.073	1.354	3.807
66	COc1cc(C(F)(F)F)ccc1-c1cc(C(N)=O)c(NC(N)=O)s1	0	1	11	3	4	6	347.23	107.44	-2.675	3.032	3.807
67	N=C(N)NC(=N)NCCc1ccccc1	1	0	6	5	2	6	190.14	97.78	-2.605	0.237	3.17
68	CC(C)NCC(O)COc1cccc2ccccc21	0	0	11	2	3	6	238.18	41.49	-3.577	2.578	3.585
69	CC(O)(CNC1CC1)COc1ccccc1-c1cc(C(N)=O)c(NC(N)=O)s1	1	1	11	5	6	10	380.3	139.7	-3.262	1.886	3.807
70	COCCN1CCC(Oc2ccccc2-	1	1	11	3	6	9	380.3	119.91	-3.262	2.104	3.807

	c2cc(C(N)=O)c(NC(N)=O)s2)C1										
71	NC(=O)Nc1sc(-c2ccccc2OCC2CCCNC2)cc1C(N)=O	1	1	11	4	5	7	352.29	119.47	-3.254	2.383	3.807
72	C[N+]1(C)CCCC(c2cc(-c3c(O)cccc3OCC3CC3)nc(N)c2C#N)C1	1	0	12	2	5	5	364.27	92.16	-3.853	3.651	3.807
73	CC(C)NCC(O)COc1ccccc1-c1cc(C(N)=O)c(NC(N)=O)s1	1	1	11	5	6	10	368.28	139.7	-3.17	1.742	3.807
74	C[N+]1(C)C2CC(OC(=O)C(O)(c3cccs3)c3cccs3)CC1C1OC12	1	2	10	1	6	5	370.34	59.06	-3.435	2.346	3.585
75	CC(C)N(CCC(C(N)=O)(c1ccccc1)c1ccccn1)C(C)C	1	0	12	1	3	8	310.25	59.22	-3.901	3.362	3.807
76	N=C(NC(=O)c1nc(Cl)c(N)nc1N)Nc1ccccc1	0	0	12	5	6	5	293.63	142.8	-2.51	1.071	3.907
77	CC(C)NCC(O)COc1ccc2(Cunha-Vaz)ccc21	0	0	10	3	3	6	228.16	57.28	-3.243	1.424	3.459
78	CCCCc1oc2ccccc2c1C(=O)c1cc(I)c(OCCN(CC)CC)c(I)c1	0	0	16	0	4	11	616.08	42.68	-3.995	6.936	4.17

79	CN1C2CCC1CC(OC(=O)C(CO)c1ccccc1)C2	1	0	6	1	4	5	266.19	49.77	-3.556	1.931	3
80	CC(N)COc1ccccc1-c1cc(C(N)=O)c(NC(N)=O)s1	1	1	11	4	5	7	316.25	133.46	-2.95	1.731	3.807
81	CC(C)(C)NCC(O)c1c(O)cc(O)c1	1	0	6	4	4	4	206.13	72.72	-3	1.519	2.807
82	NC(=O)Nc1sc(-c2ccc(OC3CCNC3)cc2)cc1C(N)=O	1	1	11	4	5	6	328.26	119.47	-3.057	1.745	3.807
83	CN(C)CCCN1c2cccc2CCc2ccccc21	0	0	12	0	2	4	256.22	6.48	-3.974	3.875	3.7
84	COc1ccc(C2Sc3cccc3N(CCN(C)C)C(=O)C2OC(C)=O)cc1	1	1	12	0	6	7	388.31	59.08	-3.685	3.369	3.907
85	CCNC(=O)C1OC(n2cnc3c2nc(NCCNC(=O)Nc2cc[n+](C)cc2)nc3NC(CC)CC)C(O)C1O	0	0	16	7	11	15	532.35	191.46	-3.397	0.24	4.248
86	NC(=O)Nc1sc(-c2cc(F)ccc2OC2CCNC2)cc1C(N)=O	1	1	11	4	5	6	347.26	119.47	-2.972	1.884	3.807
87	Cc1noc(C)c1S(=O)(=O)N1CC=C(c2cc(C(N)=O)c(NC(N)=O)s2)CC1	0	2	10	3	7	6	406.34	161.62	-2.747	1.42	4

88	COC(=O)C1CC(Oc2ccccc2-c2cc(C(N)=O)c(NC(N)=O)s2)CN1	1	1	11	4	7	8	384.28	145.77	-3.09	1.287	3.907
89	CC(C)NCC(O)COc1ccc(CC(N)=O)cc1	1	0	6	3	4	8	244.16	84.58	-3.13	0.452	3
90	COCC1CC(Oc2ccccc2-c2cc(C(N)=O)c(NC(N)=O)s2)CN1	1	1	11	4	6	8	368.28	128.7	-3.17	1.76	3.807
91	CC(C)NCC(O)COc1cccc1-c1cc(C(N)=O)c(NC(N)=O)s1	1	1	11	5	6	10	368.28	139.7	-3.17	1.742	3.807
92	Cc1c(C(C)N2CCOCC2)cc(C(=O)NCc2ccc(S(C)(=O)=O)cc2)c(=O)n1-c1cccc(C(F)(F)F)c1	0	1	18	1	7	9	547.38	97.71	-3.725	3.891	4.524
93	NC(=O)Nc1sc(-c2ccccc2OC2CNC(CO)C2)cc1C(N)=O	1	1	11	5	6	7	356.27	139.7	-3.073	1.106	3.807
94	CN1CCN(CCCN2c3ccccc3Sc3ccc(Cl)cc32)CC1	0	1	12	0	4	4	349.76	9.72	-3.715	4.58	3.7
95	NCCOc1ccccc1-c1cc(C(N)=O)c(NC(N)=O)s1	1	1	11	4	5	7	304.24	133.46	-2.838	1.342	3.807

96	COc1ccc(-c2cc(C(N)=O)c(NC(N)=O)s2)c(O)c1	1	1	11	4	5	5	294.22	127.67	-2.719	1.719	3.807
97	N#Cc1ccc(-c2ccc(CC(C#N)NC(=O)C3(N)CCOCC3)cc2)cc1	0	0	12	2	5	6	352.26	111.93	-3.777	2.284	4
98	C=CCN(C)CCOc1ccccc1-c1cc(C(N)=O)c(NC(N)=O)s1	0	1	11	3	5	10	352.29	110.68	-3.254	2.501	3.907
99	CC(=O)Nc1cc(Cl)c(O)cc1OCC(C)(O)CNC1CCN(Cc2ccc(Cl)cc2)CC1	0	0	12	4	6	10	465.18	94.06	-3.669	4.041	3.807
100	NC(=O)Nc1sc(-c2ccc(O)cc2O)cc1C(N)=O	1	1	11	5	5	4	282.21	138.67	-2.593	1.416	3.807
101	OCCN1CCN(CCCN2c3ccccc3Sc3ccc(Cl)cc32)CC1	1	1	12	1	5	6	377.77	29.95	-3.698	3.943	3.7
102	NC(=O)Nc1sc(-c2cc(Cl)ccc2OC2CCNC2)cc1C(N)=O	1	1	11	4	5	6	363.72	119.47	-2.972	2.399	3.807
103	COc1ccc(CC2NCC(O)C2OC(C)=O)cc1	0	0	6	2	5	5	246.15	67.79	-3.13	0.502	3

104	C[N+]1(C)C2CC(OC(=O)C(O)(c3cccs3)c3cccs3)CC1C1OC12	1	2	10	1	6	5	370.34	59.06	-3.435	2.346	3.585
105	CN1C2CCC1CC(OC(=O)C(CO)c1ccccc1)C2	1	0	6	1	4	5	266.19	49.77	-3.556	1.931	3
106	NC(=O)Nc1sc(-c2ccccc2OCC(O)CNC2CC2)cc1C(N)=O	1	1	11	5	6	10	368.28	139.7	-3.17	1.496	3.807
107	CCNC(=O)C1OC(n2cnc3c2nc(C(=O)NCNC(=O)Nc2cc[n+](C)cc2)nc3N)C(O)C1O	1	0	16	7	11	12	500.30	222.52	-3.038	-2.46	4.322
108	OCc1cc(C(O)CNCCCCCCOCCCCc2ccccc2)ccc1O	0	0	12	4	5	16	378.27	81.95	-4.089	4.107	3.7
109	NC(=O)COc1ccc(-c2cc(C(N)=O)c(NC(N)=O)s2)cc1	1	1	11	4	5	7	320.24	150.53	-2.753	0.869	3.907
110	Cc1ccc(O)c(C(=O)NC2CCC(NC(=O)c3cc(F)cnc3Oc3cccc(-c4ccc(CN5CC(C)NC(C)C5)cc4CN4CCOCC4)c3)CC2)c1	0	0	24	4	9	13	711.51	128.29	-4.563	6.179	4.755

111	CC(Oc1ccccc1-c1cc(C(N)=O)c(NC(N)=O)s1)C(N)=O	1	1	11	4	5	7	332.25	150.53	-2.866	1.257	3.907
112	CN1N=C2CCN(C(=O)C(COCc3ccccc3)NC(=O)C(C)(C)N)CC2(Cc2ccccc2)C1=O	0	0	12	2	6	11	470.33	117.33	-3.942	1.715	4.087
113	COc1cc2nc(N3CCN(C(=O)c4ccco4)CC3)nc(N)c2cc1OC	0	0	16	1	8	5	362.24	106.95	-3.262	1.785	4.17
114	O=C1Nc2nc(-c3c(O)cccc3OCC3CC3)cc(C3CCCNC3)c2CO1	0	0	12	3	6	5	370.25	92.71	-3.685	3.772	3.807
115	CCNC(=O)C1OC(n2cnc3c2nc(NCCNC(=O)Nc2cc[n+](C)cc2)nc3N)C(O)C1O	0	0	16	7	11	11	472.29	205.45	-3.016	-1.778	4.248
116	CNC(=C[N+](=O)[O-])NCCSCc1csc(CN(C)C)n1	1	2	5	2	8	10	310.29	83.33	-2.51	1.322	3
117	CCNC(=O)C1OC(n2cnc3c2nc(NCCNC(=O)Nc2ccncc2)nc3NC(CC)CC)C(O)C1O	0	0	16	7	12	15	520.34	200.47	-3.326	0.811	4.248
118	NC(=O)Nc1sc(-c2ccccc2OC2CCNC2)cc1C(N)=O	1	1	11	4	5	6	328.26	119.47	-3.057	1.745	3.807

119	NC(=O)Nc1sc(-c2ccccc2OC2CCCNCC2)cc1C(N)=O	1	1	11	4	5	6	352.29	119.47	-3.254	2.526	3.807
120	C#CCN(C)C(C)Cc1ccccc1	0	0	6	0	1	4	170.15	3.24	-3.535	2.183	3
121	Cc1ccc(NC(=O)c2ccc(CN3CCN(C)CC3)c2)cc1Nc1nccc(-c2cccnc2)n1	0	0	24	2	7	8	462.36	86.28	-4.083	4.59	4.7
122	C[N+](C)(C)CC(O)COc1ccccc1-c1cc(C(N)=O)c(NC(N)=O)s1	1	1	11	4	5	9	368.28	127.67	-3.17	1.45	3.807
123	COc1cc(Cc2cnc(N)nc2N)cc(OC)c1OC	1	0	12	2	7	5	272.17	105.51	-2.928	1.258	3.7
124	CCOC(=O)Nc1nc(C(N)=O)c(NC(N)=O)s1	1	1	5	4	6	7	262.18	149.43	-1.853	0.301	3.17
125	CCS(=O)(=O)c1ccc(-c2cc(C(N)=O)c(NC(N)=O)s2)cc1	1	2	11	3	5	6	338.30	132.35	-2.753	1.798	4
126	CCNC(=O)C1OC(n2cnc3c2nc(NCCNC(=O)Nc2ccncc2)nc3N)C(O)C1O	0	0	16	7	12	11	460.28	214.46	-2.931	-1.208	4.248
127	CC(C)[N+]1(C)C2CCC1CC(OC(=O)C(CO)c1ccccc1)C2	1	0	6	1	3	6	302.22	46.53	-3.821	2.854	3

128	CCN(CC)CCNC(=O)c1ccc(N)cc1	1	0	6	2	3	7	214.16	58.36	-3.126	1.34	3
129	NC(=O)Nc1sc(-c2ccccc2OCC2CCNC2)cc1C(N)=O	1	1	11	4	5	7	340.27	119.47	-3.158	1.993	3.807
130	CCCNCC(O)COc1ccccc1C(=O)CCc1ccccc1	0	0	12	2	4	11	314.23	58.56	-3.901	3.241	3.807
131	NC(=O)Nc1sc(-c2ccccc2OCC(O)CNC2CC2)cc1C(N)=O	1	1	11	5	6	10	368.28	139.7	-3.17	1.496	3.807
132	Cc1nc(C(=O)NC2CCC(n3c(=O)c4cc(F)cnc4n(-c4cccc(-c5ccc(CCCN6CCNCC6)cc5)c4)c3=O)CC2)cs1	0	1	28	2	10	10	641.51	114.15	-4.24	4.87	5
133	N#Cc1c(N)nc(-c2c(O)cccc2OCC2CC2)cc1C1CCCNC1	0	0	12	3	6	5	340.25	104.19	-3.698	3.164	3.807
134	CCN(CC)C(=O)c1ccc(-c2cc(C(N)=O)c(NC(N)=O)s2)c(OC)c1	1	1	11	3	5	9	368.28	127.75	-3.17	2.495	3.907
135	NC(=O)Nc1sc(-c2ccccc2OC2CNC(CF)C2)cc1C(N)=O	1	1	11	4	5	7	359.27	119.47	-3.073	2.083	3.807

136	COC(=O)c1ccc(-c2cc(C(N)=O)c(NC(N)=O)s2)c(O)c1	1	1	11	4	6	6	322.23	144.74	-2.753	1.497	3.907
137	Cc1cc(C(=O)NC2CCC(NC(=O)c3cc(F)cnc3Oc3cccc(-c4ccc(CCCN5CC(C)NC(C)C5)cc4)c3)CC2)nn1C	0	0	23	3	8	13	633.47	113.41	-4.402	5.808	4.7
138	CNCCCN1c2ccccc2CCc2ccccc21	0	0	12	1	2	4	244.21	15.27	-3.89	3.533	3.7
139	COc1ccccc1CNCCCCCCNCCCCCCCCCNCCCCCNCc1ccccc1OC	0	0	12	4	6	29	520.42	66.58	-4.622	7.224	3.7
140	Nc1ccc(S(=O)(=O)Nc2ccnn2-c2ccccc2)cc1	0	1	17	2	5	4	300.25	90.01	-3.041	2.255	4.322
141	CCN(CC)CCNC(=O)c1cc(Cl)c(N)cc1OC	1	0	6	2	4	8	277.62	67.59	-3.025	2.002	3
142	CCCCN1CCCCC1C(=O)Nc1c(C)cccc1C	0	0	6	1	2	6	260.21	32.34	-3.765	3.897	3
143	Cc1c(-c2ccnn2-c2ccc(C#N)cc2)cc(C(=O)NCCC[N+](C)(C)C)c(=O)n1-c1cccc(C(F)(F)F)c1	0	0	23	1	6	10	533.36	92.71	-3.92	4.715	4.755

144	CN(C)CCC=C1c2ccc cc2Sc2ccc(Cl)cc21	0	1	12	0	2	3	297.72	3.24	-3.765	5.188	3.807
145	NC(=O)COc1ccc(-c2cc(C(N)=O)c(NC(N)=O)s2)c(OCc2ccc cc2)c1	1	1	17	4	6	10	420.32	159.76	-3.356	2.448	4.392
146	NC(=O)c1cnc(N)c2c c(-c3ccccc3OC3CCNC 3)sc21	1	1	16	3	6	4	336.29	103.26	-3.344	2.385	4.17
147	COc1ccc(CC(N)C(=O)NC2C(O)C(n3cnc 4c3ncnc4N(C)C)OC 2CO)cc1	0	0	16	4	11	9	442.28	160.88	-3.292	-0.794	4.17
148	N#Cc1ccc(-n2nccc2-c2ccc(=O)n(-c3cccc(C(F)(F)F)c3) c2CN)cc1	0	0	23	1	6	5	419.28	89.63	-3.594	4.039	4.7
149	CC12CC3CC(C)(C1) CC(N)(C3)C2	0	0	0	1	1	0	158.13	26.02	-3.416	2.694	0
150	CCC(C)NCC(O)COc1 ccccc1-c1cc(C(N)=O)c(NC(N)=O)s1	1	1	11	5	6	11	380.3	139.7	-3.262	2.132	3.807
151	NC(=O)Nc1sc(-c2ccccc2OC2CCNC C2)cc1C(N)=O	1	1	11	4	5	6	340.27	119.47	-3.158	2.135	3.807

152	COc1ccc(C(NCc2ccccc2)C(=O)NC2CCC(n3c(=O)c4cc(F)cnc4n(C4CCSCC4)c3=O)CC2)cc1	0	1	23	2	9	10	593.47	107.25	-4.149	4.905	4.755
153	OC1CCCCC1N1CCC(c2ccccc2)CC1	0	0	6	1	2	2	234.19	23.47	-3.801	3.17	2.807
154	CNc1nccc(-c2cc3cc(C(=O)NC(CN(c4ccccc4)c4cccn4)C(=O)OC)ccc3(Cunha-Vaz)2)n1	0	0	28	3	8	11	494.36	125.13	-3.93	3.689	4.954
155	NC(=O)Nc1sc(-c2cc(F)cc(Br)c2OC2CCNC2)cc1C(N)=O	1	1	11	4	5	6	427.17	119.47	-2.893	2.647	3.807
156	CC[N+](C)(CC)CCOC(=O)C(O)(c1ccccc1)C1CCCCC1	1	0	6	1	3	9	314.23	46.53	-3.901	3.484	3
157	C=CC1CN2CCC1CC2C(O)c1ccnc2ccc(OC)cc21	0	0	11	1	4	4	300.23	45.59	-3.821	3.173	3.7
158	c1cnc2cc3c(cc2n1)C1CC3CNC1	1	0	11	1	3	0	198.16	37.81	-3.25	1.804	3.585
159	NCCOc1ccccc1-c1nc(C(N)=O)c(NC(N)=O)s1	1	1	11	4	6	7	306.24	146.35	-2.635	0.737	3.807

160	NC(=O)Nc1sc(-c2cccc(OC3CCNC3)c2)cc1C(N)=O	1	1	11	4	5	6	328.26	119.47	-3.057	1.745	3.807
161	CC(NC(C)(C)C)C(=O)c1cccc(Cl)c1	0	0	6	1	2	4	221.60	29.1	-3.25	3.299	3
162	CC(C)(N)C(=O)NC(COCc1ccccc1)C(=O)N1CCC2(CN(S(C)(=O)=O)c3ccccc32)CC1	0	1	12	2	6	10	492.38	122.04	-3.801	1.765	4.087
163	NC(=O)Nc1sc(-c2ccccc2OCC(O)CNCCO)cc1C(N)=O	1	1	11	6	7	11	372.27	159.93	-2.994	0.326	3.807
164	N=C(NCc1ccccc1)NC(=O)c1nc(Cl)c(N)nc1N	1	0	12	5	6	6	305.64	142.8	-2.635	0.749	3.907
165	CN1CCc2cccc3c2C1Cc1ccc(O)c(O)c1-3	0	0	12	2	3	0	250.19	43.7	-3.674	2.85	3.7
166	NC(=O)Nc1sc(-c2ccc(Cl)cc2)cc1C(N)=O	0	1	11	3	3	4	285.67	98.21	-2.683	2.658	3.807
167	CN1C2CC(OC(=O)C(CO)c3ccccc3)CC1C1OC12	0	0	6	1	5	5	282.19	62.3	-3.446	0.918	3
168	CCC(NC(C)C)C(O)c1ccc(O)c2(Cunha-Vaz)c(=O)ccc12	1	0	11	4	4	5	268.18	85.35	-3.347	1.562	3.7

169	CC1(C)Cc2c(cccc2CN2CCC3(CC2)CCN(C(=O)c2ccnc(N)c2)CC3)O1	0	0	12	1	5	4	400.31	71.69	-4.063	3.896	3.807
170	Cc1c(-c2ccnn2-c2ccc(C#N)cc2)cc(C(=O)NCCCNC(C)C)c(=O)n1-c1cccc(C(F)(F)F)c1	0	0	23	2	7	11	533.36	104.74	-3.92	5.007	4.755
171	O=C(CCCN1CCC(O)(c2ccc(Cl)cc2)CC1)c1ccc(F)cc1	0	0	12	1	3	6	352.68	40.54	-3.797	4.426	3.807
172	CC(=N)NC(CNC(=O)c1nc(Cl)c(N)nc1N)Cc1ccccc1C	1	0	12	5	6	8	353.68	142.8	-3.073	1.531	3.907
173	NC(=O)Nc1sc(-c2ccccc2OCC2CCNC2)cc1C(N)=O	1	1	11	4	5	7	340.27	119.47	-3.158	1.993	3.807
174	CC1CN(C2CC(N=[N+]=(Richa and Yazbek))C(CO)O2)C(=O)[N]C1=O	0	0	0	1	5	3	254.14	129.7	-2.236	-0.025	2.322
175	CC(C)NCC(O)COc1cc(CC(N)=O)cc1	1	0	6	3	4	8	244.16	84.58	-3.13	0.452	3
176	Cc1cccc(-c2cc(C(N)=O)c(NC(N)=O)s2)c1OC1CCNC1	1	1	11	4	5	6	340.27	119.47	-3.158	2.054	3.807

177	CNCCOc1ccccc1-c1cc(C(N)=O)c(NC(N)=O)s1	1	1	11	4	5	8	316.25	119.47	-2.95	1.603	3.807
178	CN(C)C(=O)C1CC(Oc2ccccc2-c2cc(C(N)=O)c(NC(N)=O)s2)CN1	1	1	11	4	6	8	394.30	139.78	-3.183	1.202	3.907
179	CCS(=O)(=O)N1CC=C(c2cc(C(N)=O)c(NC(N)=O)s2)CC1	1	2	5	3	5	6	340.30	135.59	-2.557	0.776	3.459
180	CN(C)C(=O)C(CCN1CCC(O)(c2ccc(Cl)cc2)CC1)(c1ccccc1)c1ccccc1	0	0	18	1	3	8	443.78	43.78	-4.339	5.088	4.322
181	CCC1(CS(=O)(=O)N2CC=C(c3cc(C(N)=O)c(NC(N)=O)s3)CC2)NC(=O)NC1=O	0	2	5	5	7	8	448.35	193.79	-2.717	-0.255	3.7
182	Cc1cccc(-c2cc(C(N)=O)c(NC(N)=O)s2)c1OC1CCNC1	1	1	11	4	5	6	340.27	119.47	-3.158	2.054	3.807
183	O=C(NCCNCC(O)COc1ccc(O)cc1)N1CCOCC1	1	0	6	4	6	10	314.19	103.29	-3.057	-0.237	3
184	CNC(=O)c1nc(-c2ccnn2-c2ccc(C#N)cc2)c(C)	0	0	23	1	7	6	461.29	105.6	-3.517	3.644	4.755

	n(-c2cccc(C(F)(F)F)c2)c1=O										
185	NCC(O)COc1ccccc1-c1cc(C(N)=O)c(NC(N)=O)s1	1	1	11	5	6	8	332.25	153.69	-2.866	0.703	3.807
186	CN(C)C(CN1c2ccccc2Sc2ccccc21)c1ccccc1	0	1	18	0	3	4	324.32	6.48	-4.087	5.592	4.248
187	C[N+]1(C)CCC(OC(=O)C(O)(c2ccccc2)C2CCCC2)C1	1	0	6	1	3	5	290.21	46.53	-3.737	2.456	3
188	NC(=O)Nc1sc(C2=CCCCC2)cc1C(N)=O	0	1	5	3	3	4	250.21	98.21	-2.78	2.295	3.17
189	CNS(=O)(=O)Cc1ccc2(Cunha-Vaz)cc(CCN(C)C)c2c1	1	1	10	2	3	6	274.24	65.2	-3.025	0.839	3.7
190	COc1ccc(CCN(C)CCC(C#N)(c2ccc(OC)c(OC)c2)C(C)C)cc1OC	0	0	12	0	6	13	416.30	63.95	-4.127	5.093	3.807
191	NC(=O)Nc1sc(-c2ccccc2OC2CCNC2)cc1C(N)=O	1	1	11	4	5	6	328.26	119.47	-3.057	1.745	3.807

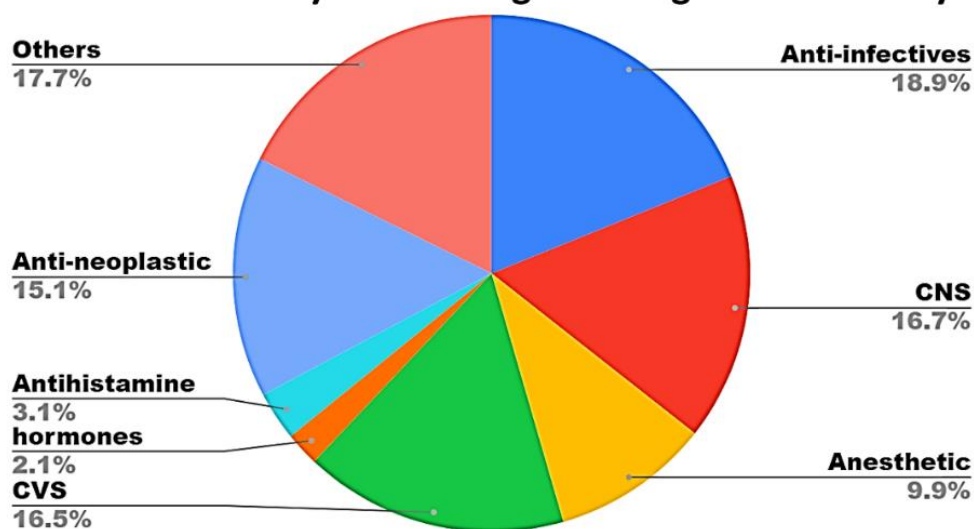|											
192	COc1cc2ncnc(Nc3c cc(F)c(Cl)c3)c2cc1O CCCN1CCOCC1	0	0	17	1	7	8	422.71	68.74	-3.516	4.276	4.17
193	CC1CN(C(=O)CN2C C(C)(C)OCC2C(=O) Nc2cc(Cl)cc3c4ccnc c4(Cunha-Vaz)c32)CC(C)O1	0	0	15	2	6	6	481.77	99.79	-3.734	2.941	4.17
194	NCCCOc1ccccc1-c1cc(C(N)=O)c(NC(N)=O)s1	1	1	11	4	5	8	316.25	133.46	-2.95	1.732	3.807

Figure 4.2: Therapeutic classification of systemic drugs causing ocular toxicity. The screening dataset consists of 424 systemic drugs causing ocular toxicity which were categorized into different categories based on their therapeutic use.

4.3.2 Machine learning model performance

A supervised machine learning model was developed to predict whether the systemic drugs causing ocular toxicity are a substrate or a non-substrate for hOCT1 based on various features. A total of six supervised learning models were implemented initially to compare their accuracy. Since the training set was small and numeric features were used, there was a possibility of overfitting, which was reduced by using a particular class of Decision trees (C4.5) as one of the base models. All six models were trained with k=5 as k-fold cross-validation.

To overcome the limitations of the individual models, we applied a consensus model based on the concept of stacking and blending, where the predictions from the test dataset of the individual model are the training data for the logistic regression model development. Compared to base models, the weighted consensus approach consistently achieved more favorable values across all evaluation metrics, indicating overall improvements in inaccuracy and stability (**Table 4.2 a-b**). ANN also classified the drugs as substrate (indicated by 1) and non-substrate (indicated by 0) of hOCT1. The model ran with 100 epochs and presented an accuracy of 80% to 85%. Predictions from the supervised and ANN model classified the drugs as substrate or non-substrate of hOCT1.

Table 4.2: Evaluation metrics of supervised learning model and artificial neural network. The predictive models were obtained by running the parameters over an artificial neural network (ANN) and various supervised machine learning algorithms such as k-Nearest neighbors (KNN), Random Forest, Decision tree C4.5, Naive Bayes, XG Boost, and Support Vector Machines (SVM). Additionally, k-fold cross-validation (k=5) was applied to accurately estimate the model's predictive performance. Table 4.2 (a) represents evaluation metrics of different folds as F1, F2, F3, F4, and F5. Table 4.2 (b) represents the overall evaluation metrics of the supervised learning model and ANN.

4.2 a)

Accuracy						
Models	**F1**	**F2**	**F3**	**F4**	**F5**	**Average**
KNN	0.69	0.85	0.92	0.79	0.74	0.80
Random Forest	0.74	0.82	0.95	0.92	0.79	0.85
Decision Tree	0.62	0.79	0.79	0.82	0.74	0.75
Naïve Bayes	0.69	0.85	0.95	0.77	0.74	0.80
XG Boost	0.74	0.85	0.92	0.82	0.82	0.83
SVM	0.56	0.82	0.87	0.69	0.74	0.74
Precision						
KNN	0.75	0.83	0.91	0.79	0.77	0.81
Random Forest	0.77	0.83	0.92	0.88	0.82	0.84
Decision Tree	0.67	0.75	0.94	0.78	0.75	0.78
Naïve Bayes	0.75	0.83	0.95	0.78	0.75	0.81
XG Boost	0.77	0.86	0.88	0.89	0.86	0.85
SVM	0.60	0.83	0.84	0.71	0.77	0.75
Recall						
KNN	0.68	0.91	0.95	0.86	0.77	0.84
Random Forest	0.77	0.86	1.00	1.00	0.82	0.89
Decision Tree	0.64	0.95	0.68	0.95	0.82	0.81
Naïve Bayes	0.68	0.91	0.95	0.82	0.82	0.84
XG Boost	0.77	0.86	1.00	0.77	0.82	0.85
SVM	0.68	0.86	0.95	0.77	0.77	0.81

F1						
KNN	0.71	0.87	0.93	0.83	0.77	0.82
Random Forest	0.77	0.84	0.96	0.94	0.82	0.87
Decision Tree	0.65	0.84	0.79	0.86	0.78	0.78
Naïve Bayes	0.71	0.87	0.95	0.80	0.78	0.82
XG Boost	0.77	0.86	0.94	0.83	0.84	0.85
SVM	0.64	0.84	0.89	0.74	0.77	0.78

4.2 b)

Metrics	Supervised learning (Average values)	ANN
Accuracy	0.79	0.80
Precision	0.81	0.85
Recall	0.84	0.80
F1 Score	0.82	0.82

4.3.3 Machine learning model predictions and characteristics of predicted OCT1 substrates

A screening dataset of systemic drugs causing ocular toxicity was screened through the developed logistic regression model and ANN model to predict their interactions with OCT1. Out of 424 molecules screened, 125 drug molecules were found to be substrates for OCT1. Since we developed the logistic regression and ANN models, predicted substrates (overlapped) from both models could be the potential substrates of OCT1. Interestingly, these drugs were not reported earlier (n=125) for any interaction with OCT1 (**Table 4.3**) and are found to be the substrate of OCT1 from our analysis.

Table 4.3: Predictions from machine learning models, indicating novel interactions between drug and OCT1 transporter, not known earlier in the literature. The developed machine learning model with an accuracy of around 80%, predicted the novel substrates of OCT1 (n=125) from our screening database of systemic drugs causing ocular toxicity (n=424). The drugs predicted as substrates from both logistic regression and artificial neural network model, are listed here.

S.No.	Names	Simplified Molecular Input Line Entry System (SMILES)
1	Diethyl carbamazine citrate	CCN(CC)C(=O)N1CCN(C)CC1
2	Amoxicillin	CC1(C)SC2C(NC(=O)C(N)c3ccc(O)cc3)C(=O)N2C1C(=O)O
3	Ampicillin	CC1(C)SC2C(NC(=O)C(N)c3ccccc3)C(=O)N2C1C(=O)O
4	Nafcillin sodium	CCOc1ccc2ccccc2c1C(=O)NC1C(=O)N2C1SC(C)(C)C2C(=O)O
5	Ticarcillin monosodium	CC1(C)SC2C(NC(=O)C(C(=O)O)c3ccsc3)C(=O)N2C1C(=O)O
6	Clindamycin	CCCC1CC(C(=O)NC(C(C)Cl)C2OC(SC)C(O)C(O)C2O)N(C)C1
7	Cefadroxil	CC1=C(C(=O)O)N2C(=O)C(NC(=O)C(N)c3ccc(O)cc3)C2SC1
8	Cefotoxin sodium	CON=C(C(=O)NC1C(=O)N2C(C(=O)O)=C(COC(N)=O)CSC12)c1ccc o1
9	Ciprofloxacin	O=C(O)c1cn(C2CC2)c2cc(N3CCNCC3)c(F)cc2c1=O
10	Tosufloxacin	NC1CCN(c2nc3c(cc2F)c(=O)c(C(=O)O)cn3-c2ccc(F)cc2F)C1
11	Minocycline hydrochloride	CN(C)c1ccc(O)c2c1CC1CC3C(N(C)C)C(=O)C(C(N)=O)=C(O)C3(O)C (=O)C1=C2O
12	Linezoid	CC(=O)NCC1CN(c2ccc(N3CCOCC3)c(F)c2)C(=O)O1
13	Nalidixic acid	CCn1cc(C(=O)O)c(=O)c2ccc(C)nc21
14	Nitrofurantoin	O=C1CN(N=Cc2ccc([N+](=O)[O-])o2)C(=O)N1
15	Sulfacetamide sodium	CC(=O)NS(=O)(=O)c1ccc(N)cc1
16	Sulfadiazine	Nc1ccc(S(=O)(=O)Nc2ncccn2)cc1
17	Sulfafurazole	Cc1noc(NS(=O)(=O)c2ccc(N)cc2)c1C
18	Sulfamethoxazole	Cc1cc(NS(=O)(=O)c2ccc(N)cc2)no1
19	Sulfamethizole	Cc1nnc(NS(=O)(=O)c2ccc(N)cc2)s1
20	Sulfanilamide	Nc1ccc(S(N)(=O)=O)cc1

21	Sulfasalazine	O=C(O)c1cc(N=Nc2ccc(S(=O)(=O)Nc3ccccn3)cc2)ccc1O
22	Sulfathiazole	Nc1ccc(S(=O)(=O)Nc2nccs2)cc1
23	Dapsone	Nc1ccc(S(=O)(=O)c2ccc(N)cc2)cc1
24	Isoniazid	NNC(=O)c1ccncc1
25	Thioacetazone	CC(=O)Nc1ccc(C=NNC(N)=S)cc1
26	Gabapentin	NCC1(CC(=O)O)CCCCC1
27	Pregabalin	CC(C)CC(CN)CC(=O)O
28	Vigabatrin	C=CC(N)CCC(=O)O
29	Clorazepate dipotassium	O=C(O)C1N=C(c2ccccc2)c2cc(Cl)ccc2NC1=O
30	Meprobamate	CCCC(C)(COC(N)=O)COC(N)=O
31	Carisoprodol	CCCC(C)(COC(N)=O)COC(=O)NC(C)C
32	Venlafaxine hydro-chloride	COc1ccc(C(CN(C)C)C2(O)CCCCC2)cc1
33	Isocarboxazid	Cc1cc(C(=O)NNCc2ccccc2)no1
34	Methylphenidate hydrochloride	COC(=O)C(c1ccccc1)C1CCCCN1
35	Quetiapine fumarate	OCCOCCN1CCN(C2=Nc3ccccc3Sc3ccccc32)CC1
36	Psilocybin.	CN(C)CCc1c(Cunha-Vaz)c2cccc(OP(=O)(O)O)c12
37	Lysergic acid diethylamide (LSD)	CCN(CC)C(=O)C1C=C2c3cccc4(Cunha-Vaz)cc(c43)CC2N(C)C1
38	Amobarbital	CCC1(CCC(C)C)C(=O)NC(=O)NC1=O
39	Butabarbital sodium	CCC(C)C1(CC)C(=O)NC(=O)NC1=O
40	Butalbital	C=CCC1(CC(C)C)C(=O)NC(=O)NC1=O
41	Pentobarbital sodium	CCCC(C)C1(CC)C(=O)NC(=O)NC1=O
42	Phenobarbital	CCC1(c2ccccc2)C(=O)NC(=O)NC1=O
43	Primidone	CCC1(c2ccccc2)C(=O)NCNC1=O
44	Secobarbital sodium	C=CCC1(C(C)CCC)C(=O)NC(=O)NC1=O
45	Allopurinol sodium	O=c1(Cunha-Vaz)cnc2(Cunha-Vaz)ncc21
46	Piroxicam	CN1C(C(=O)Nc2ccccn2)=C(O)c2ccccc2S1(=O)=O
47	Diacetylmorphine	CC(=O)Oc1ccc2c3c1OC1C(OC(C)=O)C=CC4C(C2)N(C)CCC314

48	Meperidine hydrochloride	CCOC(=O)C1(c2ccccc2)CCN(C)CC1
49	Succinylcholine chloride (suxamethonium chloride)	C[N+](C)(C)CCOC(=O)CCC(=O)OCC[N+](C)(C)C
50	Chloroprocaine hydrochloride	CCN(CC)CCOC(=O)c1ccc(N)cc1Cl
51	Prilocaine	CCCNC(C)C(=O)Nc1ccccc1C
52	Procaine hydrochloride	CCN(CC)CCOC(=O)c1ccc(N)cc1
53	Tolterodinetartrate	O=C(O)CCCSSCCCC(=O)O
54	Bethanechol chloride	CC(C[N+](C)(C)C)OC(N)=O
55	Ergometrine maleate (ergonovine)	CC(CO)NC(=O)C1C=C2c3cccc4(Cunha-Vaz)cc(c43)CC2N(C)C1
56	Methylergometrine (methylergonovine maleate)	CCC(CO)NC(=O)C1C=C2c3cccc4(Cunha-Vaz)cc(c43)CC2N(C)C1
57	Nitroglycerin	O=[N+]([O-])OCC(CO[N+](=O)[O-])O[N+](=O)[O-]
58	Methacholine chloride	CC(=O)OC(C)C[N+](C)(C)C
59	Labetalol hydrochloride	CC(CCc1ccccc1)NCC(O)c1ccc(O)c(C(N)=O)c1
60	Captopril	CC(CS)C(=O)N1CCCC1C(=O)O
61	Enalapril	CCOC(=O)C(CCc1ccccc1)NC(C)C(=O)N1CCCC1C(=O)O
62	Guanethidine monosulfate.	NC(N)=NCCN1CCCCCC1
63	Chlorothiazide	NS(=O)(=O)c1cc2c(cc1Cl)NC=NS2(=O)=O
64	Hydrochlorothiazide	NS(=O)(=O)c1cc2c(cc1Cl)NCNS2(=O)=O
65	Indapamide	CC1Cc2ccccc2N1NC(=O)c1ccc(Cl)c(S(N)(=O)=O)c1
66	Methyclothiazide	CN1C(CCl)Nc2cc(Cl)c(S(N)(=O)=O)cc2S1(=O)=O
67	Furosemide	NS(=O)(=O)c1cc(C(=O)O)c(NCc2ccco2)cc1Cl
68	Methylprednisolone	CC1CC2C3CCC(O)(C(=O)CO)C3(C)CC(O)C2C2(C)C=CC(=O)C=C12
69	Prednisolone	CC12CC(O)C3C(CCC4=CC(=O)C=CC43C)C1CCC2(O)C(=O)CO
70	Prednisone	CC12CC(=O)C3C(CCC4=CC(=O)C=CC43C)C1CCC2(O)C(=O)CO
71	Tranexamic acid	NCC1CCC(C(=O)O)CC1

72	Acetohexamide	CC(=O)c1ccc(S(=O)(=O)NC(=O)NC2CCCCC2)cc1
73	Chlorpropamide	CCCNC(=O)NS(=O)(=O)c1ccc(Cl)cc1
74	Glipizide	Cc1cnc(C(=O)NCCc2ccc(S(=O)(=O)NC(=O)NC3CCCCC3)cc2)cn1
75	Tolazamide	Cc1ccc(S(=O)(=O)NC(=O)NN2CCCCCC2)cc1
76	Tolbutamide	CCCCNC(=O)NS(=O)(=O)c1ccc(C)cc1
77	Rosiglitazone maleate	CN(CCOc1ccc(CC2SC(=O)NC2=O)cc1)c1ccccn1
78	Biperiden	OC(CCN1CCCCC1)(c1ccccc1)C1CC2C=CC1C2
79	Procyclidine hydrochloride	OC(CCN1CCCC1)(c1ccccc1)C1CCCCC1
80	Dantrolene sodium	O=C1CN(N=Cc2ccc(-c3ccc([N+](=O)[O-])cc3)o2)C(=O)N1
81	Alendronate sodium	NCCCC(O)(P(=O)(O)O)P(=O)(O)O
82	Etidronate disodium	CC(O)(P(=O)(O)O)P(=O)(O)O
83	Ibandronate sodium	CCCCCN(C)CCC(O)(P(=O)(O)O)P(=O)(O)O
84	Pamidronate disodium	NCCC(O)(P(=O)(O)O)P(=O)(O)O
85	Risedronate sodium	O=P(O)(O)C(O)(Cc1cccnc1)P(=O)(O)O
86	Zoledronic acid	O=P(O)(O)C(O)(Cn1ccnc1)P(=O)(O)O
87	Penicillamine	CC(C)(S)C(N)C(=O)O
88	Azathioprine	Cn1cnc([N+](=O)[O-])c1Sc1ncnc2nc(Cunha-Vaz)c21
89	Tretinoin	CCC(C)(OO)OOC(C)(CC)OO
90	Abacavir	Nc1nc2c(ncn2C2C=CC(CO)C2)c(NC2CC2)n1
91	Didanosine	O=c1(Cunha-Vaz)cnc2c1ncn2C1CCC(CO)O1
92	Emtricitabine	Nc1nc(=O)n(C2CSC(CO)O2)cc1F
93	Stavudine	Cc1cn(C2C=CC(CO)O2)c(=O)(Cunha-Vaz)c1=O
94	Foscarnet sodium	O=C(O)P(=O)(O)O
95	Emedastine difumarate	CCOCCn1c2ccccc2nc1N1CCCN(C)CC1
96	Apraclonidine hydrochloride	Nc1cc(Cl)c(NC2=NCCN2)c(Cl)c1
97	Betaxolol hydrochloride	CC(C)NCC(O)COc1ccc(CCOCC2CC2)cc1
98	Levobunolol hydrochloride	CC(C)(C)NCC(O)COc1cccc2c1CCCC2=O

99	Timolol maleate	CC(C)(C)NCC(O)COc1nsnc1N1CCOCC1
100	Dorzolamide hydrochloride	CCNC1CC(C)S(=O)(=O)c2sc(S(N)(=O)=O)cc21
101	Brinzolamide	CCNC1CN(CCCOC)S(=O)(=O)c2sc(S(N)(=O)=O)cc21
102	Carteolol hydrochloride	CC(C)(C)NCC(O)COc1cccc2c1CCC(=O)N2
103	Metipranolol	CC(=O)Oc1c(C)cc(OCC(O)CNC(C)C)c(C)c1C
104	Cidofovir	Nc1ccn(CC(CO)OCP(=O)(O)O)c(=O)n1
105	Vidarabine	Nc1ncnc2c1ncn2C1OC(CO)C(O)C1O
106	Trifluridine	O=c1(Cunha-Vaz)c(=O)n(C2CC(O)C(CO)O2)cc1C(F)(F)F
107	Idoxuridine (IDU)	O=c1(Cunha-Vaz)c(=O)n(C2CC(O)C(CO)O2)cc1I
108	Acetazolamide	CC(=O)Nc1nnc(S(N)(=O)=O)s1
109	Methazolamide	CC(=O)N=c1sc(S(N)(=O)=O)nn1C
110	Cyclopentolate hydrochloride	CN(C)CCOC(=O)C(c1ccccc1)C1(O)CCCC1
111	Tropicamide	CCN(Cc1ccncc1)C(=O)C(CO)c1ccccc1
112	Mitomycin	COC12C3NC3CN1C1=C(C(=O)C(N)=C(C)C1=O)C2COC(N)=O
113	Cocaine hydrochloride	COC(=O)C1C2CCC(CC1OC(=O)c1ccccc1)N2C
114	Chamomile	O=c1cc(-c2ccc(O)cc2)oc2cc(O)cc(O)c12
115	Chrysanthemum (lice shampoo)	CC#CC#CCc1cccc(OC)c1C(=O)OC
116	Bortezomib	CC(C)CC(NC(=O)C(Cc1ccccc1)NC(=O)c1cnccn1)B(O)O
117	Busulfan	CS(=O)(=O)OCCCCOS(C)(=O)=O
118	Capecitabine	CCCCCOC(=O)Nc1nc(=O)n(C2OC(C)C(O)C2O)cc1F
119	Carmustine	O=NN(CCCl)C(=O)NCCCl
120	Cytarabine (cytosine arabinoside)	Nc1ccn(C2OC(CO)C(O)C2O)c(=O)n1
121	Gemcitabine	Nc1ccn(C2OC(CO)C(O)C2(F)F)c(=O)n1
122	Melphalan	NC(Cc1ccc(N(CCCl)CCCl)cc1)C(=O)O
123	Tenofovir	CC(Cn1cnc2c1ncnc2N)OCP(=O)(O)O
124	Desvenlafaxine	CN(C)CC(c1ccc(O)cc1)C1(O)CCCCC1
125	Pentostatin	OCC1OC(n2cnc3c2NC=NCC3O)CC1O

4.3.4 Development of hOCT1 homolog structure

A homology model was developed for hOCT1 since it has no X-ray crystallographic structure to date (Fiser 2010). In our studies, GLUT-1 in complex with bound inhibitor (PDB ID-5EQG) was selected as a template based on the identity score, optimum resolution (lesser the value, more the similarity, 2.9 Å), degree of mutations (none), species similarity (human) and presence of bound ligand. The developed homology model of OCT1 was consistent and validated using a protein reliability report and Ramachandran plot, as shown in **Figure 4.3**.
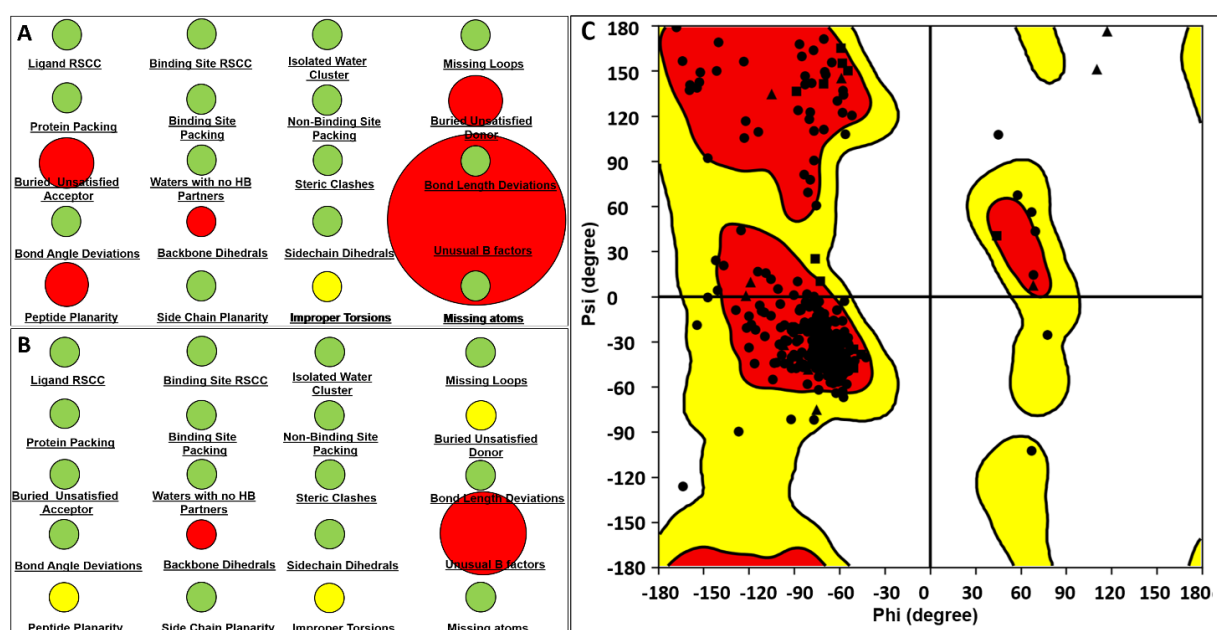

Figure 4.3: Evaluation of homology model of organic cation transporter 1 developed using human glucose transporter as template. A and B shows protein reliability report of homology model of protein backbone and region around ligand (10 Å), respectively. Various protein properties are generated based on their structure and conformations, such as steric clashes, bond length and angle deviations, backbone and sidechain dihedrals, planarity, torsions, missing atoms, and stereochemistry with their allowable limits indicating the quality of the developed protein model. C, shows Ramachandran plot of homology model, indicating the location of amino acids in favourable (Orange), allowed (Yellow), or disallowed (White) regions. It displays the protein dihedrals for all the amino acid residues in the protein where triangle represents glycine, squares represent proline and other amino acid residues are represented by circle. The developed homologue model indicates the presence of glycine (triangle) in the disallowed region, indicating the steric hindrance between the C-beta methylene group of side chains and main chain atoms. However, since glycine has no side chain (absence of methylene group), it does not possess steric hindrance and hence can be accepted in all the quadrants of the plot. Predictions from machine learning models, indicating novel interactions between drug and OCT1 transporter, not known earlier in the literature.

The prepared model had a few outliers concerning the energy dihedrals and unusual B factors because the model was built with less than 40% sequence identity. However, when the protein reliability report was generated for the region around the ligand within a radius of 10 Å, the outliers were reduced, indicating that the prepared model would not impact the molecular interactions in the binding pocket (**Figure 4.3**).

4.3.5 Molecular dynamic simulations

Molecular dynamic simulations were performed to equilibrate the docked hOCT1-ligand complex and to visualize the binding stability and interactions of drug-hOCT1. The best suitable docked pose of each ligand was selected for MD simulations based on their docking score and interactions with the protein. As these simulations are computationally extensive and require a lot of computational power and time, MD simulations were performed for randomly selected drug molecules from various therapeutic categories. The simulations indicate the ionic and hydrophobic interactions of Trp217 and Asp474 with the quaternary nitrogen of TEA and MPP, as reported earlier (Koepsell 2004, 2011; Meyer and Tzvetkov 2021). However, in the current study, the template (PDB ID: 5EQG) chosen for the homology model was different than earlier reported, which explains the additional hydrophobic interaction of TEA and MPP with other amino acids, such as Phe244 and Phe159.

MD simulations do not simulate molecules' transport direction or entry through the transporter but show molecular interactions between the docked ligand and protein, whether a substrate or non-substrate. Hence, molecular interactions were visualized only between substrates (known and predicted) and hOCT1, as shown in **Figure 4.4**.
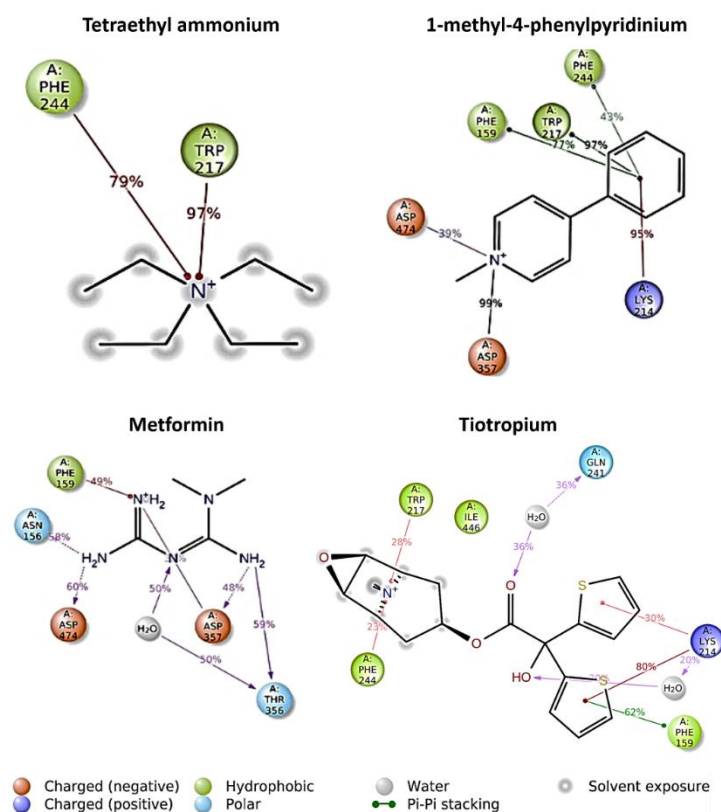
Figure 4.4: Molecular interactions of known substrates with organic cation transporter 1 for a simulation time of 100ns, evaluated by molecular dynamic simulations. Tetraethyl ammonium forms hydrophobic interactions with Trp 217 and Phe 244, 1-methyl-4-phenylpyrinidium forms hydrophobic interactions with Phe 159, Trp 217 and Phe 244, metformin forms hydrophobic interactions with Phe 159 and Tiotropium forms hydrophobic interactions with Phe 159, and Phe 244.

The RMSD plots from MD simulations represent the binding stability and equilibration of the ligand-protein complex (drug-hOCT1) (**Figure 4.5**). A significant fluctuation in the RMSD of protein indicates a conformational change during simulation. In our studies, the drug molecule's ligand RMSD was stable for most of the simulation time (**Figure 4.5**). Most of the drug substrates formed hydrophobic interactions with Trp217 (~90%) and Ile446 (~80%), followed by Lys214 (~70%), which formed hydrogen bonds, hydrophobic and ionic

interactions. The other highly interacting amino acid residues were found to be Phe159 (~60%), Ser470 (~60%), Tyr221 (~55%), Asp474 (~55%), and Phe244 (~50%).

1.Tetraethylammonium
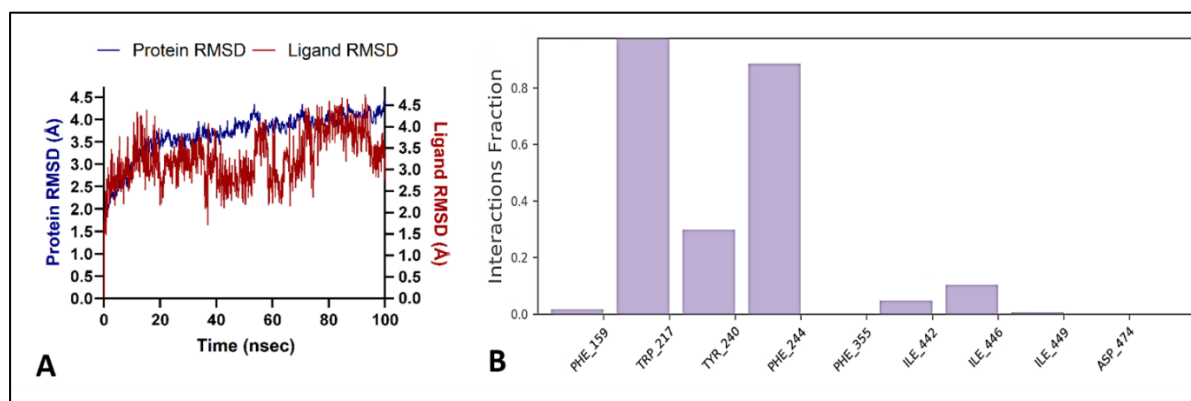
2. 1-methyl-4-phenylpyridinium
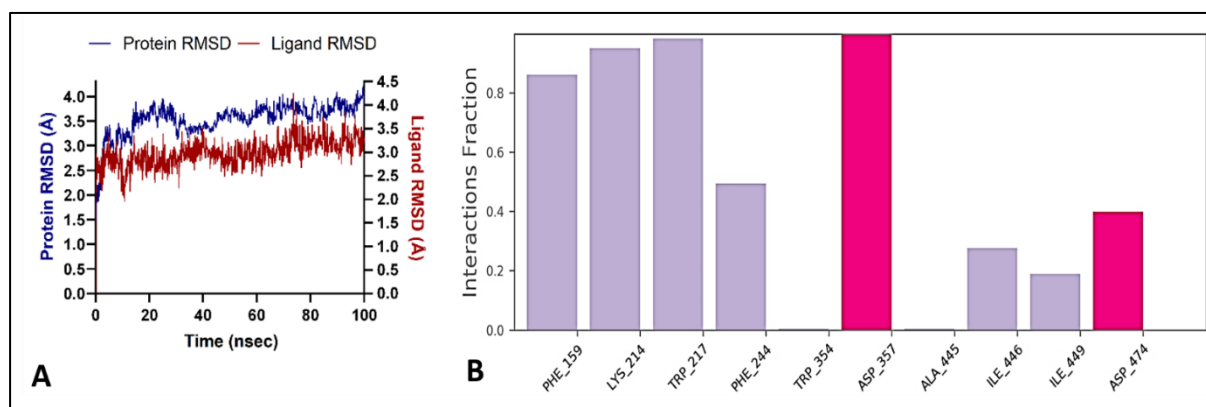
3. Metformin

4. Tiotropium

5. Cyclophosphamide
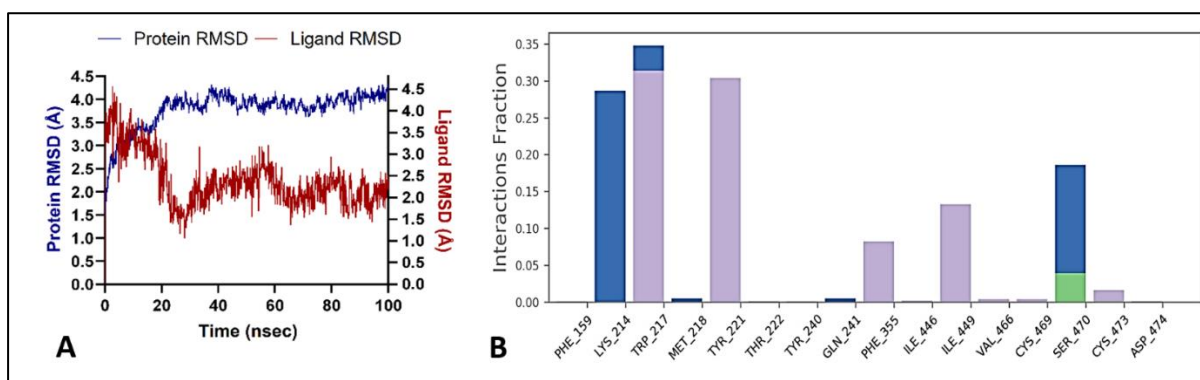
6. Risedronate
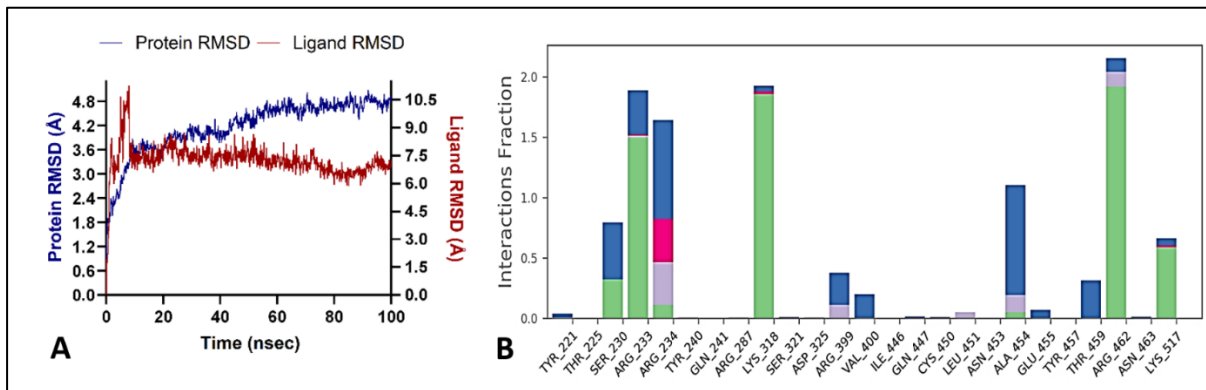
7. Captopril
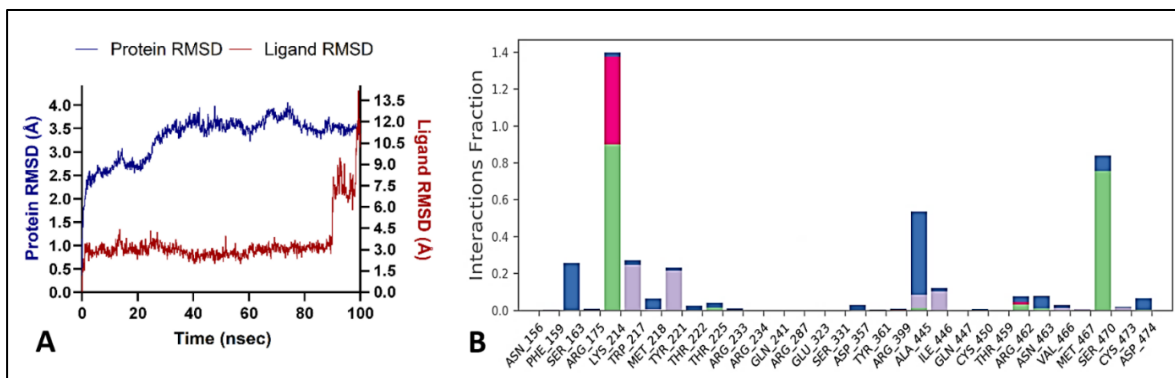
8. Acetazolamide
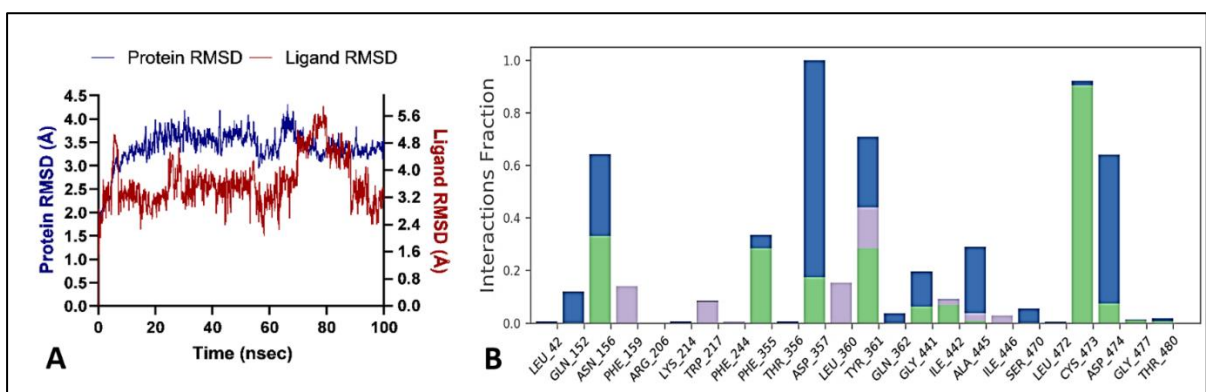
9. Sulfadiazene
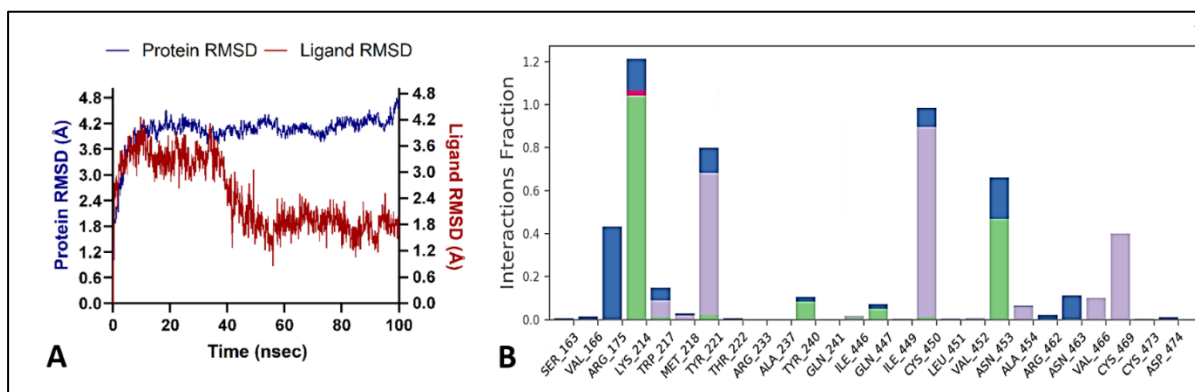
10. Enalapril
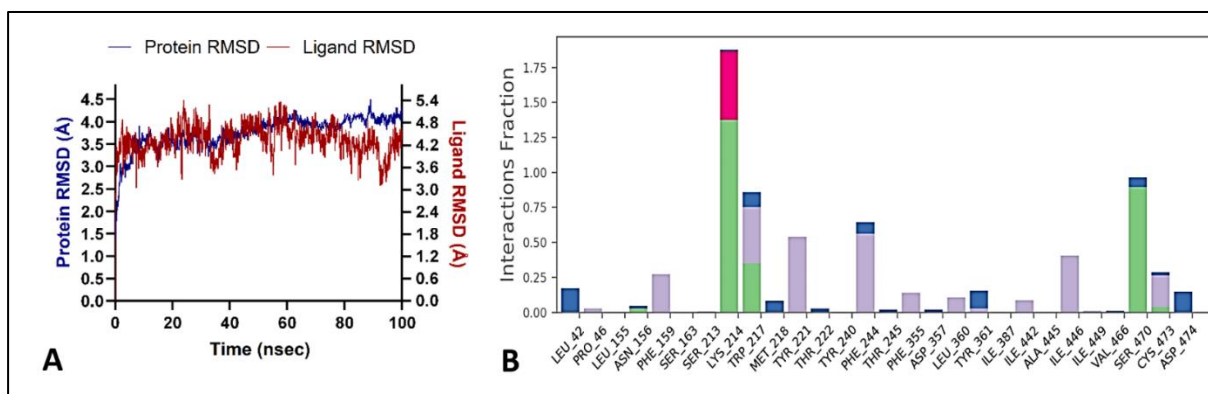
11. Bortezomib
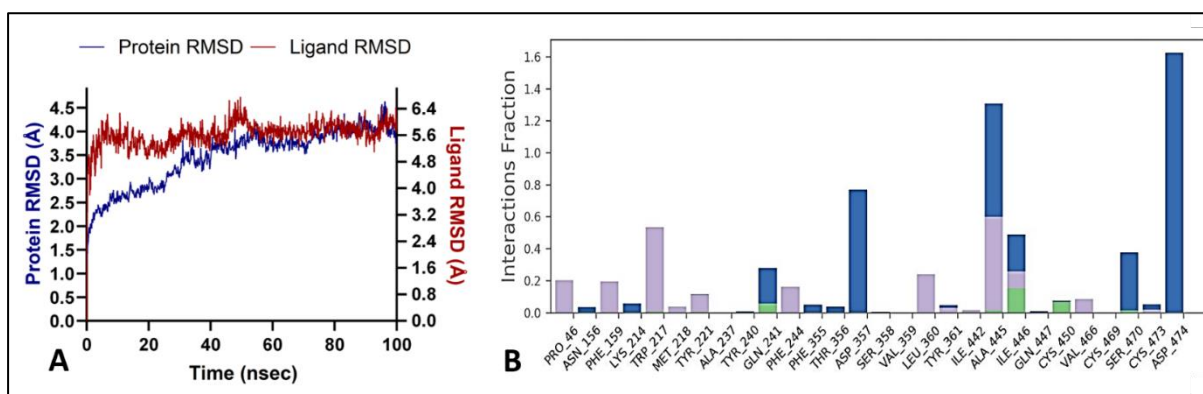
12. Cimetidine
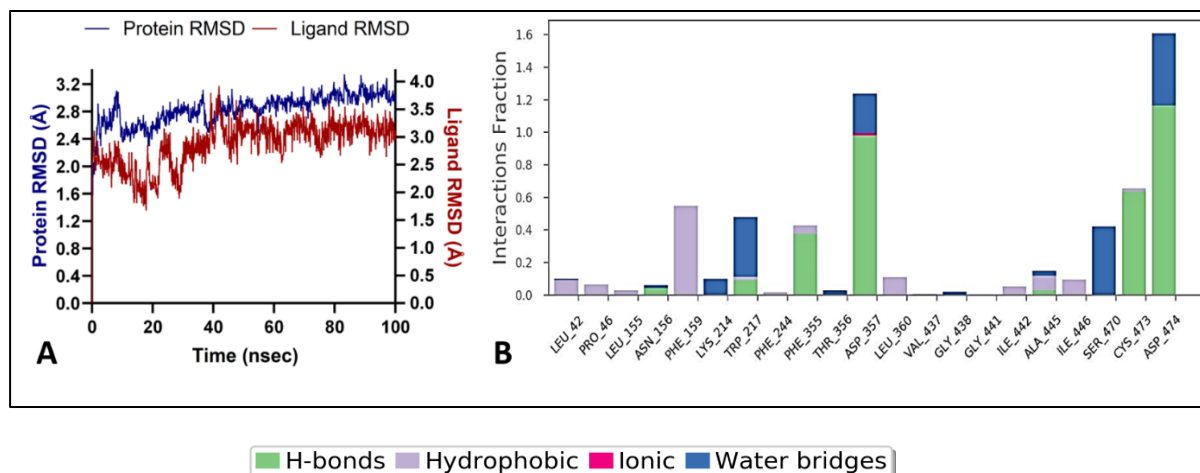
Figure 4.5: Root mean square division (RMSD) (A), and protein-ligand interactions between OCT1 substrates and hOCT1 (B), using MD sim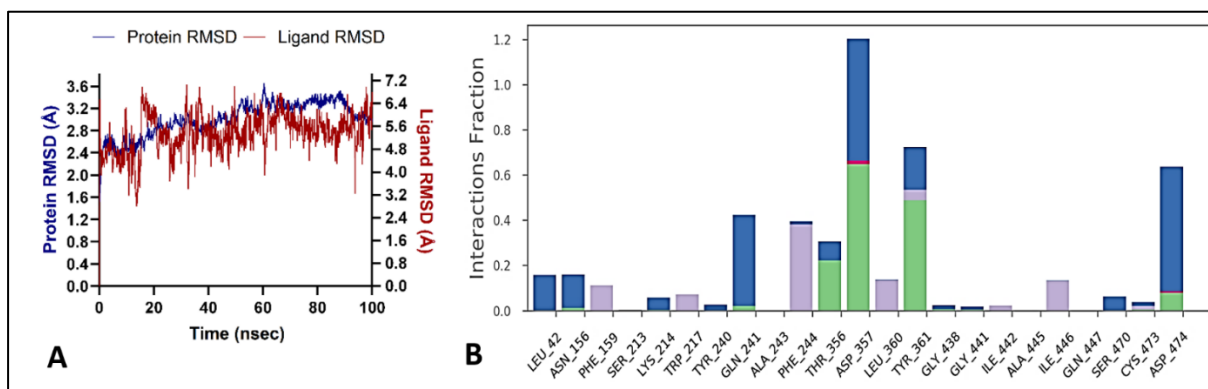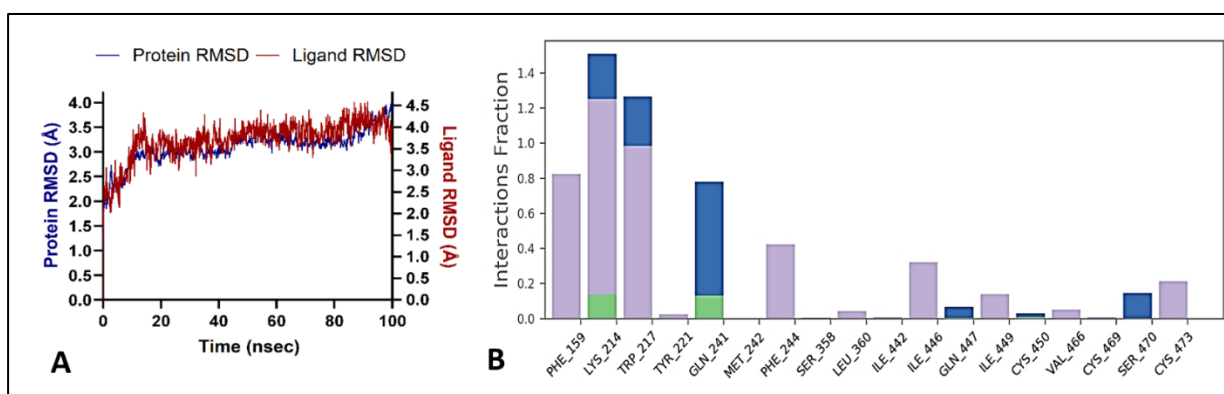ulations. A) The RMSD plots from MD simulations represent the binding stability and equilibration of the ligand-protein complex (drug-hOCT1). Whereas, ligand RMSD as plotted on Y-axis indicates stability of ligand/drug with respect to its protein and binding site. B) Various interactions are observed between ligand atoms and amino acid residues of hOCT1 such as hydrogen bonds (green), hydrophobic (purple) and ionic interactions (pink), and salt and water bridges (blue) represented in each figure. X-axis represents the interacting amino acid residue whereas the Y-axis represents the normalized simulation time of the specific interaction over the course of simulation.

4.3.6 Metadynamics simulation

Metadynamics is an atomistic computer simulation tool used to perform accelerated simulations of the biological event by forcing the system across the energy barriers using a series of well-defined Gaussian energy functions to boost the potential energy of the collective variable, thereby speeding up the process (Bussi and Laio 2020). The known substrates and non-substrates of OCT1 were used to identify the discrete pattern in their associated free energies concerning their movement during the simulations. Upon different trials, it was found that a wall length of 35 Å with a simulation time of 40 ns revealed that around 75% of substrates displayed their lowest energy state close to their initially docked

site, and 88% of non-substrates displayed their lowest energy state outside the initially

docked site, thereby validating the model with a mean accuracy of 81%. As shown in **Figure**

4.6, the energy profile patterns of substrate and non-substrate showed an intriguing pattern

as the substrate molecules displayed their lowest energy state very close to their initially

docked position, whereas the non-substrates had their lowest energy far away from their

initially docked position.
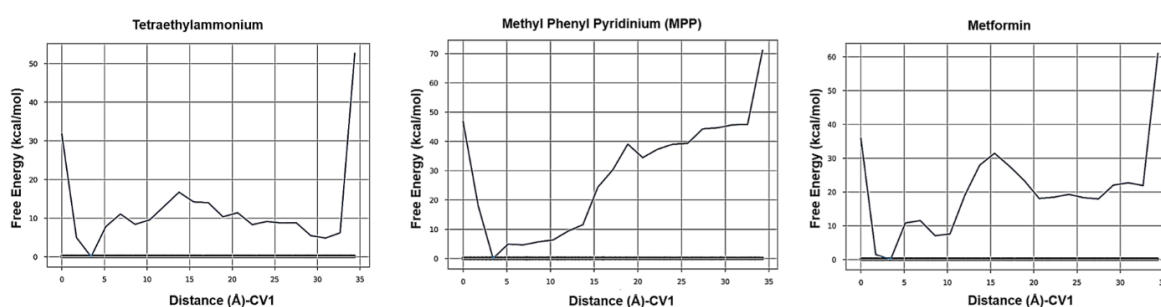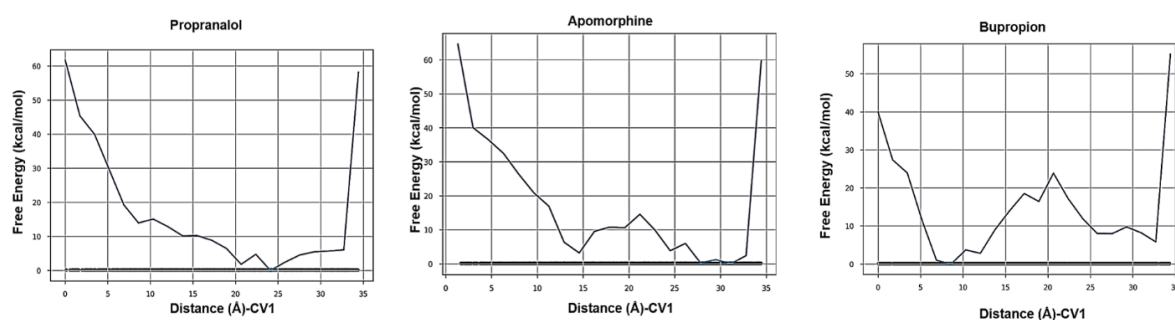
Figure 4.6: Energy profile graph of substrates (TEA, MPP, Metformin, Tiotropium) and non-substrates (Propranolol, Bupropion) of organic cation transporters, obtained through metadynamics simulation studies. TEA: Tetraethyl ammonium, MPP: 1-methyl-4-phenylpyridinium. A distance-based collective variable was used for the metadynamics simulations with a specified center of mass for protein and ligand. A total simulation time for metadynamics was set as 40 ns. The energy profile patterns indicate that the substrate molecules were stable near the binding pocket of the transporter, while non-substrates were stable outside the initial binding pocket. Therefore, the position of molecule where it possesses the minimum free energy was used to classify substrates and non-substrates.
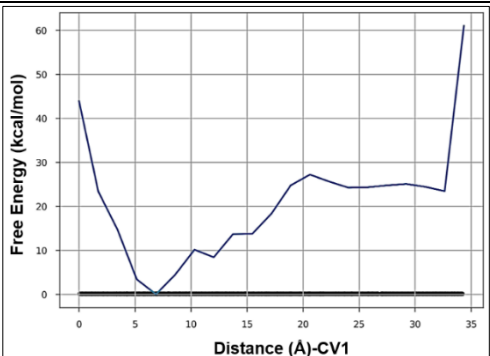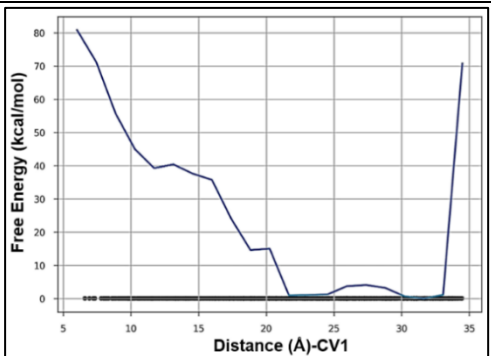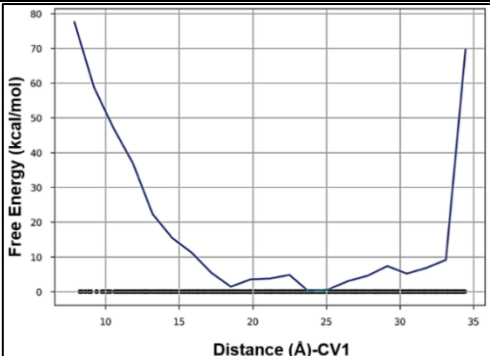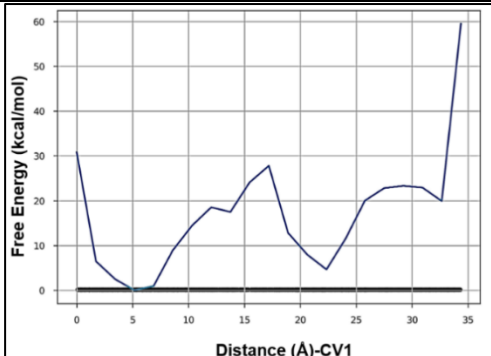
The energy profile graph for various predicted substrates and non-substrates with their

classification as substrate or non-substrate is given in **Table 4.4**. Based on the AI predictions
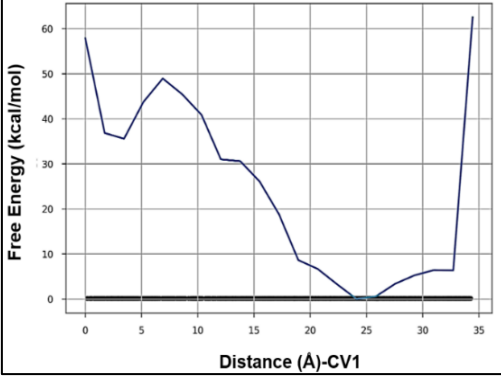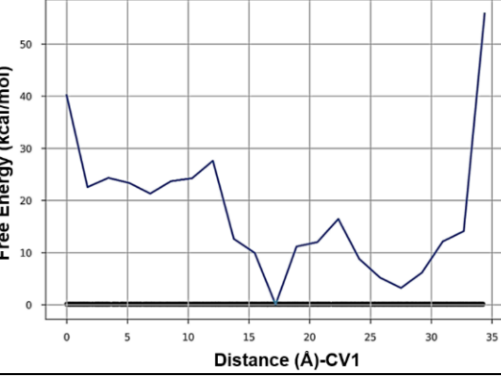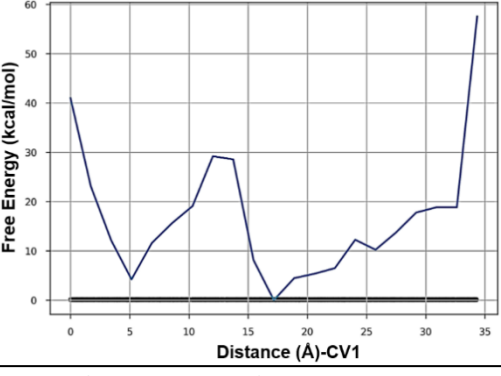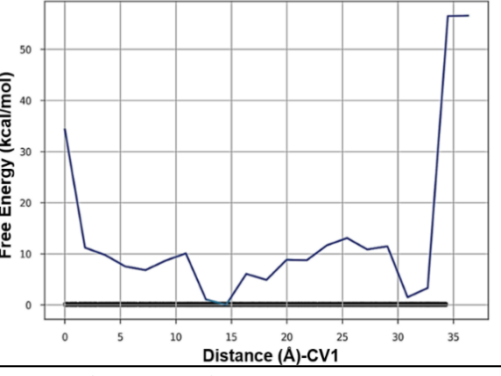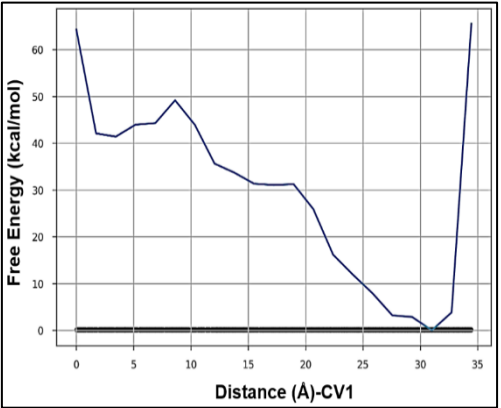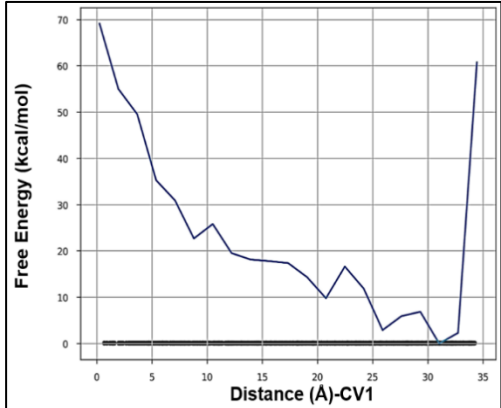
and computer simulations, some of the OCT1 predictions not known earlier are given in **Table 4.5**, along with their therapeutic class and associated ocular toxicities.
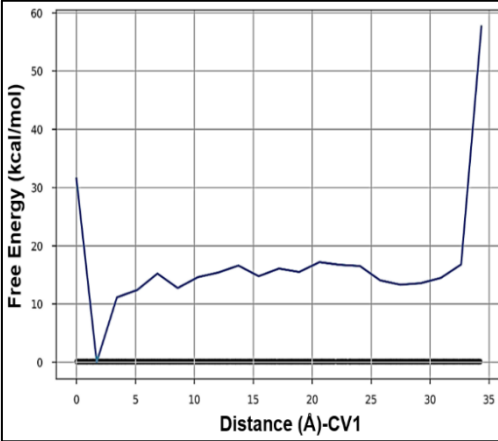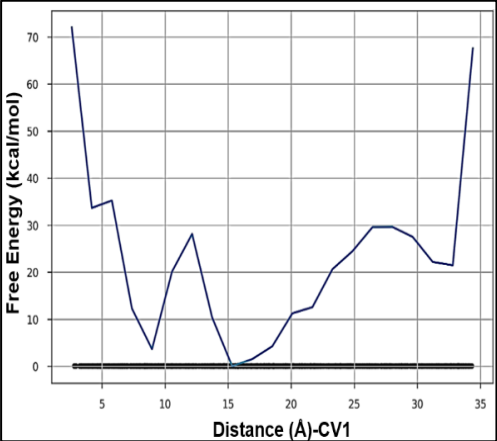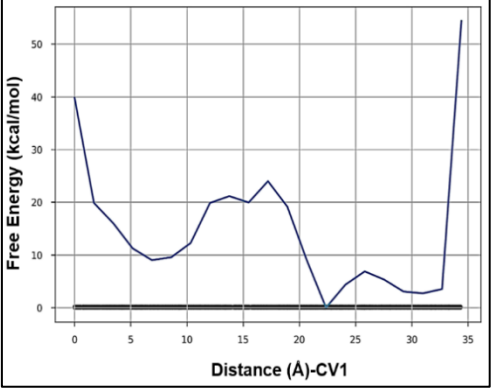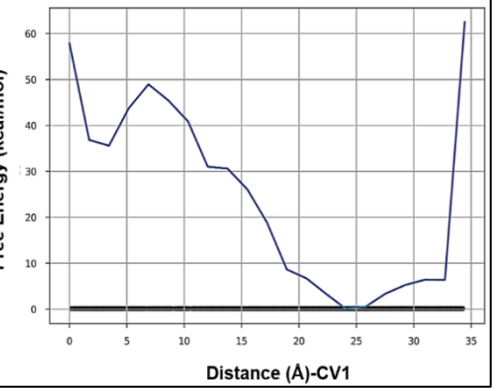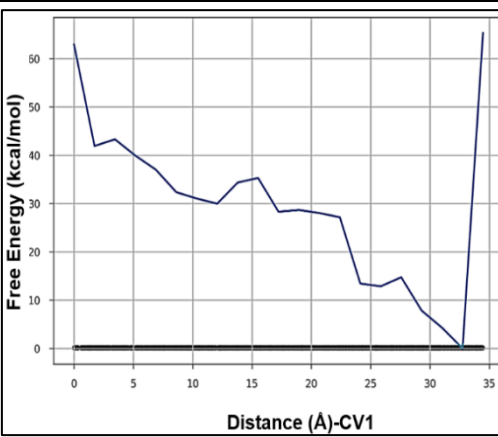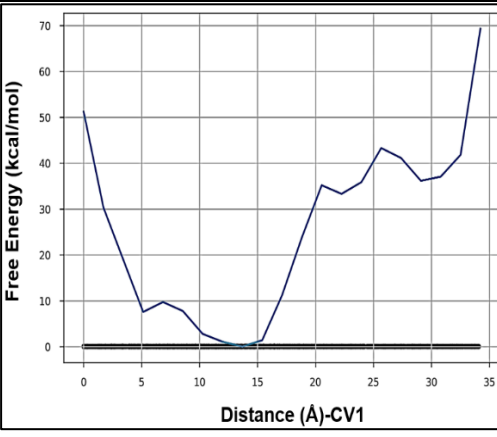
Table 4.4: Energy profile graph of predicted substrates and non-substrates from machine learning models. Predictions of organic cation transporter (OCT1) substrates from machine learning (ML) models, further validated by computer simulations (CS). The translocation of substrates was enhanced by performing metadynamics to visualize the movement of drugs along the OCT1 protein.

Drug	Metadynamics	Drug	Metadynamics
Cyclophosphamide	 **ML predictions:** Substrate **CS predictions:** Substrate	Methotrexate	 **ML predictions:** Non-substrate **CS predictions:** Non-substrate
Risedronate	 **ML predictions:** Substrate **CS predictions:** Substrate	Captopril	 **ML predictions:** Substrate **CS predictions:** Substrate
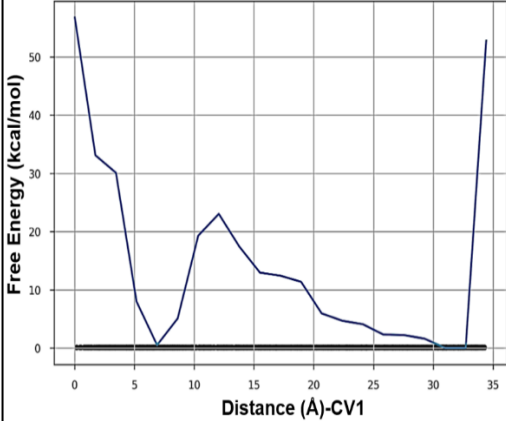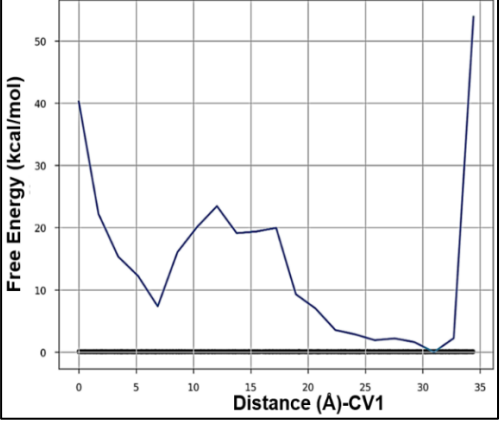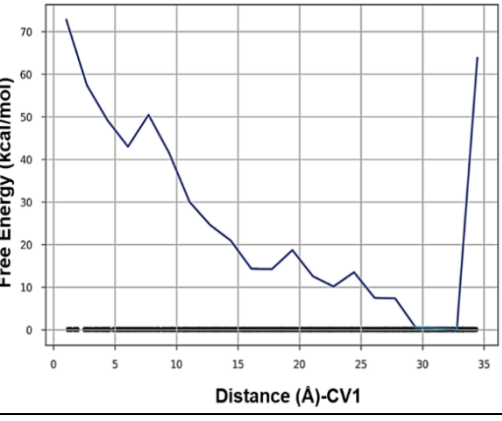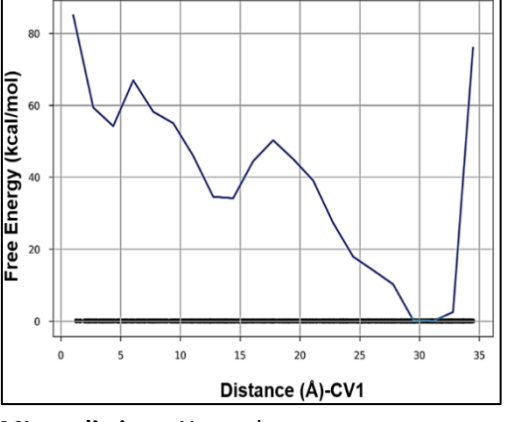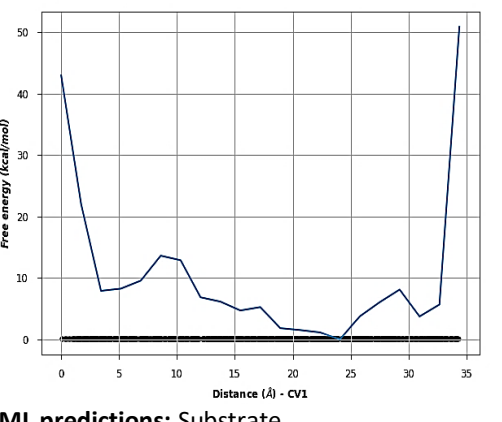
Artificial Intelligence in predicting drug Organic cation transporter interactions

Metoprolol	**ML predictions:** Substrate **CS predictions:** Non-substrate	**Reserpine**	**ML predictions:** Non-substrate **CS predictions:** Non-substrate
Chlordiazepoxide	**ML predictions:** Non-substrate **CS predictions:** Non-substrate	**Acetazolamide**	**ML predictions:** Substrate **CS predictions:** Substrate
Vesamicol	**ML predictions:** Non-substrate **CS predictions:** Non-substrate	**Timolol**	**ML predictions:** Substrate **CS predictions:** Non-substrate

Sulphanilamide

ML predictions: Substrate

CS predictions: Substrate

Ritonavir

ML predictions: Non-substrate

CS predictions: Non-substrate

Pregabalin

ML predictions: Substrate

CS predictions: Non-substrate

Metoprolol

ML predictions: Non-substrate

CS predictions: Non-substrate

Bupivacaine

ML predictions: Substrate

CS predictions: Non-substrate

Bortezomib

ML predictions: Substrate

CS predictions: Substrate

Artificial Intelligence in predicting drug Organic cation transporter interactions

Sulfadiazine

ML predictions: Substrate

CS predictions: Substrate

Labetalol

ML predictions: Substrate

CS predictions: Non-substrate

Enalapril

ML predictions: Substrate

CS predictions: Substrate

Broxyquinoline

ML predictions: Non-substrate

CS predictions: Non-substrate

Arformoterol

ML predictions: Non-substrate

CS predictions: Non-substrate

Piroxicam

ML predictions: Substrate

CS predictions: Substrate

Busulfan	
	ML predictions: Substrate
	CS predictions: Substrate

Glipizide	
	ML predictions: Substrate
	CS predictions: Substrate
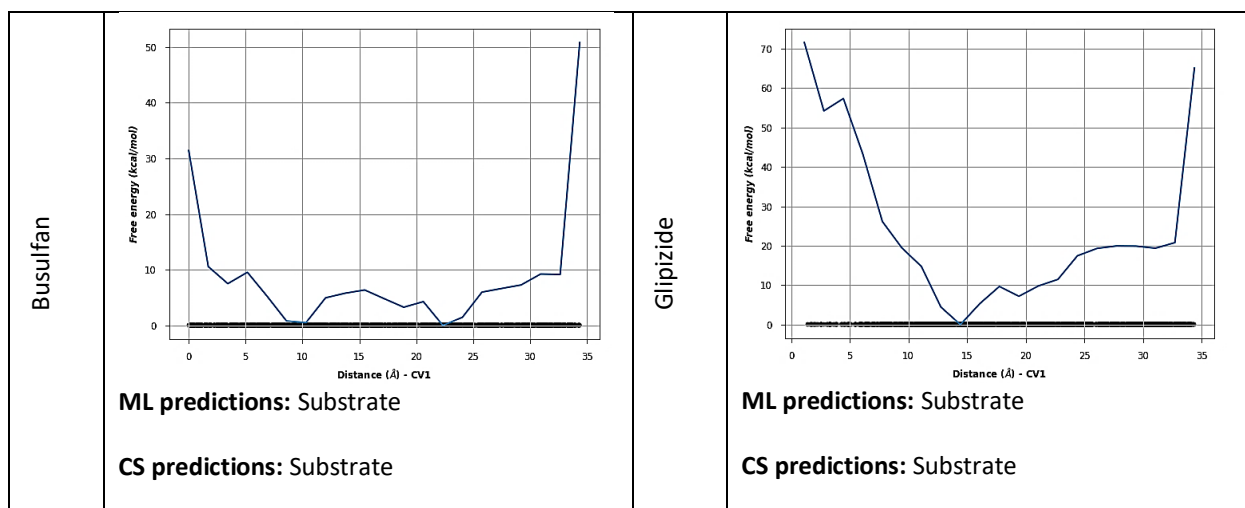
Table 4.5: Predicted organic cation transporters 1 (OCT1) substrates and their associated ocular toxicities. Predictions of OCT1 substrates from machine learning models, further validated by molecular dynamic simulations and metadynamics, revealed drug-OCT1 interactions which were not known earlier.

S.No	Predicted OCT1 substrates	Therapeutic class	Associated ocular toxicities when administered systemically
1	Cyclophosphamide	Anti-neoplastic	Visual Impairment, Inflammation, Lacrimation, Blurred Vision
2	Risedronate	Calcium regulators	Eye Inflammation (Iritis, Uveitis), Eye Pain, Redness
3	Captopril	Angiotensin-converting enzyme inhibitor	Eye Swelling, Blurred Vision
4	Acetazolamide	Anti-viral	Transient Myopia, Photosensitivity
5	Sulphanilamide	Antiobiotic	Glaucoma, Conjunctivitis, Keratitis, decreased vision
6	Sulphadiazine	Antiobiotic	Ophthalmic Suspension Include: Cataract, Dizziness, Eye Discharge, Eyelid Edema, Eyelid Erythema, Eye Irritation, Eye Pain, Eye Pruritus,

			Ocular Hyperemia, and Visual Disturbance (Blurry Vision).
7	Enalapril	Angiotensin-converting enzyme inhibitor	Swelling of eyes, Blurred vision, Conjunctivitis, Dry eyes, Tearing
8	Bortezomib	Anti-neoplastic	Ophthalmic Herpes, Diplopia, Blurred Vision, Conjunctival Infection, Irritation, Necrosis in the eyes, reduced Eyesight, Blurred Vision

4.4 Discussions

Chronic disease patients (cancer, arthritis, cardiovascular diseases) undergo long-term systemic drug treatment. Membrane transporters in ocular barriers could falsely recognize these drugs and allow their trafficking into the eye from systemic circulation (Gao et al. 2015; Hafey et al. 2022; Taylor-Wells and Meredith 2014). Hence, despite their pharmacological activity, these drugs accumulate and cause toxicity at the off-target site, such as the eye. Since around 40% of clinically used drugs are organic cation in nature, we aimed to understand the drug-OCT1 interactions. We applied machine learning techniques and computer simulation models in the current study to predict the potential OCT1 substrates. The developed model predicted the potential substrates for OCT1 among systemic drugs causing ocular toxicity – not known earlier, such as cyclophosphamide, bupivacaine, bortezomib, sulphanilamide, tosufloxacin, topiramate, and many more (**Table 4.5**).

Preparing a dataset with necessary features is the key to a successful model since the physicochemical and structural properties of drugs play a crucial role in their binding with the transporters (Ozdemir and Susarla 2018). Initially, various constitutional, molecular, charge and physicochemical features were obtained for substrate and non-substrates of OCT1.

Artificial Intelligence in predicting drug Organic cation transporter interactions

Several structural and physicochemical features such as logP, weight, number of sulfur atoms, and others were selected based on their correlation values, a few of which has also been previously reported (Baidya et al. 2020). The prepared dataset has a wide range of physicochemical property values which were normalized before the training. K-fold cross-validation (k=5) was added to the model, which divides the dataset into k- subsets (or folds) of equal size to test the data on 1-fold and use (k-1) folds to train the model. The process is repeated k-times for validation, each for a different fold. Consensus modeling can improve the overall performance of the machine learning model, which comprises several aggregation techniques to obtain better results by combining the strengt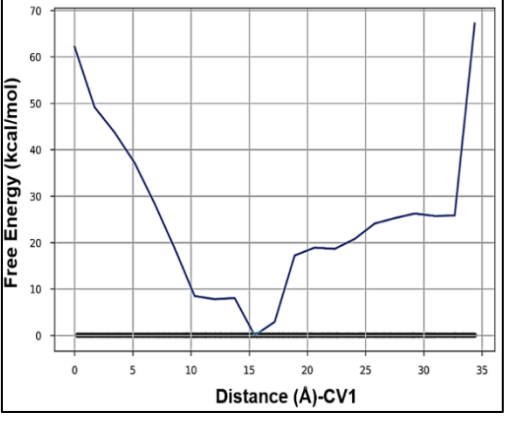hs of individual algorithms. The developed artificial intelligence model predicted novel OCT1 substrates where more than 43% of anti-infectives (35 out of 80), 28% of CNS (20 out of 71), 21% of CVS (15 out of 70), and 12% of anti-neoplastic (8 out of 64) from our dataset were predicted as OCT1 substrates.

Further, computer simulations were performed to visualize the interactions between various drugs and hOCT1 at an atomic level and validate the predictions from machine learning models. Since the sequence identity between the template (5EQG) and target (OCT1) was less than 40%, energy-based modeling was performed to develop the homolog. The earlier homology model of OCT1 was developed with a template showing only 29% amino acid sequence similarity; however, the quality of the model was evaluated based on the location of substrate-binding amino acids in a single structural epitope and contact with hydrophilic molecules indicating the reliability of the model (Popp et al. 2005). In our studies, these amino acids were located in the core protein region facing the hydrophilic/aqueous medium. The Ramachandran plot showed that the majority (99.27% for hOCT1) of the amino acid residue lies in the favorable and allowed region, indicating the model's suitability for further

interaction studies (Ramachandran and Sasisekharan 1968). The prepared model was energy minimized and used to perform further computational studies.

The available literature offers limited predictive value for drug-OCT1 interactions due to structural differences among the substrates (Meyer and Tzvetkov 2021). Due to the poly-specific nature of OCT1, there is a possibility for the studied drugs to bind at different binding sites and therefore, while performing docking, a grid was generated around the protein rather than a specific site. As reported earlier, the docked structures of TEA and MPP showed interactions with similar amino acids (Phe159, Trp217, Phe244, Asp474) (Koepsell 2004), validating our homology model and demonstrating that the ligand was docked precisely at the binding pocket of the hOCT1 protein.

MD simulations are known to be independent of the simulation box size when it exceeds a distance of at least 10 Å or three solvation layers from the protein to the box edge, based on which we fixed our simulation box size as 10 Å distance from each side of the protein (Gapsys and de Groot 2020). Most of the reported literature supports the simulation time of 100 ns to visualize the interactions between ligands and proteins (Amir et al. 2019; Ghosh et al. 2021; Koshy et al. 2010; Schlessinger et al. 2018). Hence 100 ns was chosen as the appropriate time for MD simulations. In our simulation studies, few deviations were observed with protein RMSD; however, the order changes were within 1 to 3 Å, which is acceptable (Weng et al. 2021). Whereas ligand RMSD as plotted on the secondary Y-axis, indicates the stability of the ligand/drug concerning its binding site (Hermanto et al. 2022). However, a second RMSD shift was observed after 90ns for captopril, indicating the drug movement away from the binding pocket (Al-Karmalawy et al. 2021). For other drugs such as cyclophosphamide, risedronate,

and sulfadiazine, initial fluctuations in RMSD were observed, however as the simulation progressed, these fluctuations were minimized (Cyclophosphamide ~25 ns, Risedronate ~10 ns, Sulfadiazine ~50 ns). Such fluctuations may arise as the initial docked pose of the ligand might not be the most stable conformation when presented in the solvation medium (Shoichet et al. 1999). MD simulations could enable the alteration of ligand conformation to achieve a stable state, indicated by initial ligand RMSD fluctuations (Liu and Kokubo 2017). Ligand-protein interactions were used to visualize the interactions between ligand atoms and amino acid residues of hOCT1, such as hydrogen bonds, hydrophobic and ionic interactions, and salt and water bridges (de Freitas and Schapira 2017). Nevertheless, we were not able to visualize the movement of molecules across the transporter by MD simulations, and therefore the equilibrated structure of drug-hOCT1 was further subjected to metadynamics. Since the conventional MD simulations require a longer duration to simulate the transport movement across the transporter, which is practically not feasible owing to the tremendous amount of computational resources, hardware capacity, and time required for simulating at an atomistic level – metadynamics simulations can be used as an alternative tool to visualize these movements.

The metadynamics approach is employed to visualize biological processes like the transport of a ligand molecule through the transporters (ligand-protein equilibrated complex) (Nagy et al. 2021). Apart from improving the simulation timescale, metadynamics also enhances the sampling method by utilizing collective variables whose values directly influence the biological process (Valsson et al. 2016). This study employed metadynamics simulations to classify systemic drugs causing ocular toxicity as substrates and non-substrates of hOCT1. The rationale for selecting drugs (AI predictions) for metadynamics simulation was based on their

clinical use and the associated toxicities. To ensure the diversity, the drugs were selected from multiple therapeutic categories such as anti-infectives (6), cardiovascular drugs (9), central nervous system drugs (4), and anti-neoplastic (3). The distinct pattern of metadynamics graphs indicates that the substrate molecules were more stable near the binding pocket of the transporter, while non-substrates were stable outside the initial binding pocket. The molecule position with minimum free energy was used to classify the systemic drugs causing ocular toxicity as substrates and non-substrates of hOCT1.

Earlier studies proved the functional role of OCT1 in the eye in transporting various cationic molecules from systemic circulation to the ocular tissues (Nirmal, Sirohiwal, et al. 2013a; Nirmal J 2010; Velpandian, Nirmal, Sirohiwal, et al. 2012). Our current study focuses on drug-OCT1 interactions indicating membrane transporters could be a potential portal for the systemic drugs (29% of 424 drugs from our database) into the eye. Several beta-blockers, including Atenolol, Nadolol, Labetalol, and Pindolol, were found to be substrates for OCT1, as reported earlier using in vitro studies (Guo et al. 2018; Misaka et al. 2016). Interestingly, from our predictions, 33 out of 62 (53%) sulfur-containing drugs were predicted as OCT1 substrates, including busulfan, tamsulosin, dapsone, sulphanilamide, sulfacetamide, and sulphadiazine, indicating the presence of the sulfur group could be one of the crucial features of OCT1 substrate. Moreover, based on the correlation analysis performed during training dataset preparation, the number of sulfur atoms in the molecular structure was selected as one of the essential features to be identified as OCT1 substrate. However, a careful interpretation and more detailed invitro and invivo studies are required to confirm this finding. A recent study also reported that sulfur could be an additional factor facilitating the transport of drugs through OCT1 (Redeker et al. 2022). Hence, understanding the structural

and physicochemical properties of drugs responsible for their interaction with other membrane transporters expressed in the ocular barriers could delineate the molecular mechanisms responsible for the entry of systemic drugs into the eye – leading to ocular toxicity.

4.5 Conclusion

In our study, we used machine learning, MD simulations, and metadynamics to predict the drug-OCT1 interactions. These interactions could help in understanding the entry of systemic drugs (cations) into the eye through OCT1. The findings from our study are: a) predictions from the artificial intelligence model revealed potential OCT1 substrates (n=125) – not known earlier, b) our predictions demonstrate that the sulfur-containing drugs could be an additional factor facilitating the transport of OCT1 substrates, c) metadynamics studies can be used to classify the drugs as substrate or non-substrate based on their free energy concerning their movement during the simulations.

Though previous studies have predicted drug-OCT1 interactions using artificial intelligence, to the best of our knowledge, for the first time in the current study, we have used metadynamics for classifying drugs as substrates and non-substrates for the transporters. This high-throughput screening approach can be further explored to advance the understanding of drug interactions with other transporters. However, these predictions need further validation by in vitro and in vivo studies to improve our understanding of the drug-OCT1 interactions and the entry of systemic drugs into the eye.

Chapter 5

Evaluation of drug substrate interaction with OCT transporters in the in vivo model
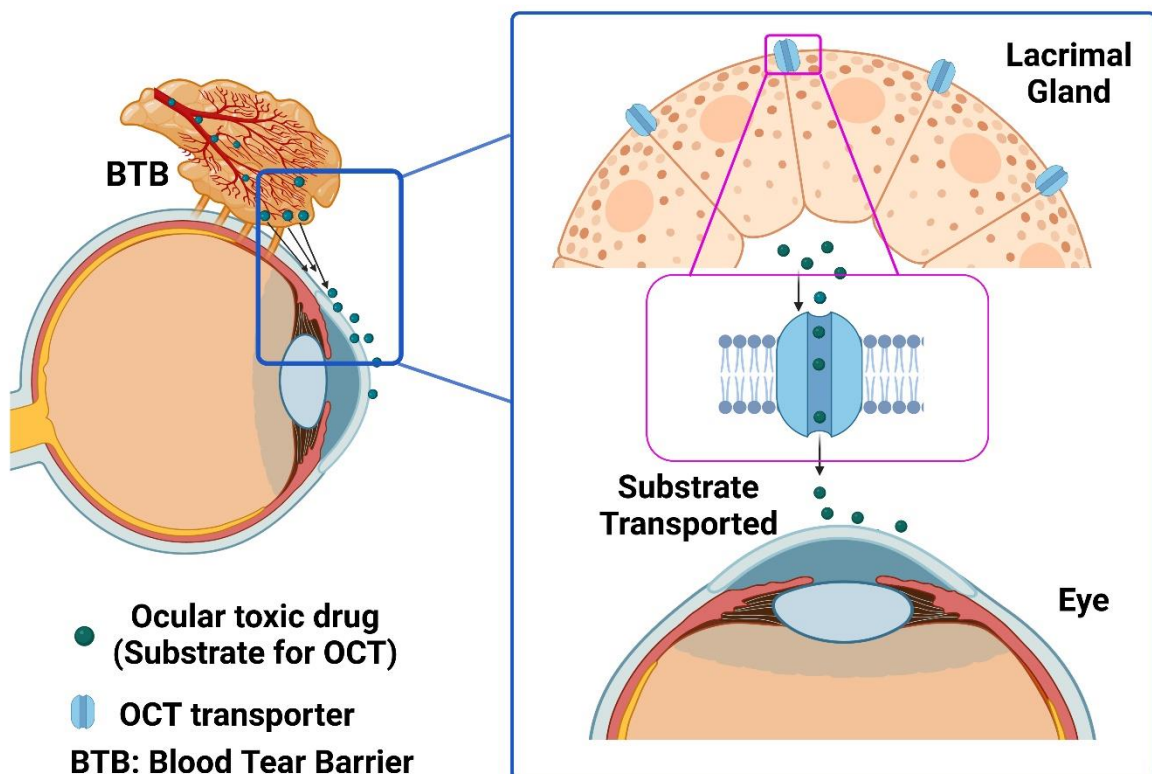
Functional role of organic cation transporters in lacrimal gland

5.1 Introduction

Chronic diseases are defined as the state of illness that continues for more than a year and requires medical care on a routine basis (Prevention 2022). According to the Centers for Disease Control and Prevention, every one in three individuals around the world suffers from multiple chronic diseases. Hence, the patients must adhere to long-term medication usage for efficient clinical outcomes – some continuing for a lifetime (Unni 2023). However, chronic medications can lead to other unwanted adverse effects due to off-target accumulation of the drugs. One such organ is the eye, the most dominant of human senses, which can affect the quality of life (Burton et al. 2021). Hundreds of drugs (anti-cancer, cardiovascular drugs, central nervous system drugs) have been reported to accumulate in the eye and show ocular toxicity, such as retinal toxicity, cataract, and dry eye, which varies with the dose and duration of the usage (Castells et al. 2002; Constable et al. 2022a; Li et al. 2008; Liu et al. 2018; Moorthy and Valluri 1999; Mukhtar and Jhanji 2022; Prakash et al. 2019; Richa and Yazbek 2010; Santaella and Fraunfelder 2007).

Ocular damages can be reversible but can also be irreversible even upon discontinuing the medication, such as maculopathy and keratopathy caused by amiodarone (Bratulescu et al. 2005). There are several cases reported for irreversible lacrimal duct stenosis in women who consumed Methotrexate, Fluorouracil, and Cyclophosphamide for early-stage breast cancer (Stevens and Spooner 2001). A retrospective cohort study showed that several anti-cancer agents (v-raf murine sarcoma viral oncogene homolog B1 (BRAF) inhibitors, Mitogen-activated protein kinase-kinase (MEK) inhibitors, Immune checkpoint inhibitors, therapeutic

antibodies) could cause ocular toxicities such as inflammatory uveitis, dry eye, and Central serous retinopathy (Vishnevskia-Dai et al. 2021).

One unexplored research area for understanding systemic drugs' ocular toxicity is their entry mechanism into the eye. The complex anatomy of the eye with tight ocular barriers can hinder the entry of xenobiotics into the eye (Cunha-Vaz 1979). The eye demands a high supply of nutrients, vitamins, and other endogenous molecules that are supplied by membrane transporters for normal functioning (Kato et al. 2008). More than 850 transporter genes have been recognized to transport the endogenous molecules and remove the waste products from the tissue (Venter et al. 2001). Uptake transporters belonging to the solute carrier (SLC) family, such as glucose transporter (GLUT), taurine transporter, amino acid transporter, nucleoside transporter, folate transporter, organic anion (OAT) and organic cation transporters (OCT), mediate the translocation of endogenous molecules from blood to ocular tissues across various barriers (Liu and Liu 2019; Mannermaa et al. 2006).

The OCTs are one of the highly expressed uptake transporters in various ocular barriers that are of clinical relevance since nearly 40 % of FDA-approved drugs exists as cations at physiological pH – one of the key determining factors for OCT substrates (Neuhoff et al. 2003). Among the various isoforms of OCT, isoform 1 (OCT1) is highly expressed in ocular tissues and, therefore, is essential to understand its functional role in drug disposition from systemic circulation to the eye. OCT1 transporters are reported to express in the cornea, iris-ciliary body (blood-aqueous barrier), retina and retinal pigment epithelium (blood-retinal barrier), and other ocular tissues which could be responsible for the entry of organic cations into the eye (Garrett et al. 2008; Nirmal, Sirohiwal, et al. 2013a; Zhang et al. 2008). Entry of drugs from

the systemic circulation to the precorneal area could be attributed to the tear secretion from the lacrimal gland – however, the expression of membrane transporters in the lacrimal gland is unexplored (Velpandian, Nirmal, Sirohiwal, et al. 2012). Studies have reported the presence of water transporter channels and nucleoside transporters in the lacrimal gland involved in drug disposition from blood to tear (Ding et al. 2010; Sharma et al. 2021; Ubels et al. 2006).

In the current study, we aim to understand the functional role of OCT1 in the lacrimal gland as a gateway for the entry of systemically administered drugs to the eye. Our previous study used an artificial intelligence model and computer simulations that predicted n=125 novel OCT1 substrates which were not reported earlier (Malani et al. 2023). To confirm these predictions using in vivo experimental model, we took an advantage of the presence of OCT1 in the cornea and performed topical tear kinetics for initial rapid screening. Drugs were selected based on their physicochemical properties and clinical relevance. Further, tear kinetics were performed for the selected drugs administered intravenously to delineate the role of OCT1 in the entry of systemically administered drugs through lacrimal gland. We have also shown the gene and protein expression of OCT1 in rabbit lacrimal gland along with its localization in the cornea and lacrimal gland.

5.2 Materials and Methods
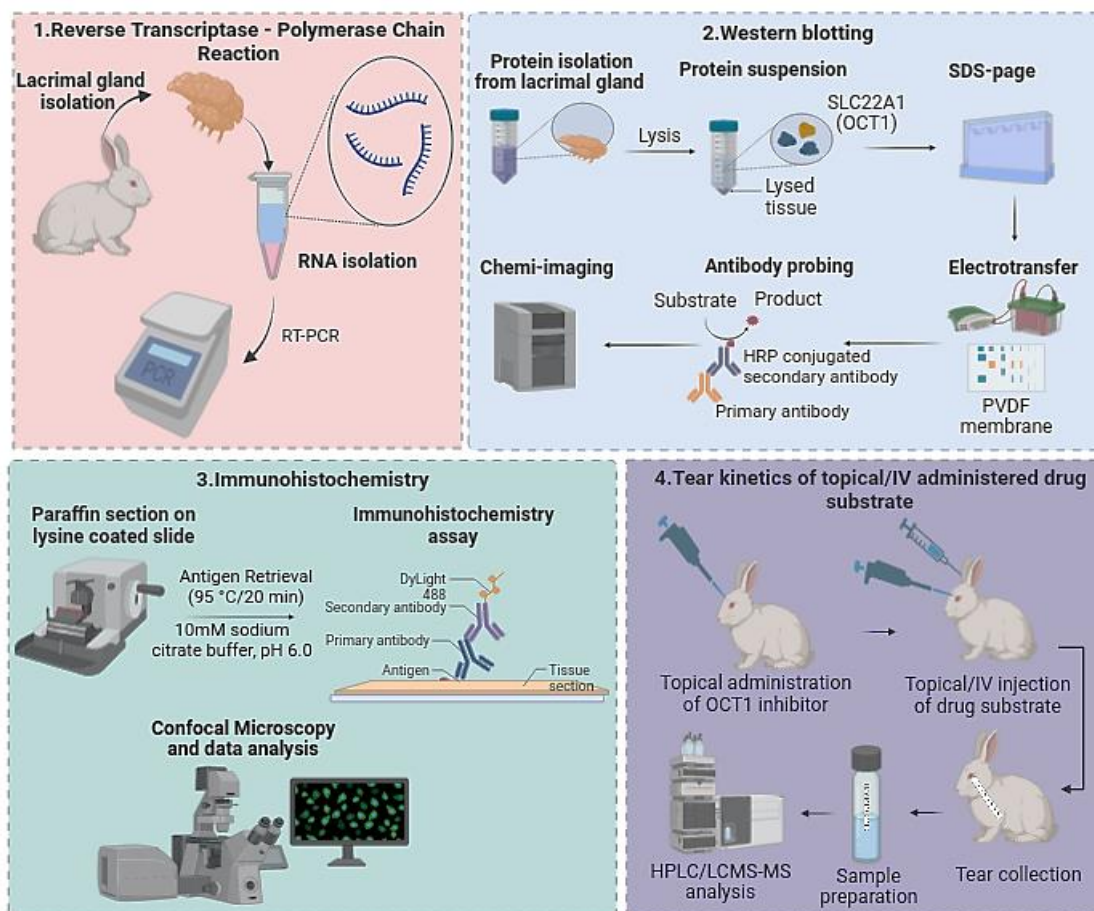
Figure: Workflow of chapter 5 (Objective 2).

5.2.1 Materials

Tri reagent and fluoroshield were procured from Sigma Aldrich, USA. cDNA synthesis kit and PCR master mix were purchased from Takara, Japan. Primers were obtained from G.M. Biotech, India. Bradford reagent and all Western blot reagents were of molecular biology grade from HiMedia, India. Glipizide, Busulfan, Pregabalin, Piroxicam, Cyclophosphamide of Active Pharmaceutical Ingredient (API) grade were purchased from Carbanio, India. Atropine sulphate and Quinidine sulphate were purchased Sigma, USA.

5.2.2 Animals

Rabbits were procured from VAB-Bioscience Pvt. Ltd. (India). Rabbits were handled according to the National Research Council's Guide for the Care and Use of Laboratory Animals (8th edition) guidelines. All the experiments were approved by the Institutional Animal Ethics Guideline, BITS-Pilani, Hyderabad, India, and were performed according to the Association for Research in Vision and Ophthalmology guidelines. Animals were kept under a 12-hour light-dark cycle with ad-libitum access to food and water.

5.2.3 Histology of the lacrimal gland:

Lacrimal gland was excised from rabbit and fixed in 4% paraformaldehyde for 48 h. Histology was performed as per our previously reported method (Malani and Nirmal 2022). Tissue samples were dehydrated using an increasing concentration of ethanol from 50 to 100%, and cleared with xylene to remove the alcohol. The paraffin blocks were prepared and 5 μm sections were cut. The sections were stained with hematoxylin and eosin stain and visualized under microscope to study the histological changes.

5.2.4 Expression of OCT1 in lacrimal gland:

The lacrimal gland was excised from rabbits to confirm the presence of OCT1 in the lacrimal gland and snap frozen in liquid nitrogen, which was transferred to -80°C until further analysis (Honkanen et al. 2020).

5.2.4.1 Gene expression of OCT1 in lacrimal gland by Polymerase Chain Reaction

The lacrimal gland (n=3) was thawed and homogenized using a bead homogenizer (Minilys, Bertin). RNA was isolated using TRI reagent, and the pellet was dissolved in 50 μl RNase-free

water (Gottshall et al. 2008). RNA isolated from rabbit liver was used as a positive control. Complementary DNA (cDNA) was synthesized using 1 µg RNA with a random hexamer and oligo dT primers per the manufacturer's instructions (One script, Takara). Real-time polymerase chain reaction (RT-PCR) was performed for OCT1 and beta-actin gene using their specific primers at annealing temperatures of 54 °C and 56 °C, respectively (rabbit OCT1, Forward: GACAGCAGAGAGAAGAGAGAGA, Reverse: AGAGAGAATGCCGTAGGATTTG; rabbit Beta-actin Forward: GCTTCTAGGCGGACTGTTAG, Reverse: CGAATAAAGCCATGCCAATCTC).

5.2.4.2 Protein expression by Western Blotting

Lacrimal gland was homogenized using radioimmunoprecipitation assay (RIPA) buffer with protease inhibitor, phenyl methyl sulfonyl fluoride (PMSF), and ethylene diamine tetra acetic acid (EDTA). Tissue samples were agitated at 4°C for 1 h and then centrifuged at 7500 g for 10 mins at 4 °C. The supernatant was collected and total protein was quantified using Bradford reagent. The protein sample was prepared by denaturation at 95 °C for 10 mins and loaded (30 µg) onto 12 % acrylamide gel. Protein was separated based on molecular weight and transferred to a polyvinylidene difluoride (PVDF) membrane. Membranes were then blocked using 3% bovine serum albumin for 1 h at room temperature. Further, the membrane was incubated with primary antibody (Recombinant Anti-SLC22A1/OCT1 antibody, Abcam (ab181022)) at 1:5000 dilution overnight at 4 °C. The membrane was washed thrice with 1X tris buffered saline with 0.1% tween 20 (TBST), 20 mins for each wash, and then incubated with secondary antibody (Goat secondary antibody-HRP conjugated) at 1:2000 dilution for 1 h at room temperature. After incubation, the membrane was washed thrice with 1X TBST as mentioned above and immunoreactivity to the target protein was detected by enhanced chemiluminescent reagent using ChemDoc (Fusion Solo S, Vilber) (Mahmood and Yang 2012).

5.2.4.3 Localization by Immunohistochemistry

For immunohistochemistry, paraffin-embedded sections were deparaffinized and rehydrated using xylene, followed by decreasing the concentration of ethanol (100%, 90%, 70%, 50%) and finally washed with water. Antigen epitopes were retrieved using 10 mM sodium citrate buffer, pH 6.0, heated at 95 °C for 20 mins. Slides were allowed to cool at room temperature for 20 mins. Further, the sample was blocked with 1 % BSA for 1 h at room temperature and then incubated with primary antibody (1:500 dilution) (Monoclonal Anti-SLC22A1, 2C5, Novus Biologicals) overnight at 4°C. The slides were then washed thrice and re-incubated with fluorescence conjugated secondary antibody (Novus Biologicals (NB7570)) for 1 h at room temperature and counter-stained with 1 µg/ml 4',6-diamidino-2-phenylindole (DAPI) for 20 mins at room temperature. After thorough washing, sections were mounted with a Fluoroshield and visualized under a confocal microscope (Leica, Germany).

5.2.5 Tear Kinetics of topically administered predicted substrates in the presence and absence of OCT1 blockers

Among the predicted substrates, topical tear kinetics studies were performed for Piroxicam, Pregabalin, Glipizide, Busulfan, and Cyclophosphamide in the presence and absence of OCT1 blocker (Atropine and Quinidine).

5.2.5.1 Preparation of substrate and blocker solutions

The drugs were weighed per their equivalent weight from their respective salt forms. Piroxicam (3.01 mM) and Pregabalin (6.28 mM) were dissolved in 5% dimethyl sulphoxide (DMSO) in phosphate buffered saline (PBS), pH 7.4. Glipizide (2.24 mM) was dissolved in 6%

DMSO and 12% ethanol in PBS, pH 7.4. Busulfan (4.01 mM) was dissolved in 10% DMSO in water, and cyclophosphamide (3.01 mM) was dissolved in PBS, pH 7.4. Both atropine (3.45 mM) and quinidine (3.08 mM) were dissolved in PBS, pH 7.4. All the solutions were filtered using a 0.22 μm filter before administration (Nirmal, Singh, et al. 2013a).

5.2.5.2 Topical administration of substrate and blockers and sample collection

Tear kinetics of topically administered substrate and blockers were performed in New Zealand White rabbits (Nirmal, Singh, et al. 2013a). Topical drops (50 μl) of substrates and blockers were administered using a calibrated pipette in the right eye, whereas the left eye served as control. Rabbits were divided into three groups for each tested drug: Group 1: Control (Only substrate), Group 2: Atropine pre-treated (Substrate + Atropine), and Group 3: Quinidine pre-treated (Substrate + Quinidine). In all the groups, the substrate was administered in the right eye, whereas in the pre-treated group, blockers were administered 30 min before the substrate administration. Tears were collected at pre-determined time points (5 min, 15 min, 30 min, 1 h, 2 h) after substrate administration by placing the Schirmer strips in the lateral canthus of the treated eye. The tears were allowed to flow till the 10 mm mark, and the strip was cut and stored at -80 °C till further analysis by the developed Liquid chromatography-mass spectrometry (LCMS-MS) or High-performance liquid chromatography (HPLC) method.

5.2.6 Tear Kinetics of intravenously administered substrates in the presence and absence of OCT1 blockers

5.2.6.1 Preparation of substrate and blocker solutions

For intravenous administration of substrate (Cyclophosphamide, 40 mg/ml) solution was prepared in 0.9% sodium chloride (saline), pH 7.4. Drug was weighed and transferred to a

sterile container, followed by the addition of sterile saline to obtain the desired concentration. For topical administration of blockers, atropine (3.45 mM) and quinidine (3.08 mM) were dissolved in PBS, pH 7.4. All the solutions were filtered using a 0.22 µm sterile filter before administration.

5.2.6.2 Intravenous administration of substrate and topical administration of blockers and sample collection

To understand the functional role of OCT1 in lacrimal gland for the uptake of systemic drugs, tear kinetics of intravenously (i.v.) administered substrates (15.5 mg/kg) was performed with topically administered blocker in New Zealand White rabbits (Nirmal, Sirohiwal, et al. 2013a; Sharma et al. 2021). Animals were divided into three groups for each drug: Group 1: Control (Only substrate, iv), Group 2: Atropine pre-treated (Substrate, i.v. + Atropine, Topical), and Group 3: Quinidine pre-treated (Substrate, i.v. + Quinidine, Topical). The substrate was administered as an intravenous bolus injection through the marginal ear vein in all the groups. In blocker pre-treated groups, topical drops (50 µl) of blocker were administered in the right eye 30 mins before substrate administration, using a calibrated pipette. After substrate administration, tears were collected at pre-determined time points (5 mins, 15 mins, 30 mins, 1 h, 2 h) and stored at -80 °C till further analysis.

5.2.7 Sample processing and analysis

The tear samples were thawed, and 0.2 ml of extraction solvent was added (**Table 5.1**). The strips were soaked in extraction solvent for 1 min and vortexed at high speed for 1 min. Further, the samples were centrifuged at 7400 g for 5 mins, and the collected supernatant was injected into HPLC/LCMS-MS for drug quantification.

Table 5.1: Extraction solvents for drugs. HPLC: High Performance Liquid Chromatography, LCMS-MS: Liquid Chromatography Mass Spectrometry

S.No.	Drug	Concentration of Internal standard	Extraction solvent	Analytical Method
1	Piroxicam	-	Methanol	HPLC
2	Glipizide	-	Methanol	
3	Pregabalin	100 ng/ml Gabapentin	Methanol	LCMS-MS
4	Busulfan	100 ng/ml Dexamethasone	Acetonitrile	
5	Cyclophosphamide		0.1% Formic acid in Methanol	

5.2.8 Effect of atropine on tear secretion

Atropine solution (0.1 %) was prepared in PBS, pH 7.4 and topically administered (50 µl) to the right eye of New Zealand white rabbit using calibrated pipette. Tear flow was measured using Schirmer strip for 1 min and the reading was recorded at pre-determined time intervals till 2 h.

5.2.9 Analytical method development

5.2.9.1 High Performance Liquid Chromatography (HPLC)

HPLC method was developed for quantification of Piroxicam and Glipizide using Reverse Phase HPLC (Shimadzu). Kromasil C18 column (5 µm, 250 x 4.6 mm) column was used for separation of drugs. The validation parameters are given in the **Table 5.2**.

Table 5.2: HPLC method parameters for Piroxicam and Glipizide.

S.No.	Drug	Aqueous Phase	Organic Phase	Ratio (A:O)	Flow rate (ml/min)	Injection volume (µl)	Absorption wavelength
1	Piroxicam	10mM KH$_2$PO$_4$, pH 4.9	Acetonitrile	60:40	1	10	360 nm
2	Glipizide			55:45			230 nm

5.2.9.2 Liquid Chromatography Mass Spectrometry (LCMS-MS)

LCMS-MS method was developed for the quantification of Pregabalin, Busulfan, and Cyclophosphamide using LCMS-MS, Shimadzu, 8040. Zorbax SB-C18, 4.6 x 50 mm, 3.5 µm column was used for separation of drugs. Electrospray ionization (ESI) was used for the production of ions with positive ionization mode for all drugs. Nebulizing gas flow of 3 L/min, DL temperature of 250 °C, Heat block temperature of 400 °C and Drying gas flow of 15 L/min was set for all the drugs. The validation parameters are given in the **Table 5.3 and 5.4**.

Table 5.3: Liquid chromatography parameters for Pregabalin, Busulfan, and Cyclophosphamide.

S.No.	Drug	Aqueous Phase	Organic Phase	Ratio (A:O)	Flow rate (ml/min)	Injection volume (µl)
1	Pregabalin	0.1% Formic acid	Acetonitrile	Gradient	0.6	2
2	Busulfan	10 mM Ammonium formate		10:90	0.3	10
3	Cyclophosphamide	5 mM ammonium formate with 0.1% formic acid		10:90	0.4	10

Table 5.4: Mass spectrometry parameters for Pregabalin, Busulfan, and Cyclophosphamide. ISTD: Internal standard.

S.No.	Drug	ISTD	m/z Transition	ISTD Transition	Collision energy (Drug, ISTD)
1	Pregabalin	Gabapentin	160.2→54.9	172.1→154.1	
2	Busulfan	Dexamethasone	264.1 → 151.0	393 →147.0	-11, -23
3	Cyclophosphamide		261.70→140.0	393→147.0	-22, -30

5.2.10 Statistical analysis

All the data is represented as mean ± Standard error mean (SEM) with at least n=3. Student's t-test (unpaired) was used to compare the statistical difference between two groups, whereas Two-way ANOVA was used to compare the statistical difference between more than two groups using Dunnett's test. GraphPad Prism (Ver 8.0) was used to calculate significant differences.

5.3 Results

5.3.1 Histology of the lacrimal gland

The eye is surrounded by fat tissues; therefore, histology was performed as per our previously reported method to confirm the isolated tissue as a lacrimal gland (Malani and Nirmal 2022) (**Figure 5.1**). Lacrimal gland consists of acinar cells which secretes into intralobular and interlobular ducts further converging to form intralobar and interlobar ducts. The tear is secreted from the main excretory duct to the ocular surface (Bromberg et al. 1994; Schechter et al. 2010a).
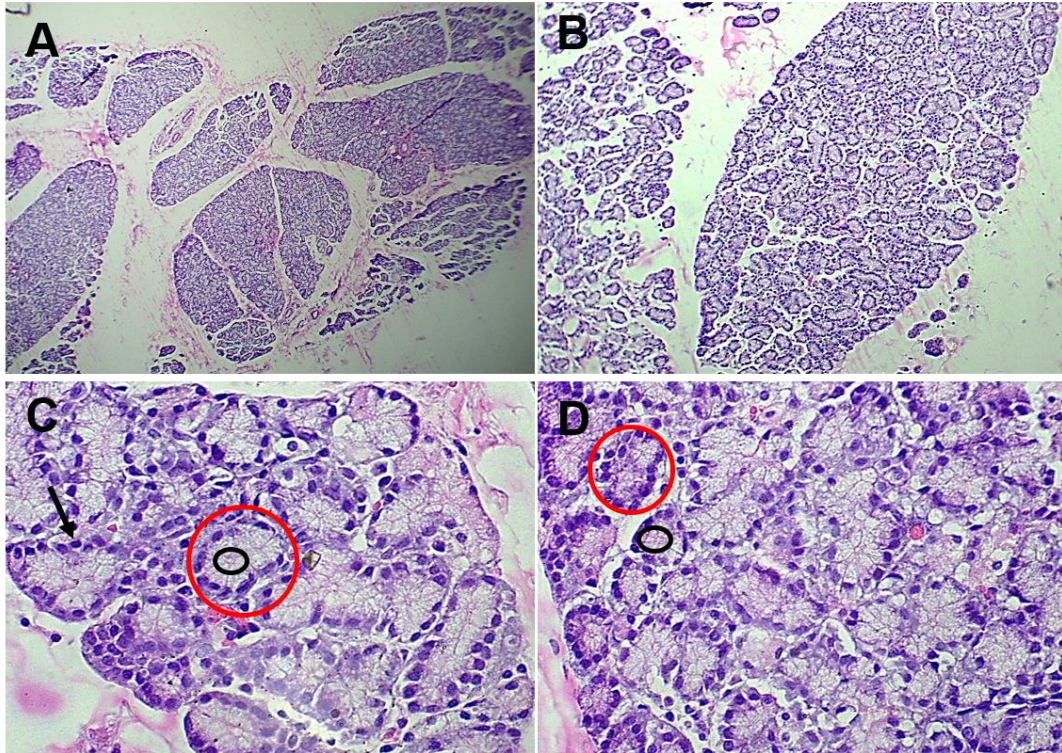
Figure 5.1: Histology of rabbit lacrimal gland. Paraffin sections of rabbit lacrimal gland stained with Hematoxylin and Eosin stain were visualized under light microscope, A. Under 4X, B. Under 10X, C and D. Under 40X. Black arrow indicates acinar cell; black circle indicates intercalated duct; and red circle indicates lobule of acini.

5.3.2 Expression of OCT1 in lacrimal gland

RNA was isolated using the trizol method, and RT-PCR was performed to amplify OCT1 and beta-actin genes (housekeeping gene). Liver RNA was used as the positive control. The OCT1 expression was normalized using beta-actin and was expressed in both liver and lacrimal gland with a relatively less expression in the lacrimal gland compared to liver (**Figure 5.2A**). Further, to confirm the OCT1 protein expression, western blotting was performed for proteins isolated from the lacrimal gland. The band at 61 kD indicated the presence of OCT1 protein in the lacrimal gland (**Figure 5.2B**), whereas the beta-actin band was observed around 42kD. Finally, immunohistochemistry was performed for fixed lacrimal gland tissue to visualize the localization of OCT1 in the lacrimal gland using a confocal microscope. OCT1 protein was

strongly expressed in the terminal acinar and intralobular cells with weak expression near the central excretory duct (**Figure 5.2C**). Further, OCT1 expression was also visualized in rabbit cornea by immunohistochemistry (**Figure 5.3**).
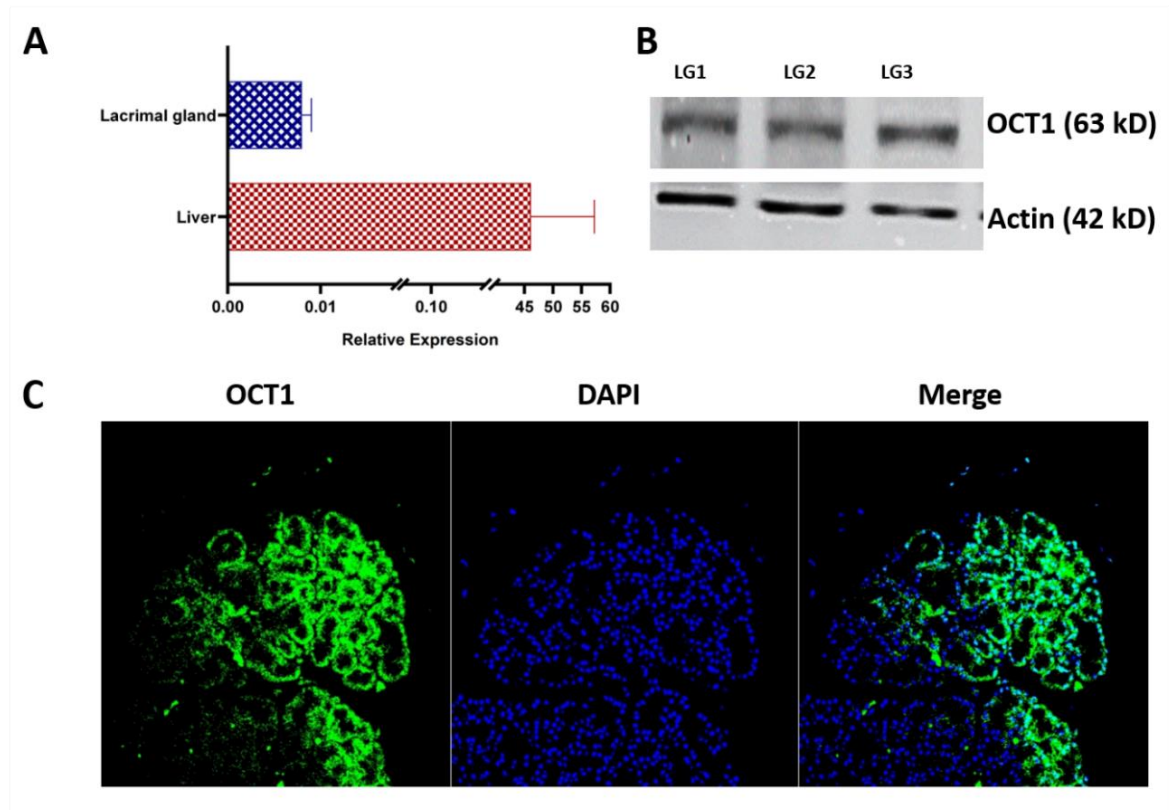
Figure 5.2: Expression of Organic cation transporter (OCT1) in rabbit lacrimal gland (LG). A. Gene expression of OCT1 was evaluated using RT-PCR studies. OCT1 was found to be expressed in lacrimal gland though less than liver. B. Western blot was performed for protein isolated from lacrimal gland (n=3) and the band near 63 kD upon reacting with Anti-SLC22A1/OCT1 antibody indicates the presence of OCT1. C. Immunohistochemistry of rabbit lacrimal gland with Anti-SLC22A1/OCT1 antibody indicates the strong expression of OCT1 in terminal acinar cells. Green signal represents OCT1, and blue signal represents nuclei stained with DAPI.

OCT1	DAPI	Merge
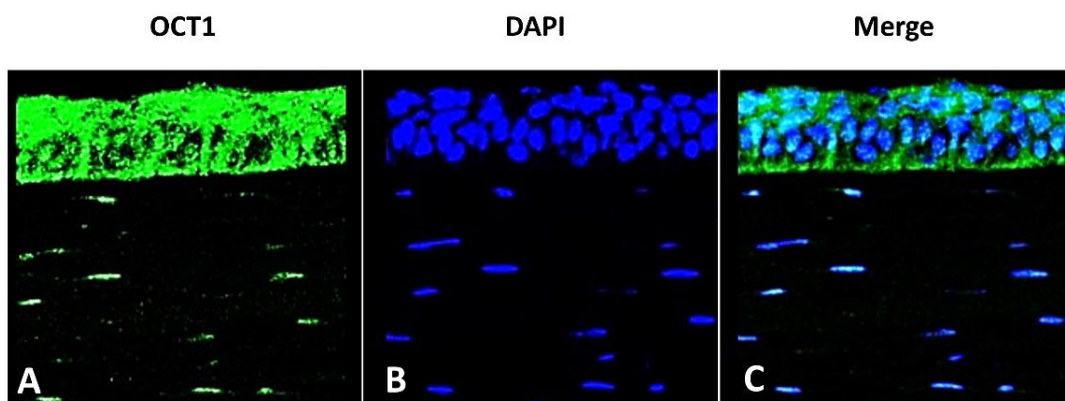
Figure 5.3: Expression of Organic cation transporter (OCT1) in rabbit cornea. Immunohistochemistry of rabbit cornea with Anti-SLC22A1/OCT1 antibody indicates the expression of OCT1 in both apical and basal side of corneal epithelium. Green signal represents OCT1, and blue signal represents nuclei stained with DAPI.

5.3.3 Topical tear kinetics of predicted OCT1 substrates

HPLC method was developed for quantification of Piroxicam and Glipizide, whereas LCMS-MS method was developed for quantification of Busulfan, Cyclophosphamide and Pregabalin. The linear regression (R^2) for all the developed methods was found to be value > 0.99 (**Figure 5.4**).
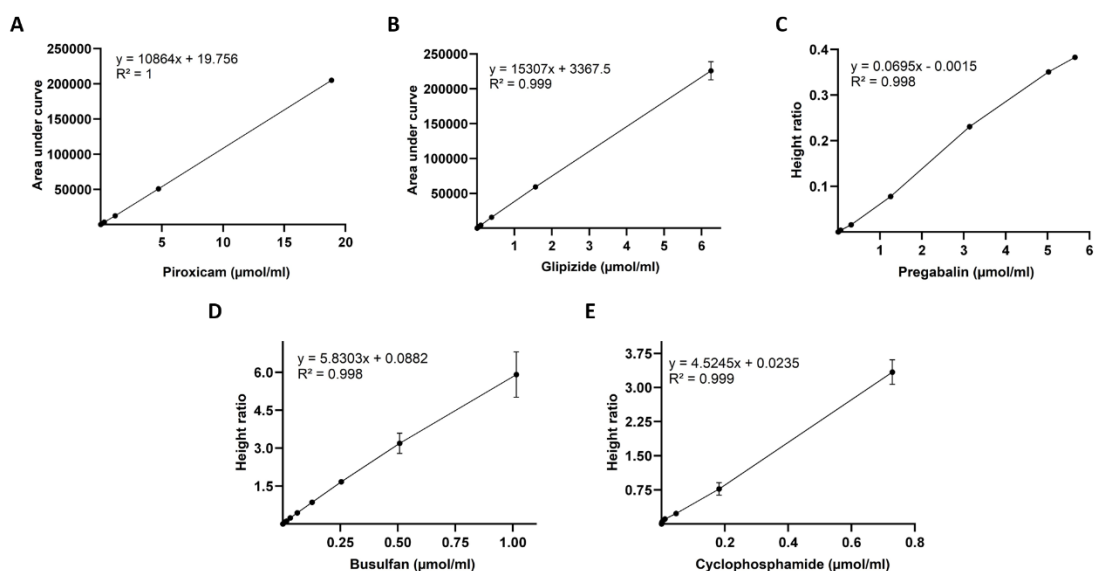
Figure 5.4: Calibration curve of drug using HPLC/LCMS-MS methods. A. Piroxicam ranging from 0.0037 to 18.86 µmol/ml, B. Glipizide ranging from 0.027 to 14.02 µmol/ml, C. Pregabalin ranging from 0.006 to 5.65 µmol/ml, D. Busulfan ranging from 0.008 to 1.01 µmol/ml, and E. Cyclophosphamide ranging from 0.0007 to 0.73 µmol/ml.

Topical tear kinetics of predicted OCT1 substrates were performed for initial rapid screening to confirm the AI predictions. Predicted substrates were administered topically in the presence and absence of OCT1 blocker (Atropine and Quinidine), and pharmacokinetic analysis was performed (**Table 5.5**). In Piroxicam group (**Figure 5.5A**), tear concentration of Piroxicam was higher in blocker pre-treated group compared to control group at all the time points. However, significant difference was observed at 15 mins, 1 h and 2 h in atropine pre-treated group and at 15 mins, and 30 mins in quinidine pre-treated group. In Busulfan group (**Figure 5.5B**), tear concentration of Busulfan was higher in blockers pre-treated group compared to control group at all time points. However, significant difference was observed at 30 mins, 1 h, and 2 h in atropine pre-treated group, and at all time points except 5 mins in quinidine pre-treated group. In Glipizide group (**Figure 5.5C**), tear concentration of Glipizide was higher in atropine pre-treated group compared to control group at all time points with significant difference at 5 mins. In quinidine pre-treated group, Glipizide concentration was higher at all time points except 30 mins than control group with significant difference at 5 mins. In Pregabalin group (**Figure 5.5D**), tear concentration of Pregabalin was higher in atropine pre-treated group compared to control group with significant difference at 30 mins. In quinidine pre-treated group, Pregabalin concentration was less than control group with significant difference at 15 mins and 2 h. In Cyclophosphamide group (**Figure 5.5E**), tear concentration of cyclophosphamide was higher in control group compared to atropine pre-treated group at all time points with significant difference at 15 mins. In quinidine pre-treated, Cyclophosphamide concentration was higher than control group at all time points with significant difference at 15 mins.

Table 5.5: Pharmacokinetic parameters of topically administered predicted substrates in presence and absence of Organic cation transporter (OCT1) blockers (Atropine, 3.45 mM and Quinidine, 3.08 mM).

Pharmacokinetic parameters of topically administered substrates in tears			
Drug	C_{max} (µmol/mL)	$AUC_{(0-2h)}$ (µmol/mL*h)	$AUC_{(0-2h)}$ fold difference
1) Piroxicam (3.01 mM) [a]			
Control	2.13	0.43	-
Atropine pre-treated	3.13	0.82	1.90
Quinidine pre-treated	3.37	0.72	1.67
2) Busulfan (4.01 mM) [a]			
Control	10.47	1.05	-
Atropine pre-treated	13.51	2.10	2.01
Quinidine pre-treated	26.34	6.14	5.88
3) Glipizide (2.24 mM) [a]			
Control	10.81	1.04	-
Atropine pre-treated	4.20	0.51	0.49
Quinidine pre-treated	4.95	0.73	0.70
4) Pregabalin (6.28 mM) [a]			
Control	79.14	8.23	-
Atropine pre-treated	66.72	8.15	0.99
Quinidine pre-treated	70.76	6.35	0.77
4) Cyclophosphamide (3.01 mM) [a]			
Control	114.31	17.94	-
Atropine pre-treated	117.29	15.40	0.86
Quinidine pre-treated	106.09	21.58	1.20

[a] Concentration of substrates administered topically (50 µl).

C_{max}: Maximum concentration, AUC: Area under curve.
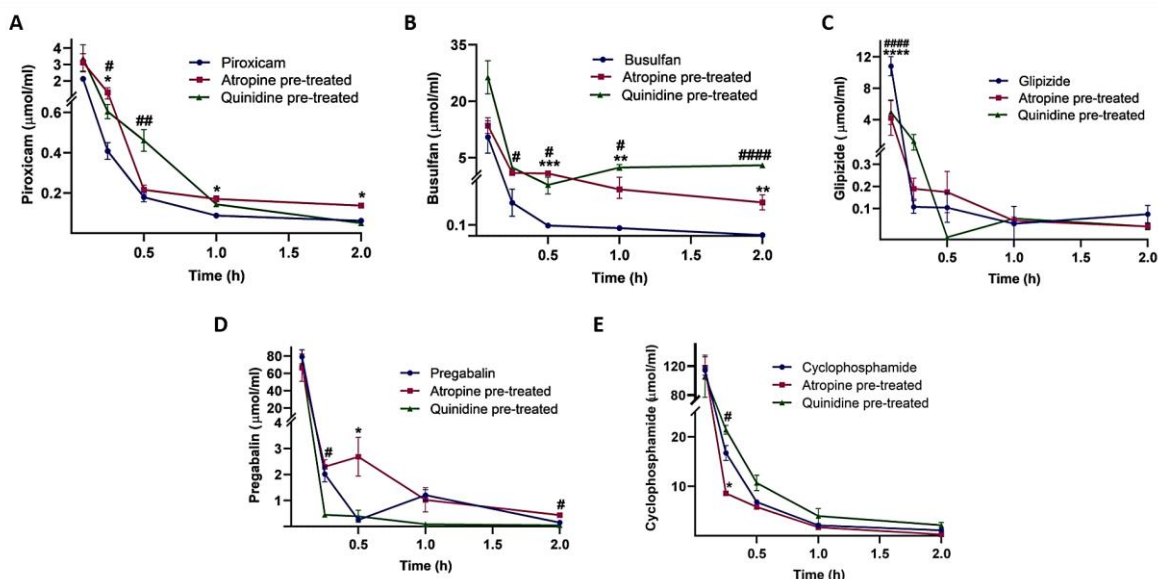
Figure 5.5: Tear kinetics of topically administered substrates (0.1%) in presence and absence of topical Organic cation transporter (OCT1) blocker (0.1% Atropine and 0.1% Quinidine). A. In Piroxicam group, tear concentration of Piroxicam was higher in blocker pre-treated group compared to control group at all the time points. However, significant difference (Student's t-test) was observed at 15 mins, 1 h and 2 h in atropine pre-treated group (*p<0.1) and at 15 mins, and 30 mins in quinidine pre-treated group (#p<0.1, ##p<0.01). B. In Busulfan group, tear concentration of Busulfan was higher in blockers pre-treated group compared to control group at all time points. However, significant difference (Student's t-test) was observed at 30 mins, 1 h, and 2 h in atropine pre-treated group, **p<0.01, ***p<0.001) and at all time points except 5 mins in quinidine pre-treated group (#p<0.1, ####p<0.0001). C. In Glipizide group, tear concentration of Glipizide was higher in atropine pre-treated group compared to control group at all time points with significant difference (Student's t-test) at 5 mins (****p<0.0001). In quinidine pre-treated group, Glipizide concentration was higher at all time points except 30 mins than control group with significant difference (Student's t-test) at 5 mins (####p<0.0001). D. In Pregabalin group, tear concentration of Pregabalin was higher in atropine pre-treated group compared to control group with significant difference (Student's t-test) at 30 mins (*p<0.1). In quinidine pre-treated group, Pregabalin concentration was less than control group with significant difference at 15 mins and 2 h (#p<0.1). E. In Cyclophosphamide group, tear concentration of cyclophosphamide was higher in control group compared to atropine pre-treated group at all time points with significant difference (Student's t-test) at 15 mins (*p<0.1). In quinidine pre-treated, Cyclophosphamide concentration was higher than control group at all time points with significant difference (Student's t-test) at 15 mins (#p<0.1).

5.3.4 Intravenous tear kinetics of OCT1 substrates

LCMS-MS method was developed to quantify Cyclophosphamide (**Figure 5.4**). In cyclophosphamide group, the substrate's tear concentration was higher in the control group than in the topically administered blocker pre-treated group (**Table 5.6**). The $AUC_{(0-2h)}$ of

cyclophosphamide was found to be 1.7-fold less in the atropine pre-treated group and 2.4-fold less in the quinidine pre-treated group when compared to the control group (**Figure 5.6**).

Table 5.6: Pharmacokinetic parameters of intravenously administered substrate in presence and absence of topical Organic cation transporter (OCT1) blockers (Atropine, 3.45 mM and Quinidine, 3.08 mM).

Pharmacokinetic parameters of intravenously administered substrates in tears			
Drug	**C_{max} (µmol/mL)**	**AUC (µmol/mL*h)**	**AUC fold difference**
1) Cyclophosphamide (15.5 mg/kg) [a]			
Control	174.59	212.93	-
Atropine pre-treated	129.39	124.84	1.71
Quinidine pre-treated	75.14	88.07	2.42

[a] Dose of substrate administered intravenously

C_{max}: Maximum concentration, AUC: Area under curve.
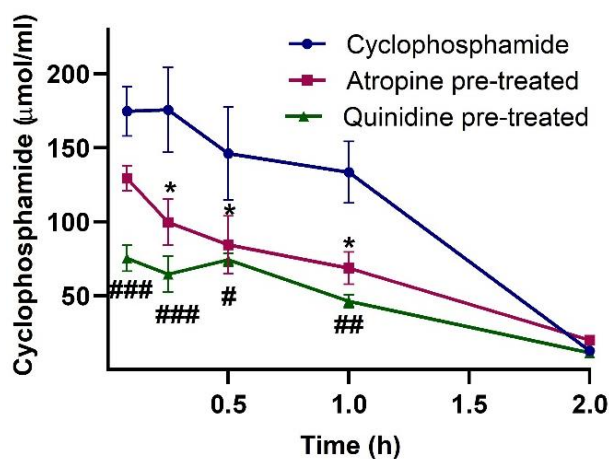
Figure 5.6: Tear kinetics of intravenously administered OCT1 substrates in presence and absence of topical Organic cation transporter (OCT1) blocker (0.1% Atropine and 0.1% Quinidine). In Cyclophosphamide group, tear concentration of Cyclophosphamide was found to be less in blockers pre-treated group than control group at all time point. Significant difference was observed at 15 mins, 30 mins and 1 h in atropine pre-treated group (****$p < 0.0001$), and at all time points except 2 h in quinidine pre-treated group (#$p < 0.1$, ##$p < 0.01$, ###$p < 0.001$).

5.3.5 Effect of atropine on tear secretion

The effect of topically administered 0.1% Atropine (50 µl) on tear secretion was evaluated for up to 2 h. The tear secretion did not change significantly after a one-time administration of 0.1% Atropine (**Figure 5.7**).
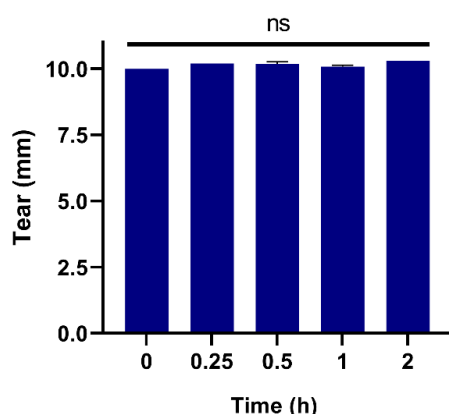
Figure 5.7: Effect of Atropine on tear secretion. Atropine (0.1 %) was administered topically in the right eye of New Zealand White rabbit and tear secretion was measured for 1 min at each time point till 2 h. No significant difference (One-way ANOVA) was observed in tear secretion till 2 h after atropine drop administration when compared before administration (Time 0 h).

5.4 Discussions

Several systemic drugs used for acute and chronic diseases are known to cause ocular toxicities, which could be reversible or irreversible, leading to vision loss (Castells et al. 2002; Constable et al. 2022a; Li et al. 2008; Liu et al. 2018; Moorthy and Valluri 1999; Mukhtar and Jhanji 2022; Prakash et al. 2019; Richa and Yazbek 2010; Santaella and Fraunfelder 2007). Therefore, it is crucial to understand the entry mechanism of systemic drugs into the eye despite ocular barriers. We hypothesized that the systemic drugs (cations) are falsely recognized as substrates by OCT1 in the lacrimal gland and facilitate entry into the anterior eye segment. OCT1 is reported to be highest expressed isoform in the ocular tissues and therefore the functional role of OCT1 in lacrimal gland was evaluated (Zhang et al. 2008).

Functional role of organic cation transporters in lacrimal gland

Human and rabbit lacrimal glands are known to share more similarities when compared to mice or rats and is widely used as an animal model for preclinical ocular studies (Schechter et al. 2010a). Hence, the lacrimal gland was isolated from rabbits to evaluate the OCT1 expression in the lacrimal gland using RT-PCR, Western blotting and Immunohistochemistry (Honkanen et al. 2020). Both OCT1 gene and protein was expressed in the lacrimal gland. IHC studies revealed that localization of OCT1 was not uniform throughout the lacrimal gland due to the heterogeneous nature of acinar cells concerning their functions (Bromberg et al. 1994; Djeridane 1994). Several proteins are known to be expressed only in a specific subset of acinar cells. The expression of OCT1 found uniquely in terminal acinar cells indicates these cells possess a particular transport function associated with the primary secretion of lacrimal fluid (Bromberg et al. 1994; Schechter et al. 2010a). The presence of several organic amines, such as epinephrine, dopamine, histamine, and serotonin, in the tear explains the presence of OCT1 in the lacrimal gland (Martin and Brennan 1993, 1994; Van Haeringen 1981a). For the first time, the current study reported the presence of OCT1 in the lacrimal gland.

Earlier studies have reported the gene expression of OCT1 in rabbit cornea; however, its localization was not reported (Zhang et al. 2008). This study reported the expression of OCT1 in both the apical and basal surfaces of the cornea. The OCT1 is positioned apical (tear) to basolateral (aqueous humor) in the cornea as indicated from previously reported studies where the concentration of well-known OCT1 substrate tetraethyl ammonium, when administered topically in the presence of OCT1 blocker, increased in the tear (Nirmal, Singh, et al. 2013a). This leads to an understanding that when a substrate is administered topically in the presence of an OCT1 blocker, it prevents the corneal uptake of the substrate, inhibiting the entry from tear to aqueous humor and increasing the substrate's precorneal

concentration (Nirmal, Singh, et al. 2013a). In the present study, Piroxicam, Busulfan, and Cyclophosphamide showed significant fold differences between the control and blockers pre-treated group. Whereas Pregabalin and Glipizide, did not show significant difference in control and blockers pre-treated group which could be due to their physicochemical properties. Our studies indicated that the molecules with a molecular weight between 200 to 400 g/mol and the presence of sulfur moiety in their structure could be one of the critical factors for substrate recognition by OCT1 (Redeker et al. 2022). We also found that around 53% of OCT1 substrates show at least one sulfur group in their structure (Malani et al. 2023). The in vivo studies confirm that the predicted molecules were OCT1 substrates, validating the AI predictions.

Cyclophosphamide, a predicted substrate was used to delineate the functional role of OCT1 in the lacrimal gland. Cyclophosphamide was chosen as the substrate for intravenous administration due to its water solubility. The intravenous dose of Cyclophosphamide was decided based on its clinical dose. However, since the study aims only proof-of-concept that systemic drugs reach the eye through transporters in the lacrimal gland, a sub-therapeutic dose was chosen which is also followed in other transporter studies (Sharma et al. 2021). The human dose was converted to rabbit equivalent dose based on body surface area by dividing or multiplying the human dose (mg/kg) by the correction factor ratio as given in the reported literature (FDA 2005).

The reference body weight for rabbits is 1.8 kg; therefore, to convert the human dose into rabbit effective dose, the human dose was multiplied 3.1 times or divided by 0.324 times.

Based on this conversion, the Cyclophosphamide dose was chosen as 15.5 mg/kg (40 mg to 50 mg/kg in a span of 2 to 5 days) for intravenous injection (FDA 2013; Kim et al. 2011).

Due to intravenous administration of substrate, 100% bioavailability is achieved, which results in rapid absorption in the lacrimal gland indicated by the presence of substrate in tears, which decreased over a period. Based on the tear kinetics of intravenously administered cyclophosphamide, we propose that the OCT1 in the lacrimal gland is positioned from the basal to the apical side. Earlier studies have reported nucleoside transporters in the lacrimal gland positioned from the apical side acinar cells (Sharma et al. 2021).

Also, studies have reported that the drug reaches lacrimal gland when administered topically. Cyclosporine when administered topically was detected in the lacrimal gland at sufficient levels to treat dry eye (Acheampong et al. 1999; Weiss and Kramer 2019). Therefore, topical route of administration was selected for administration of blockers to block the OCT1 transporters in the lacrimal gland. Atropine and Quinidine was chosen as the blockers for OCT1. Since, most of the molecules show overlapping specificity for the transporters and also the experimental conditions determine the fate of substrates, it is recommended to use at least two blockers (Koepsell et al. 2007). Atropine shows highest affinity towards OCT1 transporter whereas Quinidine shows affinity to all three isoforms of OCT (Koepsell et al. 2007). The use of atropine in eye is known to cause dry eye which could be attributed to reduced tear secretion and result in the decreased substrate level in tears (Burgalassi et al. 1999). However, our studies indicated that one-time administration of 0.1 % atropine did not significantly alter the tear secretion till 2 h.

Several drugs have been reported for off-target accumulation, leading to unwanted exposure and, therefore, causing toxicity. Earlier studies have reported the role of transporters in off-target accumulation leading to toxicity, such as cisplatin and ifosfamide induced nephrotoxicity due to their interaction with OCT in kidney (Filipski et al. 2009). Doxorubicin, an anticancer drug is known to cause cardiac toxicity upon its interaction with OCT transporters (Huang et al. 2018; Huang et al. 2020). Even ocular uptake of vigabatrin (an anti-epileptic drug) was attributed to the taurine transporters present in the posterior segment of the eye (Police et al. 2020a). Though several drugs have been reported to cause ocular toxicity, their entry mechanism in the eye is not clear. Many systemic drugs which are known to be OCT1 substrates could also enter the eye through OCT1 transporters and cause ocular toxicity, such as Ethambutol induced optic neuritis, Trimethoprim induced conjunctival and scleral infection, Diltiazem induced edema and retinopathy, Ipratropium induced glaucoma, Verapamil induced dry eye, and Amantadine induced edema and cataract (Fraunfelder and Fraunfelder 2021; Hendrickx et al. 2013; Manisha 2023; Saxena et al. 2021). Our current study could open a new research direction to understand and prevent the ocular toxicity caused by systemic drugs. The study indicates that transporters such as OCT1 and other uptake transporters in the lacrimal gland play a vital role in the drug disposition from blood to tear. Therefore, understanding the drug-transporters interaction and the role of membrane transporters at ocular barriers could facilitate the prevention or timely intervention of ocular toxicity caused by systemic drugs.

5.5 Conclusions

The localization of OCT1 was found to be in both the apical and basal sides of the rabbit cornea. Topical tear kinetics studies showed difference in the predicted substrate

pharmacokinetics which could be due to their physiochemical properties, and the concentration used to perform the study. The developed AI model can be used as a screening platform to understand and predict the drug-transporter interaction in the initial drug discovery phase to avoid future unseen toxicities.

The expression and localization of OCT1 in rabbit lacrimal glands were reported for the first time in this study. Moreover, the functional role of OCT1 in the lacrimal gland was confirmed by tear kinetics of intravenously administered OCT1 substrates. The topical administration of the blocker revealed the uptake positioning of OCT1 in the lacrimal gland from basal (blood) to apical side (tear). More studies are required to understand the role of various other influx and efflux transporters as well in the lacrimal gland to decipher the role of transporters in systemic drug-induced ocular toxicity.

Chapter 6

Investigation of non-therapeutic inhibitors (Pharmaceutical excipients) to inhibit the uptake of drug substrates by OCT transporters using in vitro and in vivo models
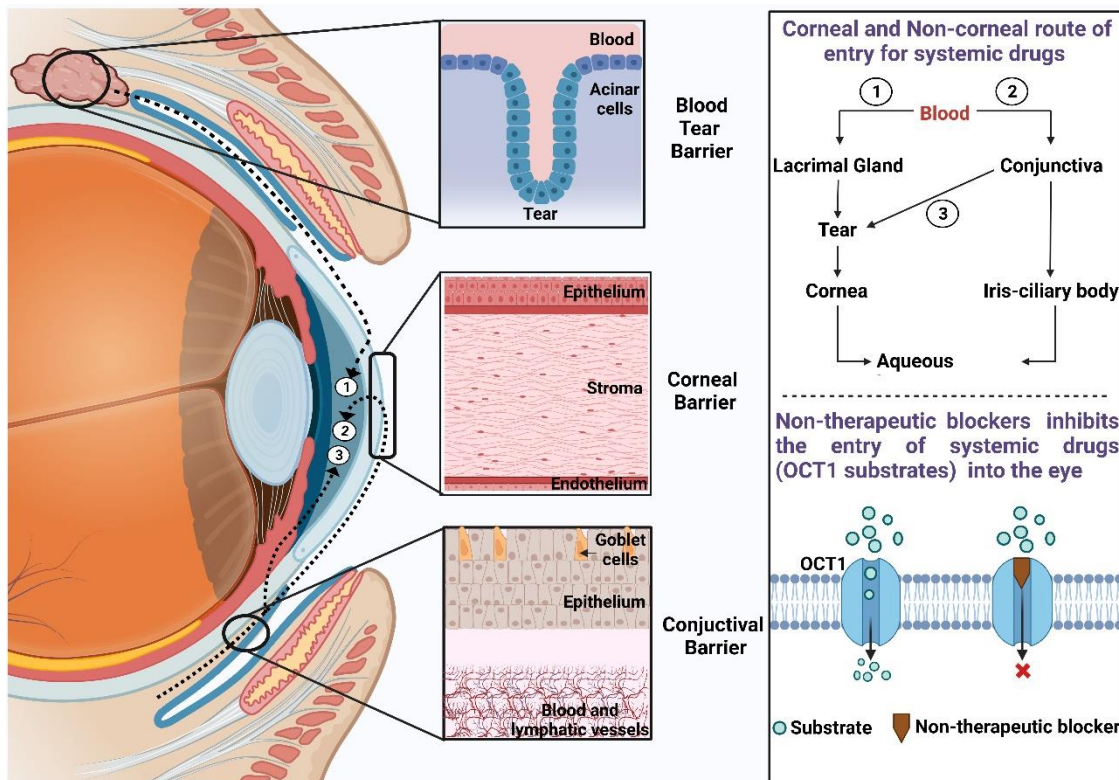
6.1 Introduction

Drugs administered for chronic medical conditions are also associated with life-threatening adverse effects. Many of the times, these effects are irreversible even upon discontinuing the medication (Curtin and Schulz 2011). Systemic drugs can enter the ocular tissues via anterior or posterior route and cause ocular toxicity which disturbs the quality of life (Garg and Yadav 2019). The blood tear barrier and blood aqueous barriers acts as the major limiting barrier in the drug absorption from systemic circulation to the anterior segment of the eye (Awwad et al. 2017). Tear fluid secreted from lacrimal gland is the major source of nourishment to the ocular surface as it consists of several proteins, lipids, hormones, neurotransmitters and other endogenous molecules (Rolando and Zierhut 2001; Van Haeringen 1981a). Therefore, the systemic drug entering the anterior segment of the eye could be attributed to tear secretion from the lacrimal gland.

Membrane transporters are crucial in drug absorption, distribution, metabolism, and excretion. Due to the evolutionary conservation of transporters, slight changes in the structure of substrates are not differentiated, leading to false recognition of the xenobiotics, including drug molecules as their substrates, and facilitating their transport across the ocular barriers. Several United States Food and Drug Administration (USFDA) approved drugs are known to interact with the transporters and act as substrates or inhibitors (Sadee and Dai 2005). Due to the ubiquitous distribution of these transporters across the body, most of the drugs administered systemically are also known to accumulate at off-target sites, which could lead to toxicity (Hafey et al. 2022).

Interaction of excipients with organic cation transporter

Ocular toxicity due to systemic drugs could also be mediated by drug uptake through membrane transporters. The presence of membrane transporters in ocular barriers is well-reported (Zhang et al. 2008). In our earlier studies, we have also shown the presence of organic cation transporters (OCT) in lacrimal gland which plays a functional role in the entry of systemic drugs into the eye. Moreover, studies have also indicated the role of transporters in drug accumulation in ocular tissues. Taurine transporters present in the BRB were found responsible for the entry of Vigabatrin into the retina, which is known to cause retinal toxicity, leading to vision loss (Police et al. 2020b). Similarly, transporters have been reported to cause toxicity in other organs, such as Cisplatin accumulation in the kidney due to organic cation transporters (Ciarimboli 2011).

Blocking the membrane transporters locally (topical eye drops) could be a possible solution to reduce or minimize the off-target (anterior eye segment) drug accumulation. As patients undergo long-term treatment with systemic drugs to treat chronic diseases, the use of an additional drug to block these transporters could be challenging due to drug-drug interactions and the pharmacological actions of the drug blockers. Therefore, we propose using non-therapeutic blockers such as excipients, which can be administered locally to block the transporters and prevent the entry of systemic drugs into the anterior segment of the eye. In the current study, we aim to block the OCT1 transporter which has been reported to be functionally active in the lacrimal gland for drug absorption from blood to tear.

Earlier, excipients used in pharmaceutical preparations were regarded as inert molecules without significant pharmacological activity. However, emerging data suggests that excipients can interact with specific transporters and thus affect the absorption and bioavailability of

drug activity (Gurjar et al. 2018). The commonly used ocular excipients include Tween, Cremophor, Poloxamer, Span, Solutol, Transcutol, Polyethylene glycol, Soluplus, Tocopheryl polyethylene glycol 1000 succinate (TPGS), Hydroxy propyl methyl cellulose which are reported to block the uptake and efflux transporters in vitro, such as OCT, organic anion transporter (OAT), and P-glyco protein (Pgp), and breast cancer resistance protein (BCRP) (Thakkar 2015). Tween 20, Tween 60, and Tween 80 have shown inhibitory effects for OCT1 and OCT2 transporters in renal proximal tubular cell lines (Soodvilai et al. 2017b). However, the potential of excipients to block the activity of OCT1 transporter in vivo for ocular applications is not explored.

The current study aims to screen the potential of various ocular excipients to block the OCT1 transporter using in vitro studies. Further, these interactions are confirmed in vivo by topical administration of blockers to inhibit the entry of systemically administered drugs into the eye.

6.2 Materials and Methods
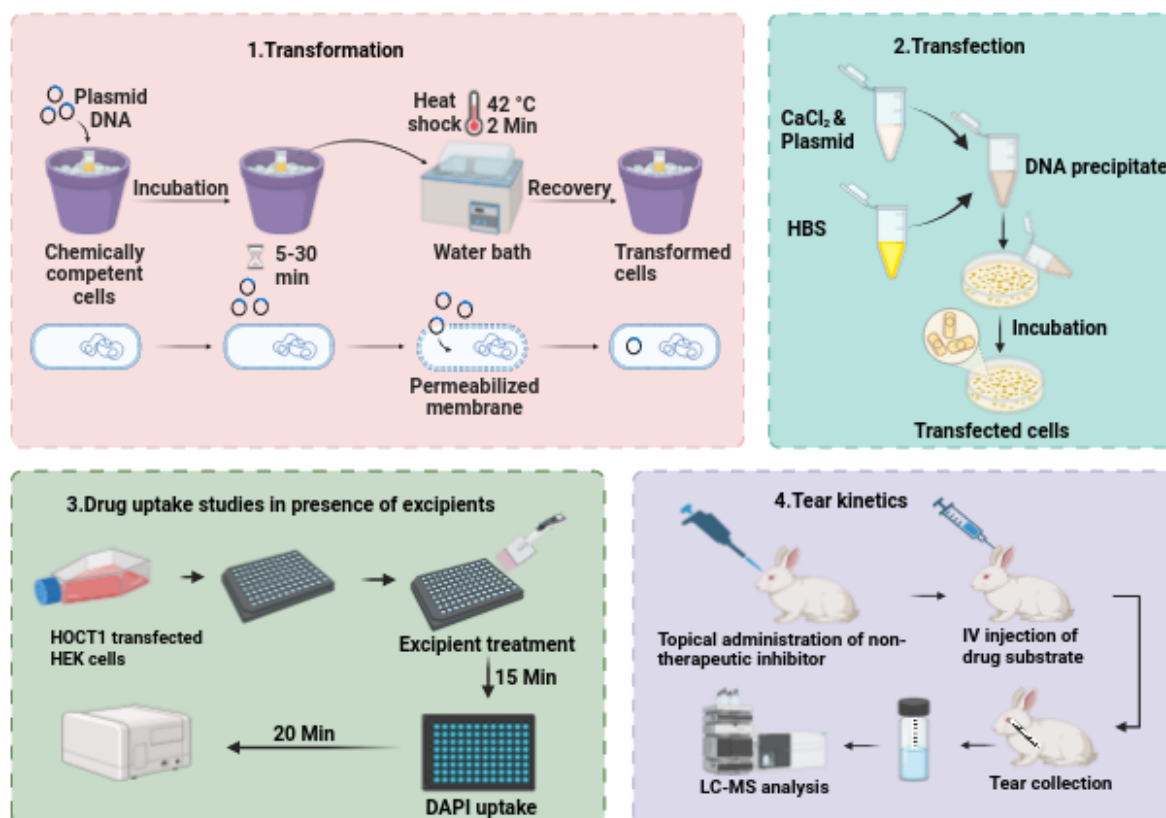
Figure: Workflow of chapter 6 (Objective 3).

6.2.1 Materials

HiPer® plasmid DNA cloning and DNA extraction teaching kit were obtained from HiMedia, India. hOCT1 plasmid was a generous gift from Prof. Kathleen Giacomini, University of California. A black 96-well plate was obtained from Nunc, Thermo Fischer, USA. All cell culture-related materials were procured from HiMedia, India. DAPI was obtained from Sigma Aldrich, USA. LC-MS/MS solvents were procured from Fisher Scientific, USA. All other reagents used were of the highest grade purchased. Milli-Q water was used throughout the experiment unless otherwise mentioned.

6.2.2 Bacterial culture, Cells, and Animals

Human Embryonic Kidney (HEK) 293 cells were obtained as a gift from the Biology Department, BITS-Pilani, Hyderabad campus. Rabbits were procured from VAB-Bioscience Pvt. Ltd. (India). Rabbits were handled according to the National Research Council's Guide for the Care and Use of Laboratory Animals (8th edition) guidelines. All the experiments were approved by the Institutional Animal Ethics Guideline, BITS-Pilani, Hyderabad, India, and all the experiments were performed according to the Association for Research in Vision and Ophthalmology guidelines. Animals were kept under a 12-hour light-dark cycle with ad-libitum access to food and water.

6.2.3 Transformation of hOCT1 plasmid in *Escherichia coli*

The hOCT1 plasmid was transformed into *Escherichia coli* by heat shock method as per manufacturer's instruction (HiMedia, India). Briefly, a sensitive *E. coli* culture was used to transform the hOCT1 pcDNA5 plasmid (which contains the Ampicillin resistance gene). The culture was grown in Ampicillin-free Luria broth overnight at 37 °C at 70 rpm. The competent cells were prepared by allowing the culture to cool down at 4 °C for 10 mins, followed by centrifugation at 4500 rpm for 10 min at 4 °C. Media was removed entirely with no traces left, and 30 ml of 0.1 M calcium chloride solution was added. The cells were resuspended uniformly and allowed to stand at 4 °C for 30 min, followed by centrifugation at 4500 rpm for 10 min at 4 °C. Finally, the pellet was resuspended in 2 ml of 0.1 M calcium chloride solution and stored on ice.

The competent E. coli (0.2 ml) were mixed with 10 µl of the hOCT1 plasmid in a sterile 2 ml tube and incubated on ice for 30 min. The tubes were transferred to a pre-heated water bath

at 42 °C for 2 mins, followed by immediate transfer on ice. After 5 to 10 min, 0.8 ml of Luria broth was added, and tubes were stored at 37 °C for 1 h. To isolate the hOCT1 transformed colonies, the mixture (0.2 ml) was spread plate on Luria agar plates with Ampicillin and incubated at 37 °C for 48 h.

6.2.4 Isolation of hOCT1 containing plasmid from *Escherichia coli*

The transformed colonies were picked and grown in Luria broth. A single isolated colony was transferred to 2 ml broth and grown overnight at 37 °C at 70 rpm. Further, the inoculum was transferred to 50 ml broth and grown overnight at 37 °C at 70 rpm. On the following day, the cell suspension was centrifuged at 1500 rpm for 5 min and washed with 1X phosphate-buffered saline (PBS). The plasmid was isolated from the cells using an alkaline lysis method per the manufacturer's instructions (HiMedia, India). The final product was resuspended in 0.6 ml of elution buffer and evaluated for purity by measuring the $A_{260/280}$ and $A_{260/230}$ values using Nanodrop.

6.2.5 Transfection of hOCT1 plasmid in Human Embryonic Kidney (HEK 293) cells

HEK 293 cells were seeded in a black tissue culture 96-well plate (Nunc, Thermo Fischer) (0.8 x 10^3 per well) in Minimum Essential Eagle Media supplemented with 10 % fetal bovine serum and incubated at 37 °C and 5 % CO_2. After 24 to 30 h, when the cells were 60 to 70 % confluent, the transfection was performed after media replacement using the calcium phosphate method, as reported earlier, with few modifications (Graham and van der Eb 1973; Jordan et al. 1996). Briefly, the plasmid was mixed with 2.5 M of calcium chloride solution, and the volume was made up of water (Solution A) such that the concentration of calcium chloride was 250 mM. Solution A was mixed with an equal volume of 2X Hepes Buffered Saline (HBS)

(Solution B), followed by immediate vortexing. Solution A and B (10 µl) were mixed with a final calcium chloride concentration of 12.5 mM, transferred to cells, and incubated at 37 °C and 5 % CO_2. After 3 h, the media was removed, and the cells were washed with sterile PBS. Further, the cells were incubated with media at 37 °C and 5 % CO_2 for 24 to 48 h. The transfected cells were used for uptake studies.

The overexpression of hOCT1 was confirmed by performing transfection in 24-well plate. Briefly, 2.0×10^4 cells were seeded per well and transfection was performed according to optimized parameters. After 24 h of incubation, RNA was isolated from the cells using the Trizol method. Complementary DNA (cDNA) was synthesized using 1 µg RNA with a random hexamer and oligo dT primers per the manufacturer's instructions (One script, Takara). Real-time polymerase chain reaction (RT-PCR) was performed for the hOCT1 gene using specific primers at annealing temperatures of 54°C, (Human OCT1, Forward: CATAGCCCTCATCACCATTGA, Reverse: GTGCAGGTCAGGTGAGATAAA).

6.2.6 Transporter uptake studies

4',6-diamidino-2-phenylindole (DAPI) is known to be a substrate for OCT1, which emits fluorescence when bound to adenine and thymine base pairs in double-stranded DNA. The transfected HEK-293 cells with hOCT1 plasmid were used to perform a DAPI uptake assay per the previously reported method (Yasujima et al. 2011). Cells were washed with 0.1 ml of Hank's buffer, followed by DAPI treatment at different concentrations and varying uptake times. Cold Hank's buffer (0.1ml) was used to terminate the DAPI uptake, followed by twice washing with buffer. Further, the cells were incubated in 0.1 ml of Hank's buffer, and the DAPI uptake was measured by recording the fluorescence with excitation and emission of 350 nm

and 450 nm using a spectrofluorometer (Spectra Max M4, Molecular Devices). The uptake

kinetics (K_m and V_{max}) were measured using Michaelis Menten's equation by measuring the

accumulation of DAPI over a period of time.

6.2.7 Excipient screening to block OCT1 using in vitro studies

To evaluate the safe range of the excipients to be screened as inhibitors of OCT1, a cell

viability assay was performed using 3-(4,5-Dimethylthiazol-2-yl)-2,5-Diphenyltetrazolium

Bromide (MTT) assay. Briefly, HEK-293 cells seeded in a 96-well plate were treated with

various excipients (1 to 100 µg/ml) used in ocular formulations. After 4 h, the cells were

washed and treated with 0.25 mg/ml MTT dye. Further, cells were incubated at 37 °C for 4 h,

and the dye was discarded. The formazan crystals were dissolved in dimethylsulphoxide, and

the absorbance was measured at 585 nm using a spectrophotometer (Spectra Max M4,

Molecular Devices). The percentage cell viability was calculated as mentioned in Equation 1.

% Cell viability = (Absorbance of test/Absorbance of control) * 100   --------- Equation 1

HEK 293 cells were transfected in a 96-well plate, and a DAPI uptake assay was performed, as

mentioned above. The uptake of DAPI was measured in the presence and absence of

excipients and known blockers (Positive control). The cells were pre-treated with varying

concentrations of excipients for 15 min prior to DAPI treatment. The cells were washed after

excipient treatment, followed by the addition of DAPI, and the uptake was performed for 20

mins. Experimental conditions for each step were maintained at 37 °C and pH 7.4. The

fluorescence was measured at an excitation and emission of 350 nm and 450 nm using a

spectrofluorometer. The active uptake of DAPI due to hOCT1 was calculated as mentioned in

Equation 2. The inhibitory potential of excipients was calculated by measuring percentage uptake.

Active uptake = Uptake in plasmid treated cells – Uptake in vector treated cells --- Equation 2

6.2.8 Tear Kinetics of intravenously administered substrate in the presence and absence of excipients

6.2.8.1 Preparation of substrate and blocker solutions

For intravenous administration of OCT1 substrate, Cyclophosphamide (15.5 mg/kg) was prepared in 0.9% sodium chloride (saline), pH 7.4. The drug was weighed and transferred to a sterile container, followed by the addition of sterile saline to obtain the desired concentration. For topical administration of excipients, Tween 20 (0.40 mM) and Poloxamer 407 (P 407) (14.28 mM) were dissolved in PBS, pH 7.4. All the solutions were filtered with a 0.22 μm sterile filter before administration.

6.2.8.2 Intravenous administration of substrate and topical administration of excipients and sample collection

Tear kinetics of intravenously (iv) administered substrate and topically administered excipient was performed in New Zealand White rabbits (Nirmal, Sirohiwal, et al. 2013a; Sharma et al. 2021). Animals were divided into three groups for each drug: Group 1: Control (Only substrate, iv), Group 2: Tween 20 pre-treated (Substrate, iv + Tween 20, Topical), and Group 3: P 407 pre-treated (Substrate, iv + P 407, Topical). The substrate was administered as an intravenous bolus injection through the marginal ear vein in all the groups. In excipient pre-treated groups, topical drops (50 μl) of excipients were administered in the right eye 30 mins

before substrate administration, using a calibrated pipette. After substrate administration, tears were collected and stored at pre-determined time points (5 mins, 15 mins, 30 mins, 1 h, 2 h). Parallely, blood samples were collected at each time point in an ethylene diamine tetra acetic acid (EDTA) coated tube and plasma was separated by centrifugation at 3000 g for 10 mins at 4 °C and further stored at -80 °C till further analysis.

6.2.8.3 Sample processing and analysis

The tear samples were thawed, and 0.2 ml of extraction solvent (100 ng/ml dexamethasone in Methanol with 0.1% formic acid). The strips were soaked in extraction solvent for 1 minute and vortexed at high speed for 1 minute. Further, the samples were centrifuged at 7400 g for 5 mins, and the collected supernatant was injected into LCMS-MS for drug quantification.

6.2.9 Data analysis

All the experiments were performed in triplicates. The data is represented as mean ± standard error mean (SEM). The values were considered significant if $p < 0.1$. GraphPad Prism (Ver 8.0) was used to calculate significant differences. The statistical analysis was performed using student's t-test and Two-way ANOVA (Dunnett's test). The uptake experiments were performed in at least n=4 and were repeated twice to thrice. Active uptake was determined by subtracting the substrate uptake in mock cells (vector-treated) from the uptake in transfected cells. The molar concentration of a substrate, which produces 50% of the maximum possible response for that substrate (IC_{50}), was obtained.

6.3 Results

6.3.1 Transformation and isolation of hOCT1 plasmid in *E. coli*

The plasmid pcDNA5 with the hOCT1 gene was transformed into *E. coli* using the heat shock method. The cells transformed with hOCT1 plasmid containing the Ampicillin resistance gene could grow on an Ampicillin-containing agar plate (**Figure 6.1**). A single isolated transformed colony with hOCT1 containing plasmid was selected and amplified in E. coli. The total yield of the hOCT1 plasmid was 2.8 µg/µl with $A_{260/280}$ and $A_{260/230}$ values of 2.07 and 2.26, respectively.
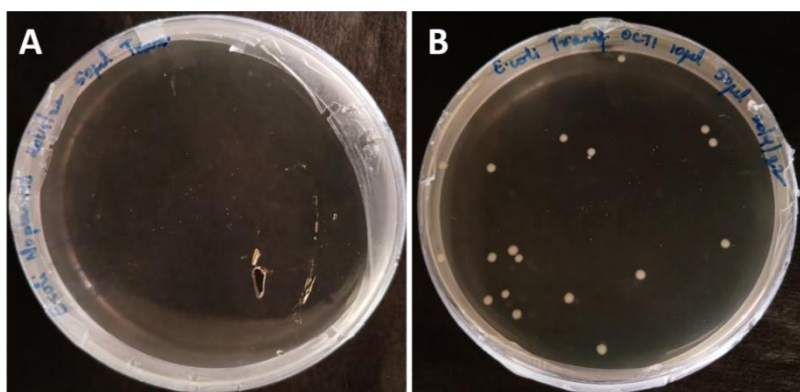
Figure 6.1: Transformed colonies of *E. coli* on Luria agar plate. Transformation was performed in Ampicillin sensitive E. coli (DH5α) using heat shock method. A. Transformation without plasmid. No colonies were observed due to absence of ampicillin resistance plasmid. B. Transformation with hOCT1 plasmid. Single isolated colonies were observed due to presence of Ampicillin resistance gene in hOCT1 plasmid.

6.3.2 Upregulation of hOCT1

Plasmid with the hOCT1 gene was transfected in HEK293 cells using the calcium phosphate precipitation method in a 96-well plate. DAPI uptake studies were performed to optimize the transfection parameters. From our studies, the transfection was found to be more efficient in the absence of glycerol. (**Table 6.1, Figure 6.2**). The precipitate formation and addition to the cells within 1 min of mixing were highly efficient compared to 5 min and 20 min. The plasmid DNA with 0.125 µg per well was sufficient to be entrapped into the calcium phosphate

precipitates and enhance the gene upregulation. Therefore, 0.125 µg of hOCT1 plasmid per well with a precipitate forming time of 1 min and the absence of glycerol was suitable for performing transfection in HEK 293 cells. Wells treated with vector DNA was considered as the negative control. Gene expression studies performed for transfected HEK293 cells in 24-well plate indicated that the expression of OCT1 was higher in transfected cells compared to their control group (non-transfected) (**Figure 6.3**).

Table 6.1: Transfection optimization parameters. Transfection was performed in presence and absence of glycerol (permeation enhancer) with different time of precipitate formation (1, 5, and 20 min) and different concentration of plasmid DNA (0.125 and 0.5 µg per well). SD (Standard Deviation).

Category	Precipitate formation time (min)	Plasmid (µg)	Uptake rate (FL/20min)	SD	Active uptake
Vector		0.125	13.74	1.50	0.00
Without glycerol	1	0.125	44.59	9.40	**30.85**
		0.5	31.20	2.82	**17.46**
	5	0.125	3.94	0.06	-9.80
		0.5	7.93	0.77	-5.81
	20	0.125	12.28	4.79	-1.46
		0.5	35.58	12.36	**21.84**
With glycerol	1	0.125	30.12	8.22	**16.38**
		0.5	9.41	2.42	-4.33
	5	0.125	10.19	1.37	-3.56
		0.5	16.53	0.48	2.79
	20	0.125	3.86	2.08	-9.88
		0.5	7.33	2.38	-6.41
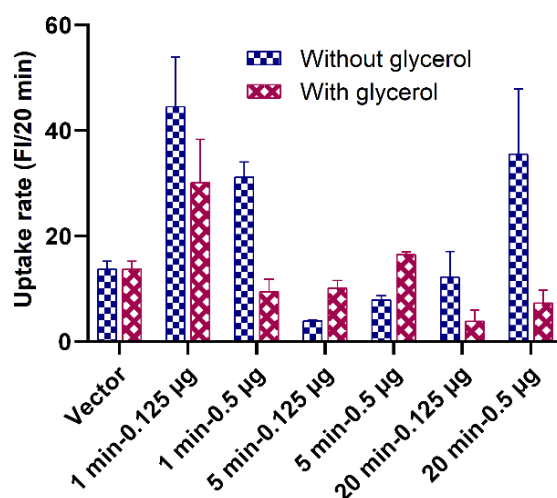
Figure 6.2: DAPI uptake studies to optimize transfection parameters. DAPI is a known fluorescent substrate of OCT1. The transfection parameters were optimized for HEK 293 cells (96-well plate) based on the DAPI uptake rate. The absence of glycerol with 0.125 µg plasmid DNA per well and 1 min of precipitate formation time resulted in the highest DAPI uptake which was considered as optimum parameters for further assays.
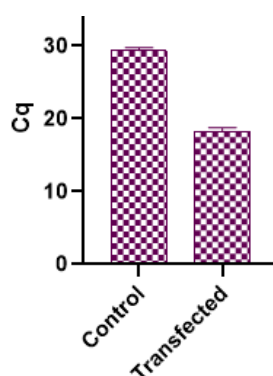
Figure 6.3: Gene expression of hOCT1 in HEK 293 transfected cells. The transfected cells with hOC1 plasmid showed lower Cq (Quantification cycle) when compared to non-transfected cells (control) indicating overexpression of hOCT1 in transfected cells.

6.3.3 DAPI uptake studies using in vitro studies

DAPI was chosen as a model substrate to screen the excipients as an inhibitor of OCT1. HEK-293 cells transiently transfected with hOCT1 plasmid were used for DAPI uptake studies. DAPI uptake was performed at 0.5, 1, 2, 5, and 10 µM concentrations (**Figure 6.4**) to determine the K_m and V_{max} for DAPI uptake through OCT1. The uptake increased proportionately from 0.5

µM to 2 µM, beyond which the uptake saturation was observed. The K_m value for saturable

OCT1-mediated uptake was 3.75 µM with a V_{max} of 142.96 ± 19.54 Fl/20 min.
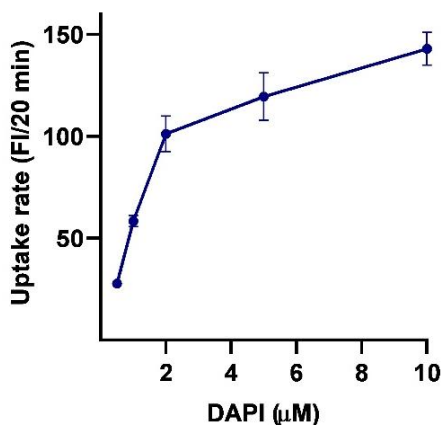
Figure 6.4: Concentration dependent uptake of DAPI. The specific uptake rate of DAPI was evaluated at pH 7.4 and 37 °C for 20 mins at varying concentrations of DAPI. The uptake of DAPI increased linearly till 2 µM and then attained saturation. The K_m value for DAPI uptake through OCT1 was found to be 3.75 µM.

Further, the uptake time was optimized using 1 µM DAPI incubated for 10, 20, and 30 mins,

and the increase was seen till 30 mins (**Figure 6.5**). However, the carrier-mediated uptake

through concentration-dependent transporters is reported to be sensitive to shorter

durations, and as reported earlier , 20 minutes was considered suitable for DAPI uptake

(Yasujima et al. 2011). Due to its fluorescence property, DAPI as a substrate could help in

initial high-throughput screening of OCT1 inhibitors. Moreover, the upregulation of specific

transporter genes minimizes the accumulation through other transporters.
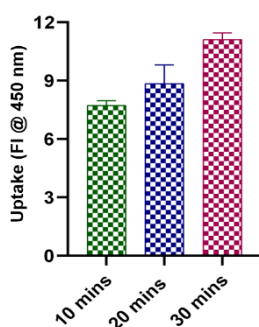
Figure 6.5: Time dependent uptake of DAPI. The specific uptake rate of DAPI was evaluated at pH 7.4 and 37 °C at 1 µM for varying uptake time. The uptake of DAPI increased till 30 mins; however, it was not linear.

6.3.4 Excipient screening as an inhibitor of OCT1

Excipients were screened as potential inhibitors of OCT1 in HEK 293 hOCT1 transfected cells. Initially, cell viability of excipients was performed on HEK-293 cells. The cells were treated with different concentrations (1, 10, and 100 µg/ml) of excipients for 4 h. Since the excipients were used to block the transporter (not more than 1 h), the toxic effect of excipients on cells was studied only for 4 h. All the tested excipients, carboxymethyl cellulose (CMC), polyvinyl pyrrolidone (PVP) K30, Tween-80, and polyvinyl alcohol (PVA) were found to be safe till 100 µg/ml concentration; however, triton-X was found to be safe only till 10 µg/ml concentration (**Figure 6.6**).
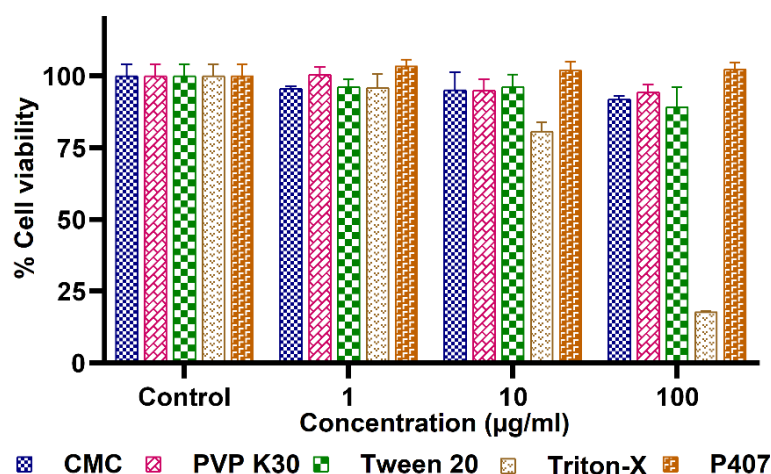
Figure 6.6: In vitro safety studies by MTT reagent. Human embryonic kidney cells were used to assess the In vitro safety of CMC (Carboxymethyl cellulose), PVP K30 (Polyvinyl pyrrolidone), Tween 20, Triton X and P407 (Poloxamer 407). All the polymers were found to safe till 100 µg/ml except Triton X which decreased cell viability above 10 µg/ml.

DAPI uptake was inhibited using OCT1 blockers – TEA and Quinidine, whereas various polymers and excipients such as Triton X-100, Tween 20, PVP K30 (Polyvinyl pyrrolidone), and P407 (Poloxamer) were evaluated for their inhibitory potential to block OCT1. Among OCT1 blockers, only TEA blocked the uptake of DAPI with an IC_{50} value of 2.16 ± 0.39 µM, whereas

quinidine could not block DAPI uptake. Among the tested polymers and surfactants, Tween 20 and Poloxamer 407 inhibited DAPI uptake with an IC_{50} value of 2.26 ± 0.82 μM and 1.41 ± 0.0.23 mM, respectively.
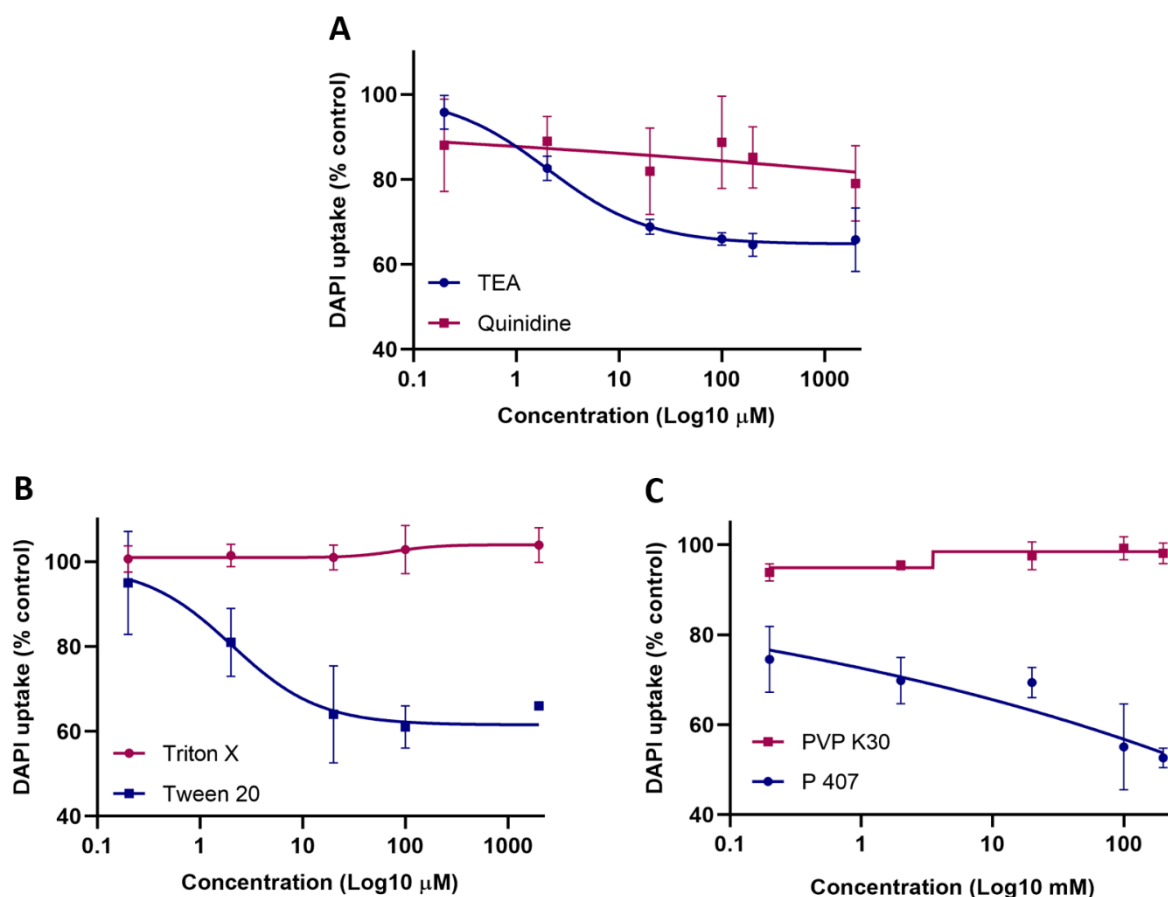
Figure 6.7: Inhibitory potency of therapeutic OCT1 blockers and excipients to block OCT1 transporter. DAPI uptake was performed at 37 °C for 20 min in presence of, A. OCT1 blockers – Tetraethyl ammonium (TEA), and Quinidine, B. Surfactants – Triton X-100, and Tween 20, and C. Polymers – PVP K30 (Polyvinyl pyrrolidone), and P407 (Poloxamer). TEA inhibited DAPI uptake with IC_{50} value of 2.16 ± 0.39 μM whereas Tween 20 and P407 showed IC_{50} value of 2.26 ± 0.82 μM and 1.41 ± 0.23 mM, respectively.

6.3.5 Therapeutic potential of topically administered excipients to block the entry of systemic drugs into the anterior segment of the eye

LCMS-MS method was developed to quantify Cyclophosphamide. Tear kinetics of intravenously administered Cyclophosphamide (OCT1 substrate) was performed in the presence and absence of Tween 20 and Poloxamer 407 (OCT1 blockers). In all the groups, the

tear concentration of Cyclophosphamide decreased from 5 min to 2 h. The substrate's tear concentration was higher in the control group than in the topically administered blocker pre-treated group at all time points (**Figure 6.8**). The $AUC_{(0-2h)}$ of Cyclophosphamide was 2-fold less in the Tween 20 pre-treated group and 1.7-fold less in the Poloxamer 407 pre-treated group compared to the control group (**Table 6.2**). Tween 20 was able to block the OCT1 at a concentration of 0.40 mM; Poloxamer 407 showed similar activity at a higher concentration (14.28 mM), indicating Tween 20 as the better blocker for OCT1.

Table 6.2: Pharmacokinetic parameters of intravenously administered substrate in presence and absence of topical non-therapeutic Organic cation transporter (OCT1) blockers (Tween 20, 0.40 mM and Poloxamer 407 (P 407), 14.28 mM).

Pharmacokinetic parameters of intravenously administered substrates in tears			
Drug	**C_{max} (µmol/ml)**	**$AUC_{(0-2h)}$ (µmol/ml*h)**	**$AUC_{(0-2h)}$ fold difference**
1) Cyclophosphamide			
(15.5 mg/kg) [a]			
Control	174.59	212.93	-
Tween 20 pre-treated	142.00	109.90	1.94
P 407 pre-treated	182.38	122.17	1.74

[a] Dose of substrate administered intravenously

C_{max}: Maximum concentration, AUC: Area under curve
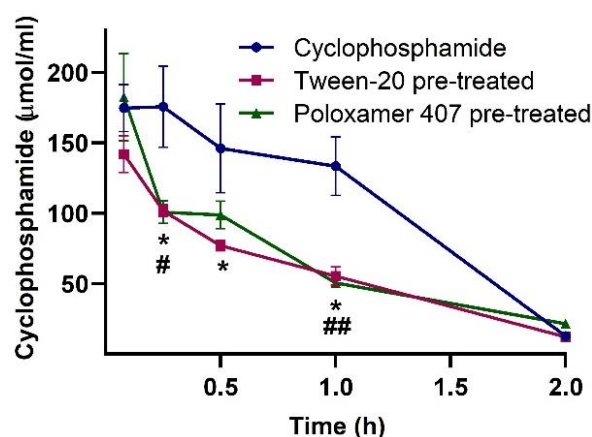
Figure 6.8: Tear kinetics of intravenously administered OCT1 substrates in presence and absence of topical non-therapeutic Organic cation transporter (OCT1) blocker (Tween 20 and P407). The tear concentration of Cyclophosphamide was found to be less in excipients pre-treated group than control group at all time point. Significant difference was observed at 15 mins, 30 mins and 1 h in Tween 20 pre-treated group ($*p<0.1$), and at 15 min and 1 h in Poloxamer 407 pre-treated group ($\#p<0.1$, $\#\#p<0.01$).

6.4 Discussions

With more than 1000 genes identified for encoding the transporter proteins, it has become crucial to understand the interactions of drugs with membrane transporters (Elbourne et al. 2016; Sahoo et al. 2014). It is now evident that by exploiting the transporters, the fate of drugs can also be altered. Since the transporters are not tissue-specific, the drug accumulates at an off-target site (Peng et al. 2020). Similarly, systemic drugs enter the eye through these transporters and accumulate in various ocular tissues (Nirmal, Sirohiwal, et al. 2013a). OCT1 in the lacrimal gland mediates the transport of systemic drugs (cations) into the anterior segment of the eye through tear secretion. Therefore, blocking the OCT1 transporters by local application of excipients as an inhibitor could minimize the drug entry into the eye. The use of excipients could also avoid drug-drug interactions while not reducing the pharmacological action of systemic drugs.

Interaction of excipients with organic cation transporter

The plasmid with the hOCT1 gene was transformed in E. coli to amplify the gene. The Ampicillin resistance gene in plasmid pcDNA5 cloned with hOCT1 was used as a selective marker to isolate the transformed colonies (containing hOCT1 plasmid) on Ampicillin-containing agar plates (Pope and Kent 1996). The selected colonies produced hOCT1 plasmid, further isolated using ethanol precipitation with similar yield and quality as reported earlier (Au - Desjardins and Au - Conklin 2010; Kachkin et al. 2020).

DAPI uptake was performed with a reported concentration (1 μM) and uptake time (20 min) for optimizing the transfection parameters (Yasujima et al. 2011). Glycerol and other chemicals, such as chloroquine and butyrate are known to improve the permeation of plasmid into the cells during transfection (Kumar et al. 2019). However, the use of chloroquine and butyrate can be extremely beneficial or harmful and therefore, transfection was performed in the presence and absence of glycerol to optimize the suitable conditions. But from our studies and other studies the absence of glycerol for HEK cells resulted in higher transfection, possibly due to the reported toxicity of glycerol on cells (Jordan et al. 1996).

Transfection was performed with varying times for calcium phosphate precipitate formation (1, 5, and 20 min) and a lower and higher amount of plasmid DNA (0.125 and 0.5 μg per well). The cells were allowed to express the gene for 24 h. The time of precipitate formation plays an essential role in the successful transfection. Prolonged time leads to an increase in precipitate size and the formation of coarse particles, further reducing transfection efficiency (Graham and van der Eb 1973).

Interaction of excipients with organic cation transporter

The optimized parameters for transfection were in line with the earlier reported studies. The pH of HBS was maintained at 7.05 to obtain a fine precipitate size. The optimum time interval between calcium chloride addition to plasmid and inoculation of this mixture to the cells is between is reported to be 1 to 20 min. Our studies found that 1 min was sufficient for the formation of DNA precipitate, as indicated by the highest DAPI uptake (Jordan et al. 1996).

Further, the time of incubation of precipitate on cells prior to overlay with fresh media is also considered to be one of the essential parameters and is reported to be optimum between 5 to 10 h (Graham and van der Eb 1973). In our studies, we incubated the cells with DNA precipitate for six h post DNA adsorption. Further, to confirm the upregulation of hOCT1, HEK 293 cells were grown in a 24-well plate and transfected with 0.5 μg of hOCT1 plasmid per well with other optimized parameters and the expression was found to be higher as indicated by lower quantification cycle value.

DAPI is a known fluorescence substrate of OCT1; however, the transport mode is suggested to differ from the typical OCT substrate – tetraethyl ammonium. But the uptake of DAPI was reportedly inhibited by various organic cations, indicating the potential use of DAPI as a substrate of OCT1 for identifying the inhibitors (Yasujima et al. 2011). Hence, in our studies, we used DAPI as a substrate to identify excipients as an inhibitor for OCT1. Based on the concentration and time-dependent uptake of DAPI, a concentration of 1 μM less than its Km value and an uptake time of 20 min was chosen for the subsequent experiments, ensuring the uptake is sensitive to various experimental conditions and inhibitors. Earlier studies reported a K_m value of 8.94 μM for DAPI uptake, which was higher than our studies, but this variability could be due to the experimental conditions (Koepsell et al. 2007; Yasujima et al. 2011). In

contrast to earlier reported studies, DAPI uptake was inhibited in presence of TEA which indicates their transport mode could be similar. However, the difference could be due to experimental conditions and the transfection efficiency (Yasujima et al. 2011).

Of the tested excipients, Tween 20 and P407 inhibited the OCT1 uptake with the highest efficiency. Tween's are reported earlier to inhibit the OCT1 uptake with the lowest IC_{50} value but show overlapping activity with different OCT isoforms (Soodvilai et al. 2017a). However, P407 was reported to show specific inhibition against OCT1; however with a 900-fold higher IC_{50} value (Otter et al. 2017). In our study, P407 showed nearly 700-fold higher IC_{50} value compared to Tween 20. OCT1 is known to transport the cation majorly; however, they are also reported for transporting a few anionic and neutral molecules (Koepsell et al. 2007). Tween and P407 are non-ionic surfactants that can also prevent transport due to non-specific interactions, such as changing the fluidity of membranes (Kabanov et al. 2003). Due to their higher molecular weight, they might inhibit the transporter without being translocating, i.e., non-competitive inhibitors. Moreover, Tween, when used in combination with oral drugs such as doxorubicin, are known to decrease the uptake of the liver due to OCT1 inhibition (Cummings et al. 1986). Tween and poloxamers also inhibit efflux transporters and enhance the drug uptake or retention time of digoxin and methotrexate (Azmin et al. 1985; Kabanov et al. 2003; Zhang et al. 2003). However, our study and other groups have also shown their potential to inhibit uptake transporters such as OCT (Otter et al. 2017; Soodvilai et al. 2017a). The inhibitory effects can be concentration-dependent and, therefore, need further studies to explore or understand their differential role in inhibiting uptake or efflux transporters. The viability assay was performed to confirm that transport inhibition was not due to toxicity,

which showed the safety of the polymers in the used range. In general, surfactants are better at altering the drug pharmacokinetics by inhibiting the transporters.

Our findings and previously reported studies indicated that Tween and Poloxamer were potent inhibitors of OCT1. Further, to explore the application of excipients as a local OCT1 blocker to minimize ocular toxicity, in vivo tear kinetics of intravenously administered OCT1 substrate were performed in the presence and absence of excipients. When administered intravenously, the tear concentration of OCT1 substrate, Cyclophosphamide, is reduced in the presence of topical excipients. Moreover, through local topical applications of blockers can block other routes of drug entry into the eye through both corneal and non-corneal routes. OCT1 is also expressed in the cornea and conjunctiva and is functionally active from tear to aqueous humor and mucous to serous side, respectively (Nirmal, Singh, et al. 2013a; Ueda et al. 2000). Therefore, topical application of non-therapeutic OCT1 inhibitors can block the OCT1 in the lacrimal gland, cornea, and conjunctiva, preventing entry from various routes into the eye and without altering systemic drugs' pharmacological action.

6.5 Conclusions

Though inert, excipients have the potential to interact with transporters and modulate their activity, further regulating the bioavailability of the drugs. Tween 20 and Poloxamer 407 showed an inhibitory effect on OCT1, indicating the use of these excipients can further affect the pharmacokinetics of organic cationic drugs. Therefore, it can be concluded that pharmaceutical excipients as non-therapeutic inhibitors could inhibit (locally in the eye by topical application without inhibiting systemic pharmacological action) the OCT1 transporters, preventing the systemic drugs from entering the eye and reducing ocular

toxicity. However, the use of transporter blockers could also prevent the entry of endogenous molecules into the eye and therefore further studies are required to study its impact on the ocular structures.

Chapter 7

Conclusions and Future Scope

Conclusions and Future scope

Systemic drugs causing ocular toxicity enter the anterior segment of the eye through membrane transporters in the lacrimal and blood aqueous barriers. Organic cation transporters (OCT) are involved in the transport of cationic drugs across biological barriers. From the current study, the developed artificial intelligence model and computer simulations revealed drug OCT1 interactions that were not reported earlier. An artificial intelligence (AI) model was used for initial high-throughput screening to classify the drug as substrate or non-substrate. Further, the interactions and movement of the drug through transporters were shown using molecular dynamics and metadynamics simulation. The in vivo topical tear kinetic studies in New Zealand white rabbits validated the AI predictions, confirming the predicted molecules as OCT1 substrates. Our studies also identified that the drug's molecular weight of 200 to 400 g/mol and sulfur moiety in the chemical structure of molecules could be one of the additional features facilitating the transport through OCT1. Therefore, the developed AI and computer simulations (CS) models can be used to understand the possible drug transporter interactions in the early phase of drug development to avoid unseen toxicities.

OCT1 is expressed in the lacrimal gland and is functionally active from the blood (basal) to the lumen (apical) side. The current study delineates the role of OCT1 transporters in the lacrimal gland as the gateway for systemic drugs (cations) into the eye through tear secretion using Cyclophosphamide as a model OCT1 substrate. Several other systemic drugs which are known to be OCT1 substrates could also enter the eye through OCT1 transporters located in different ocular barriers and cause ocular toxicity, such as Ethambutol induced optic neuritis, Trimethoprim induced conjunctival and scleral infection, Diltiazem induced edema and retinopathy, Ipratropium induced glaucoma, Verapamil induced dry eye, and Amantadine

induced edema and cataract. Though the toxicity mechanism of systemic drugs is not clear, the current work links the entry of drugs into the eye through transporters and could cause ocular toxicity.

Pharmaceutical excipients used as solubilizers, permeation enhancers, and viscosity enhancers can be potent transporters' inhibitors. The topical use of excipients can prevent the entry of systemic drugs into the eye without altering the systemic fate of the drugs. Excipients can be used as topical non-therapeutic transporter inhibitors, allowing a rapid translational research pathway to reduce the incidence of systemic drug-induced ocular toxicity (**Figure 7.1**). However, using excipients to block the transporters could also limit the secretion of ocular endogenous amines; therefore, further studies are required to study its impact on the ocular structures.

In the current work, the functional role of OCTs in the lacrimal gland, which is involved in the transport of cationic drugs, is understood; however, the question arises regarding how other drugs are being transported. This suggests that other uptake transporters might as well be present in the lacrimal gland. Therefore, we performed gene expression studies for various uptake transporters in the rabbit lacrimal gland. Genes for 10 uptake transporters were expressed in the rabbit lacrimal gland, which opens a new avenue for the futuristic work to understand the pharmacokinetics of systemic drugs through the lacrimal gland (**Figure 7.2**). However, further studies are required to understand the functional role of these transporters in the lacrimal gland and its impact on the pharmacokinetics of ocular toxic drugs. Additional mechanistic studies are also required to explore the toxicity mechanism of these drugs.

Conclusions and Future scope

Though all systemic drugs possess the ability to enter the eye, not all of them cause ocular toxicity. The underlying toxicity mechanism of selective drugs needs to be understood if it is due to differences in their physicochemical properties, dose, duration, or downstream signaling pathways.
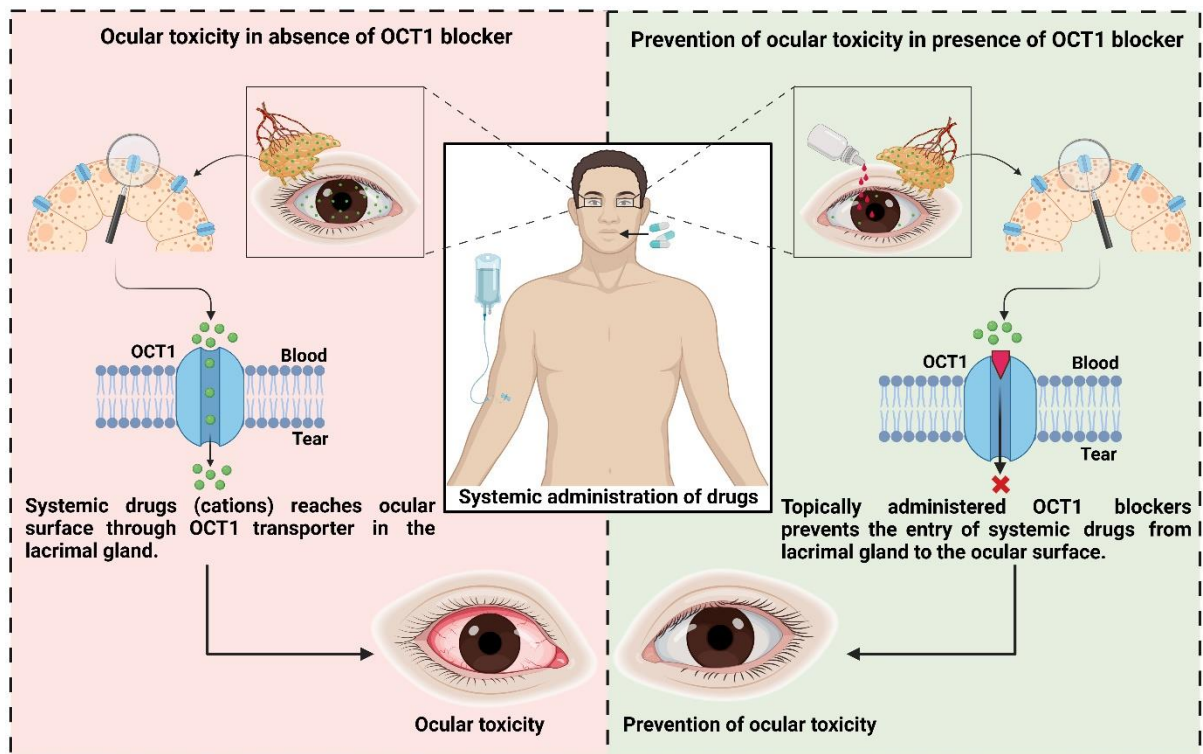
Figure 7.1: Graphical conclusion of the study. In the current study, the active role of OCT1 was delineated from blood to tear in the lacrimal gland. The systemically administered drugs (cation) were able to reach eye through OCT1 transporter in lacrimal gland. The tear concentration of drug was reduced in the presence of topically administered excipients. Therefore, the use of excipients can prevent the entry of systemic drugs causing ocular toxicity into the eye and minimize the risk of ocular toxicity.
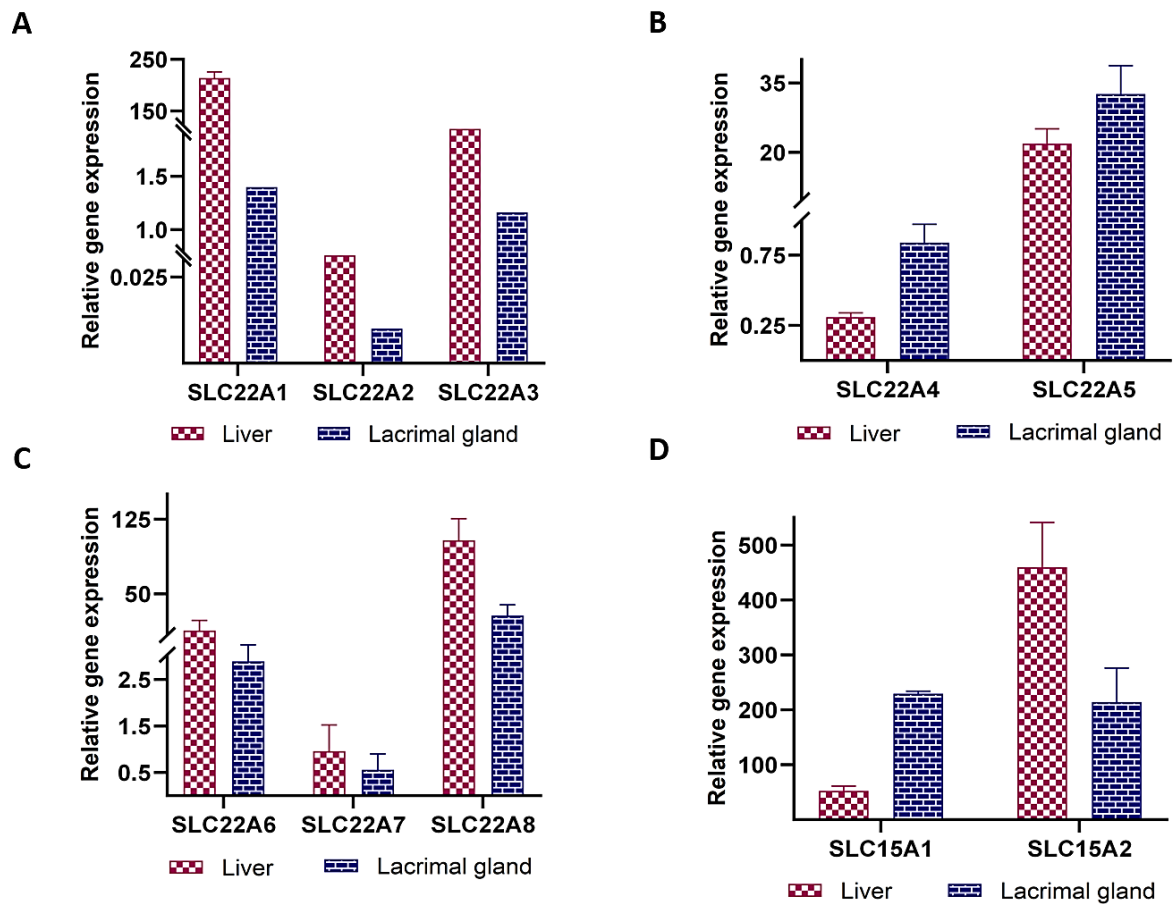
Figure 7.2: Transporter profiling in rabbit lacrimal gland. Reverse transcriptase polymerase chain reaction (RT-PCR) was performed for evaluating the expression of various uptake transporters in the rabbit lacrimal gland. Liver was used as the positive control. The relative expression of SLC22A1 (OCT1), SLC22A2 (OCT2), SLC22A3 (OCT3), SLC22A6 (OAT1), SLC22A7 (OAT2) and SLC22A8 (OAT3) was found to less in lacrimal gland compared to rabbit whereas SLC22A4 (OCTN1), SLC22A5 (OCTN2), SLC15A1 (PEPT1), SLC15A2 (PEPT2) were expressed relatively higher in lacrimal gland. SLC: Solute carrier transporters; OCT: Organic cation transporter, OAT: Organic anion transporter, PEPT: Peptide transporter.

Bibliography

Bibliography

Abdollahi, M., Shafiee, A., Bathaiee, F. S., Sharifzadeh, M., and Nikfar, S. 2004. "Drug-induced toxic reactions in the eye: an overview." *Journal of Infusion Nursing* 27 (6): 386-398.

Abraham, M. H., Kumarsingh, R., Cometto-Muniz, J. E., and Cain, W. S. 1998. "A quantitative structure–activity relationship (QSAR) for a Draize eye irritation database." *Toxicology in vitro* 12 (3): 201-207.

Acheampong, A. A., Shackleton, M., Tang-Liu, D. D.-S., Ding, S., Stern, M. E., and Decker, R. 1999. "Distribution of cyclosporin A in ocular tissues after topical administration to albino rabbits and beagle dogs." *Current eye research* 18 (2): 91-103.

Adrianto, M. F., Annuryanti, F., Wilson, C. G., Sheshala, R., and Thakur, R. R. S. 2022. "In vitro dissolution testing models of ocular implants for posterior segment drug delivery." *Drug Delivery and Translational Research* 12 (6): 1355-1375. https://doi.org/10.1007/s13346-021-01043-z.

Al-Karmalawy, A. A., Dahab, M. A., Metwaly, A. M., Elhady, S. S., Elkaeed, E. B., Eissa, I. H., and Darwish, K. M. 2021. "Molecular Docking and Dynamics Simulation Revealed the Potential Inhibitory Activity of ACEIs Against SARS-CoV-2 Targeting the h ACE2 Receptor." *Frontiers in chemistry* 9: 661230.

Alexander, J. H., van Lennep, E. W., and Young, J. A. 1972. "Water and electrolyte secretion by the exorbital lacrimal gland of the rat studied by micropuncture and catheterization techniques." *Pflugers Arch* 337 (4): 299-309. https://doi.org/10.1007/bf00586647.

Ali, A., Shah, A. A., Jeang, L. J., Fallgatter, K. S., George, T. J., and DeRemer, D. L. 2022. "Emergence of ocular toxicities associated with novel anticancer therapeutics: What the oncologist needs to know." *Cancer Treatment Reviews* 105: 102376. https://doi.org/https://doi.org/10.1016/j.ctrv.2022.102376.

Alshehri, M., and Joury, A. 2020. "Ocular Adverse Effects of Amiodarone: A Systematic Review of Case Reports." *Optometry and Vision Science* 97 (7): 536-542.

Amir, M., Mohammad, T., Kumar, V., Alajmi, M. F., Rehman, M. T., Hussain, A., Alam, P., Dohare, R., Islam, A., and Ahmad, F. 2019. "Structural analysis and conformational dynamics of STN1 gene mutations involved in coat plus syndrome." *Frontiers in molecular biosciences* 6: 41.

Ashburn, T. T., and Thor, K. B. 2004. "Drug repositioning: identifying and developing new uses for existing drugs." *Nature Reviews Drug Discovery* 3 (8): 673-683. https://doi.org/10.1038/nrd1468.

Au - Desjardins, P., and Au - Conklin, D. 2010. "NanoDrop Microvolume Quantitation of Nucleic Acids." *JoVE* (45): e2565. https://doi.org/doi:10.3791/2565.

Awwad, S., Mohamed Ahmed, A. H., Sharma, G., Heng, J. S., Khaw, P. T., Brocchini, S., and Lockwood, A. 2017. "Principles of pharmacology in the eye." *British journal of pharmacology* 174 (23): 4205-4223.

Azmin, M. N., Stuart, J. F. B., and Florence, A. T. 1985. "The distribution and elimination of methotrexate in mouse blood and brain after concurrent administration of polysorbate 80." *Cancer Chemotherapy and Pharmacology* 14 (3): 238-242. https://doi.org/10.1007/BF00258124.

Bibliography

Baidya, A. T., Ghosh, K., Amin, S. A., Adhikari, N., Nirmal, J., Jha, T., and Gayen, S. 2020. "In silico modelling, identification of crucial molecular fingerprints, and prediction of new possible substrates of human organic cationic transporters 1 and 2." *New Journal of Chemistry* 44 (10): 4129-4143.

Basile, A. O., Yahi, A., and Tatonetti, N. P. 2019. "Artificial Intelligence for Drug Toxicity and Safety." *Trends Pharmacol Sci* 40 (9): 624-635. https://doi.org/10.1016/j.tips.2019.07.005.

Bhatti, M., and Salama, A. 2018. "Neuro-ophthalmic side effects of molecularly targeted cancer drugs." *Eye* 32 (2): 287-301.

Bindiganavile, S. H., Bhat, N., Lee, A. G., Gombos, D. S., and Al-Zubidi, N. 2021. "Targeted cancer therapy and its ophthalmic side effects: a review." *Journal of Immunotherapy and Precision Oncology* 4 (1): 6-15.

Boxberger, K. H., Hagenbuch, B., and Lampe, J. N. 2014. "Common drugs inhibit human organic cation transporter 1 (OCT1)-mediated neurotransmitter uptake." *Drug Metabolism and Disposition* 42 (6): 990-995.

Bratulescu, M., Zemba, M., Gheorghieva, V., Andrei, S., Cucu, B., and Dobrescu, N. 2005. "[Ocular manifestation in amiodarone toxicity--case report]." *Oftalmologia* 49 (4): 18-23.

Brock, W. J., Somps, C. J., Torti, V., Render, J. A., Jamison, J., and Rivera, M. I. 2013. "Ocular Toxicity Assessment From Systemically Administered Xenobiotics:Considerations in Drug Development." *International Journal of Toxicology* 32 (3): 171-188. https://doi.org/10.1177/1091581813484500.

Bromberg, B. B., Hanemann, C. W., Welch, M. H., Beuerman, R. W., and Githens, S. 1994. "Carbonic anhydrase and acinar cell heterogeneity in rat and rabbit lacrimal glands." *Lacrimal Gland, Tear Film, and Dry Eye Syndromes: Basic Science and Clinical Relevance*: 31-36.

Burgalassi, S., Panichi, L., Chetoni, P., Saettone, M. F., and Boldrini, E. 1999. "Development of a simple dry eye model in the albino rabbit and evaluation of some tear substitutes." *Ophthalmic research* 31 (3): 229-235.

Burton, M. J., Ramke, J., Marques, A. P., Bourne, R. R., Congdon, N., Jones, I., Tong, B. A. A., Arunga, S., Bachani, D., and Bascaran, C. 2021. "The Lancet global health Commission on global eye health: vision beyond 2020." *The Lancet Global Health* 9 (4): e489-e551.

Bussi, G., and Laio, A. 2020. "Using metadynamics to explore complex free-energy landscapes." *Nature Reviews Physics* 2 (4): 200-212.

Castells, D. D., Teitelbaum, B. A., and Tresley, D. J. 2002. "Visual changes secondary to initiation of amiodarone: a case report and review involving ocular management in cardiac polypharmacy." *Optometry: Journal of the American Optometric Association*.

Bibliography

Chhadva, P., Lee, T., Sarantopoulos, C. D., Hackam, A. S., McClellan, A. L., Felix, E. R., Levitt, R. C., and Galor, A. 2015. "Human Tear Serotonin Levels Correlate with Symptoms and Signs of Dry Eye." *Ophthalmology* 122 (8): 1675-80. https://doi.org/10.1016/j.ophtha.2015.04.010.

Ciarimboli, G. 2011. "Role of organic cation transporters in drug-induced toxicity." *Expert opinion on drug metabolism & toxicology* 7 (2): 159-174.

Ciarimboli, G. 2020. "Regulation Mechanisms of Expression and Function of Organic Cation Transporter 1." *Front Pharmacol* 11: 607613. https://doi.org/10.3389/fphar.2020.607613.

Coleman, J. J., and Pontefract, S. K. 2016. "Adverse drug reactions." *Clin Med (Lond)* 16 (5): 481-485. https://doi.org/10.7861/clinmedicine.16-5-481.

Console, L., Scalise, M., Mazza, T., Pochini, L., Galluccio, M., Giangregorio, N., Tonazzi, A., and Indiveri, C. 2020. "Carnitine traffic in cells. Link with cancer." *Frontiers in Cell and Developmental Biology* 8.

Constable, P. A., Al-Dasooqi, D., Bruce, R., and Prem-Senthil, M. 2022a. "A Review of Ocular Complications Associated with Medications Used for Anxiety, Depression, and Stress." *Clinical Optometry* 14: 13.

---. 2022b. "A review of ocular complications associated with medications used for anxiety, depression, and stress." *Clinical Optometry*: 13-25.

Cridge, B. 2018. "Drug Transporters in Toxicology." *Open Acc J of Toxicol.* 2(3): 555588.

Cronin, M., Basketter, D., and York, M. 1994. "A quantitative structure-activity relationship (QSAR) investigation of a Draize eye irritation database." *Toxicology in vitro* 8 (1): 21-28.

Cummings, J., Forrest, G. J., Cunningham, D., Gilchrist, N. L., and Soukop, M. 1986. "Influence of polysorbate 80 (Tween 80) and etoposide (VP-16-213) on the pharmacokinetics and urinary excretion of adriamycin and its metabolites in cancer patients." *Cancer Chemotherapy and Pharmacology* 17 (1): 80-84. https://doi.org/10.1007/BF00299871.

Cunha-Vaz, J. 1979. "The blood-ocular barriers." *Surv Ophthalmol* 23 (5): 279-96. https://doi.org/10.1016/0039-6257(79)90158-9.

Curtin, F., and Schulz, P. 2011. "Assessing the benefit: risk ratio of a drug--randomized and naturalistic evidence." *Dialogues Clin Neurosci* 13 (2): 183-90. https://doi.org/10.31887/DCNS.2011.13.2/fcurtin.

Dakal, T. C., Kumar, R., and Ramotar, D. 2017. "Structural modeling of human organic cation transporters." *Computational Biology and Chemistry* 68: 153-163. https://doi.org/https://doi.org/10.1016/j.compbiolchem.2017.03.007.

Dartt, D. A. 2009. "Neural regulation of lacrimal gland secretory processes: relevance in dry eye diseases." *Prog Retin Eye Res* 28 (3): 155-77. https://doi.org/10.1016/j.preteyeres.2009.04.003.

Davies, S., Hungerford, J., Arden, G., Marcus, R., Miller, M., and Huehns, E. 1983. "Ocular toxicity of high-dose intravenous desferrioxamine." *The Lancet* 322 (8343): 181-184.

Bibliography

de Freitas, R. F., and Schapira, M. 2017. "A systematic analysis of atomic protein–ligand interactions in the PDB." *Medchemcomm* 8 (10): 1970-1981.

Development, O. f. E. C.-o. a. "OECD Guidelines for the Testing of Chemicals." *https://www.oecd-ilibrary.org/environment/oecd-guidelines-for-the-testing-of-chemicals_72d77764-en?_ga=2.96179612.1235017736.1627133985-2063296582.1616570860*.

---. "OECD Guidelines for the Testing of Chemicals, Section 1." *https://www.oecd-ilibrary.org/environment/oecd-guidelines-for-the-testing-of-chemicals-section-1-physical-chemical-properties_20745753?page=1*.

---. "OECD Guidelines for the Testing of Chemicals, Section 2." *https://www.oecd-ilibrary.org/environment/oecd-guidelines-for-the-testing-of-chemicals-section-2-effects-on-biotic-systems_20745761*.

---. "OECD Guidelines for the Testing of Chemicals, Section 3." *https://www.oecd-ilibrary.org/environment/oecd-guidelines-for-the-testing-of-chemicals-section-3-degradation-and-accumulation_2074577x*.

---. "OECD Guidelines for the Testing of Chemicals, Section 4." *https://www.oecd-ilibrary.org/environment/oecd-guidelines-for-the-testing-of-chemicals-section-4-health-effects_20745788*.

---. "OECD Guidelines for the Testing of Chemicals, Section 5." *https://www.oecd-ilibrary.org/environment/oecd-guidelines-for-the-testing-of-chemicals-section-5-other-test-guidelines_20745796*.

Dey, S., and Mitra, A. K. 2005. "Transporters and receptors in ocular drug delivery: opportunities and challenges." *Expert opinion on drug delivery* 2 (2): 201-204.

Dhananjay, P., Ramya Krishna, V., Aswani Dutt, V., and Mitra, A. K. 2013. "2 - Biology of ocular transporters: efflux and influx transporters in the eye." In *Ocular Transporters and Receptors*, edited by Mitra, A. K., 37-84. Woodhead Publishing.

Diao, L., Ekins, S., and Polli, J. E. 2010. "Quantitative structure activity relationship for inhibition of human organic cation/carnitine transporter." *Molecular pharmaceutics* 7 (6): 2120-2131.

Ding, C., Parsa, L., Nandoskar, P., Zhao, P., Wu, K., and Wang, Y. 2010. "Duct system of the rabbit lacrimal gland: structural characteristics and role in lacrimal secretion." *Invest Ophthalmol Vis Sci* 51 (6): 2960-7. https://doi.org/10.1167/iovs.09-4687.

Dintaman, J. M., and Silverman, J. A. 1999. "Inhibition of P-glycoprotein by D-alpha-tocopheryl polyethylene glycol 1000 succinate (TPGS)." *Pharm Res* 16 (10): 1550-6. https://doi.org/10.1023/a:1015000503629.

Bibliography

Djeridane, Y. 1994. "Immunohistochemical evidence for the presence of vasopressin in the rat harderian gland, retina and lacrimal gland." *Experimental eye research* 59 (1): 117-120.

Dogan, S. S., and Esmaeli, B. 2009. "Ocular side effects associated with imatinib mesylate and perifosine for gastrointestinal stromal tumor." *Hematology/oncology clinics of North America* 23 (1): 109-114.

Ebeling, M., Meyer, A. C., and Modig, K. 2020. "The rise in the number of long-term survivors from different diseases can slow the increase in life expectancy of the total population." *BMC Public Health* 20 (1): 1523. https://doi.org/10.1186/s12889-020-09631-3.

Ekins, S., Mestres, J., and Testa, B. 2007. "In silico pharmacology for drug discovery: applications to targets and beyond." *Br J Pharmacol* 152 (1): 21-37. https://doi.org/10.1038/sj.bjp.0707306.

Elbourne, Liam D. H., Tetu, S. G., Hassan, K. A., and Paulsen, I. T. 2016. "TransportDB 2.0: a database for exploring membrane transporters in sequenced genomes from all domains of life." *Nucleic Acids Research* 45 (D1): D320-D324. https://doi.org/10.1093/nar/gkw1068.

Engel, A., Oswald, S., Siegmund, W., and Keiser, M. 2012. "Pharmaceutical excipients influence the function of human uptake transporting proteins." *Molecular pharmaceutics* 9 (9): 2577-2581.

FDA. "Generally Recognized as Safe (GRAS)." *https://www.fda.gov/food/food-ingredients-packaging/generally-recognized-safe-gras*.

---. 2005. Estimating the Maximum Safe Starting Dose in Initial Clinical Trials for Therapeutics in Adult Healthy Volunteers U.S.: Food and Drug Administration.

---. 2013. Cyclophosphamide Injection. U.S.: FDA.

---. 2018. "Think It Through: Managing the Benefits and Risks of Medicines." FDA.

---. 2023. FDA Adverse Events Reporting System (FAERS). In *1997-2023*. US: US-FDA.

Filipski, K. K., Mathijssen, R. H., Mikkelsen, T. S., Schinkel, A. H., and Sparreboom, A. 2009. "Contribution of organic cation transporter 2 (OCT2) to cisplatin-induced nephrotoxicity." *Clinical Pharmacology & Therapeutics* 86 (4): 396-402.

Fiser, A. 2010. "Template-based protein structure modeling." *Methods Mol Biol* 673: 73-94. https://doi.org/10.1007/978-1-60761-842-3_6.

Fraunfelder, F. F. T., and Fraunfelder, F. R. W. 2021. "Drug-Induced Ocular Side Effects (Eighth Edition)." In *Drug-Induced Ocular Side Effects (Eighth Edition)*, edited by Fraunfelder, F. F. T. and Fraunfelder, F. R. W., iii. London: Elsevier.

Frederick T. Fraunfelder, F. W. F. 2020. *Drug-Induced Ocular Side Effects*.

Gao, B., Vavricka, S. R., Meier, P. J., and Stieger, B. 2015. "Differential cellular expression of organic anion transporting peptides OATP1A2 and OATP2B1 in the human retina and brain: implications for

Bibliography

carrier-mediated transport of neuropeptides and neurosteriods in the CNS." *Pflugers Arch* 467 (7): 1481-1493. https://doi.org/10.1007/s00424-014-1596-x.

Gapsys, V., and de Groot, B. L. 2020. "On the importance of statistics in molecular simulations for thermodynamics, kinetics and simulation box size." *Elife* 9: e57589.

Garg, P., and Yadav, S. 2019. "OCULAR SIDE EFFECTS OF SYSTEMIC DRUGS." *Era's Journal of Medical Research* 6 (1): 54-62.

Garrett, Q., Xu, S., Simmons, P. A., Vehige, J., Flanagan, J. L., and Willcox, M. D. 2008. "Expression and localization of carnitine/organic cation transporter OCTN1 and OCTN2 in ocular epithelium." *Investigative ophthalmology & visual science* 49 (11): 4844-4849.

Gherghel, D. 2020. "Ocular side effects of systemic drugs 1: Cholesterol lowering, anti-hypertensive and cardiac drugs." *Optician* 2020 (3): 8236-1.

Ghosh, R., Chakraborty, A., Biswas, A., and Chowdhuri, S. 2021. "Evaluation of green tea polyphenols as novel corona virus (SARS CoV-2) main protease (Mpro) inhibitors–an in silico docking and molecular dynamics simulation study." *Journal of Biomolecular Structure and Dynamics* 39 (12): 4362-4374.

Gokulgandhi, M. R., Vadlapudi, A. D., and Mitra, A. K. 2012. "Ocular toxicity from systemically administered xenobiotics." *Expert opinion on drug metabolism & toxicology* 8 (10): 1277-1291.

Gottshall, S. L., Tekin, S., and Hansen, P. J. 2008. "Extraction and Purification of Total RNA using Trizol or Tri Reagent." *Laboratory Procedures, PJ Hansen Laboratory, University of Florida*.

Graham, F. L., and van der Eb, A. J. 1973. "A new technique for the assay of infectivity of human adenovirus 5 DNA." *Virology* 52 (2): 456-467. https://doi.org/https://doi.org/10.1016/0042-6822(73)90341-3.

Gründemann, D., Gorboulev, V., Gambaryan, S., Veyhl, M., and Koepsell, H. 1994. "Drug excretion mediated by a new prototype of polyspecific transporter." *Nature* 372 (6506): 549-552. https://doi.org/10.1038/372549a0.

Guo, D., Yang, H., Li, Q., Bae, H. J., Obianom, O., Zeng, S., Su, T., Polli, J. E., and Shu, Y. 2018. "Selective inhibition on organic cation transporters by carvedilol protects mice from cisplatin-induced nephrotoxicity." *Pharmaceutical research* 35 (11): 1-10.

Gurjar, R., Chan, C. Y. S., Curley, P., Sharp, J., Chiong, J., Rannard, S., Siccardi, M., and Owen, A. 2018. "Inhibitory Effects of Commonly Used Excipients on P-Glycoprotein in Vitro." *Mol Pharm* 15 (11): 4835-4842. https://doi.org/10.1021/acs.molpharmaceut.8b00482.

Hafey, M. J., Aleksunes, L. M., Bridges, C. C., Brouwer, K. R., Chien, H. C., Leslie, E. M., Hu, S., Li, Y., Shen, J., and Sparreboom, A. 2022. "Transporters and Toxicity: Insights from the International Transporter Consortium Workshop 4." *Clinical Pharmacology & Therapeutics* 112 (3): 527-539.

Bibliography

Hanke, U., May, K., Rozehnal, V., Nagel, S., Siegmund, W., and Weitschies, W. 2010. "Commonly used nonionic surfactants interact differently with the human efflux transporters ABCB1 (p-glycoprotein) and ABCC2 (MRP2)." *Eur J Pharm Biopharm* 76 (2): 260-8. https://doi.org/10.1016/j.ejpb.2010.06.008.

Hayer-Zillgen, M., Brüss, M., and Bönisch, H. 2002. "Expression and pharmacological profile of the human organic cation transporters hOCT1, hOCT2 and hOCT3." *British journal of pharmacology* 136 (6): 829-836.

Helma, C., and Kazius, J. 2006. "Artificial intelligence and data mining for toxicity prediction." *Current Computer-Aided Drug Design* 2 (2): 123-133.

Hendrickx, R., Johansson, J. G., Lohmann, C., Jenvert, R.-M., Blomgren, A., Börjesson, L., and Gustavsson, L. 2013. "Identification of novel substrates and structure–activity relationship of cellular uptake mediated by human organic cation transporters 1 and 2." *Journal of medicinal chemistry* 56 (18): 7232-7242.

Hermanto, F. E., Warsito, W., Rifa'i, M., and Widodo, N. 2022. "Understanding hypocholesterolemic activity of soy isoflavones: Completing the puzzle through computational simulations." *Journal of Biomolecular Structure and Dynamics*: 1-7. https://doi.org/10.1080/07391102.2022.2148752..

Hollander, D. A., and Aldave, A. J. 2004. "Drug-induced corneal complications." *Curr Opin Ophthalmol* 15 (6): 541-8. https://doi.org/10.1097/01.icu.0000143688.45232.15.

Hollingsworth, S. A., and Dror, R. O. 2018. "Molecular dynamics simulation for all." *Neuron* 99 (6): 1129-1143.

Honkanen, R. A., Huang, L., Huang, W., and Rigas, B. 2020. "Establishment of a severe dry eye model using complete dacryoadenectomy in rabbits." *JoVE (Journal of Visualized Experiments)* (155): e60126.

Hornof, M., Toropainen, E., and Urtti, A. 2005. "Cell culture models of the ocular barriers." *European journal of pharmaceutics and biopharmaceutics* 60 (2): 207-225.

Huang, K., Magdy, T., Hu, S., Gibson, A., Sparreboom, A., and Burridge, P. 2018. "CARRIER-MEDIATED TRANSPORT OF DOXORUBICIN IN CARDIOMYOCYTES." Clinical Pharmacology & Therapeutics.

Huang, K. M., Uddin, M. E., DiGiacomo, D., Lustberg, M. B., Hu, S., and Sparreboom, A. 2020. "Role of SLC transporters in toxicity induced by anticancer drugs." *Expert opinion on drug metabolism & toxicology* 16 (6): 493-506.

Huang, Y., Dai, Z., Barbacioru, C., and Sadée, W. 2005. "Cystine-glutamate transporter SLC7A11 in cancer chemosensitivity and chemoresistance." *Cancer research* 65 (16): 7446-7454.

Hub, J. S., de Groot, B. L., Grubmüller, H., and Groenhof, G. 2014. "Quantifying artifacts in Ewald simulations of inhomogeneous systems with a net charge." *Journal of chemical theory and computation* 10 (1): 381-390.

Bibliography

Hutter, M. C. 2018. "The current limits in virtual screening and property prediction." *Future medicinal chemistry* 10 (13): 1623-1635.

Jain, S., and Ecker, G. F. 2019. "In Silico Approaches to Predict Drug-Transporter Interaction Profiles: Data Mining, Model Generation, and Link to Cholestasis." *Methods Mol Biol* 1981: 383-396. https://doi.org/10.1007/978-1-4939-9420-5_26.

Jensen, O., Brockmöller, J. r., and Dücker, C. 2021a. "Identification of novel high-affinity substrates of OCT1 using machine learning-guided virtual screening and experimental validation." *Journal of medicinal chemistry* 64 (5): 2762-2776.

---. 2021b. "Identification of Novel High-Affinity Substrates of OCT1 Using Machine Learning-Guided Virtual Screening and Experimental Validation." *Journal of Medicinal Chemistry*.

Jordan, M., Schallhorn, A., and Wurm, F. M. 1996. "Transfecting mammalian cells: optimization of critical parameters affecting calcium-phosphate precipitate formation." *Nucleic acids research* 24 (4): 596-601.

Jouan, E., Le Vee, M., Denizot, C., Da Violante, G., and Fardel, O. 2014. "The mitochondrial fluorescent dye rhodamine 123 is a high-affinity substrate for organic cation transporters (OCT s) 1 and 2." *Fundamental & clinical pharmacology* 28 (1): 65-77.

Jui-Hung Kao, T.-T. L., Cheng-Hsun Lu, Ting-Yuan Lan, Yi-Ting Hsieh, Chieh-Yu Shen, Ko-Jen Li, and Song-Chou Hsieh. 2022. "Characteristics and Potential Risk Factors of Hydroxychloroquine Retinopathy in Patients with Systemic Lupus Erythematosus: Focusing on Asian Population." *Journal of Ocular Pharmacology and Therapeutics* 0 (0): null. https://doi.org/10.1089/jop.2022.0060.

Kabanov, A. V., Batrakova, E. V., and Miller, D. W. 2003. "Pluronic® block copolymers as modulators of drug efflux transporter activity in the blood–brain barrier." *Advanced Drug Delivery Reviews* 55 (1): 151-164. https://doi.org/https://doi.org/10.1016/S0169-409X(02)00176-X.

Kachkin, D. V., Khorolskaya, J. I., Ivanova, J. S., and Rubel, A. A. 2020. "An Efficient Method for Isolation of Plasmid DNA for Transfection of Mammalian Cell Cultures." *Methods Protoc* 3 (4). https://doi.org/10.3390/mps3040069.

Kato, Y., Takahara, S., Kato, S., Kubo, Y., Sai, Y., Tamai, I., Yabuuchi, H., and Tsuji, A. 2008. "Involvement of multidrug resistance-associated protein 2 (Abcc2) in molecular weight-dependent biliary excretion of β-lactam antibiotics." *Drug metabolism and disposition* 36 (6): 1088-1096.

Kels, B. D., Grzybowski, A., and Grant-Kels, J. M. 2015. "Human ocular anatomy." *Clinics in Dermatology* 33 (2): 140-146. https://doi.org/https://doi.org/10.1016/j.clindermatol.2014.10.006.

Khuri, N., and Deshmukh, S. 2018. "Machine Learning for Classification of Inhibitors of Hepatic Drug Transporters." 2018 17th IEEE International Conference on Machine Learning and Applications (ICMLA).

Bibliography

Kim, Y. E., Yun, J. Y., and Jeon, B. S. 2011. "Effect of intravenous amantadine on dopaminergic-drug-resistant freezing of gait." *Parkinsonism & Related Disorders* 17 (6): 491-492.

Koepsell, H. 2004. "Polyspecific organic cation transporters: their functions and interactions with drugs." *Trends in pharmacological sciences* 25 (7): 375-381.

---. 2011. "Substrate recognition and translocation by polyspecific organic cation transporters."

Koepsell, H., Lips, K., and Volk, C. 2007. "Polyspecific Organic Cation Transporters: Structure, Function, Physiological Roles, and Biopharmaceutical Implications." *Pharmaceutical Research* 24 (7): 1227-1251. https://doi.org/10.1007/s11095-007-9254-z.

KONERU, P. B., LIEN, E. J., and KODA, R. T. 1986. "Oculotoxicities of systemically administered drugs." *Journal of Ocular Pharmacology and Therapeutics* 2 (4): 385-404.

Koshy, C., Parthiban, M., and Sowdhamini, R. 2010. "100 ns molecular dynamics simulations to study intramolecular conformational changes in Bax." *Journal of Biomolecular Structure and Dynamics* 28 (1): 71-83.

Kubo, Y., Tsuchiyama, A., Shimizu, Y., Akanuma, S.-I., and Hosoya, K.-I. 2014a. "Involvement of carrier-mediated transport in the retinal uptake of clonidine at the inner blood-retinal barrier." *Molecular pharmaceutics* 11 (10): 3747-3753. https://doi.org/10.1021/mp500516j.

---. 2014b. "Involvement of carrier-mediated transport in the retinal uptake of clonidine at the inner blood–retinal barrier." *Molecular Pharmaceutics* 11 (10): 3747-3753.

Kumar, P., Nagarajan, A., and Uchil, P. D. 2019. "Calcium phosphate-mediated transfection of eukaryotic cells with plasmid DNAs." *Cold Spring Harbor Protocols* 2019 (10): pdb. prot095430.

Lee, D. Y., Kim, E., and Choi, M. H. 2015. "Technical and clinical aspects of cortisol as a biochemical marker of chronic stress." *BMB Rep* 48 (4): 209-16. https://doi.org/10.5483/bmbrep.2015.48.4.275.

Lee, J., and Pelis, R. M. 2016. "Drug Transport by the Blood-Aqueous Humor Barrier of the Eye." *Drug Metab Dispos* 44 (10): 1675-81. https://doi.org/10.1124/dmd.116.069369.

Leung, S., Ashar, B. H., and Miller, R. G. 2005. "Bisphosphonate-associated scleritis: a case report and review." *South Med J* 98 (7): 733-5. https://doi.org/10.1097/01.Smj.0000152753.80490.9f.

Li, J., Tripathi, R. C., and Tripathi, B. J. 2008. "Drug-induced ocular disorders." *Drug safety* 31 (2): 127-141.

Liang, C., Peyman, G. A., and Federman, J. 1996. "Ocular toxicity of intravitreous transforming growth factor-beta 1." *Eye* 10 (6): 709-713. https://doi.org/10.1038/eye.1996.165.

Liu, C. Y., Francis, J. H., Pulido, J., and Abramson, D. 2018. "Ocular side effects of systemically administered chemotherapy." *UpToDate. Waltham, MA: UpToDate*.

Liu, H. C., Goldenberg, A., Chen, Y., Lun, C., Wu, W., Bush, K. T., Balac, N., Rodriguez, P., Abagyan, R., and Nigam, S. K. 2016. "Molecular Properties of Drugs Interacting with SLC22 Transporters OAT1,

Bibliography

OAT3, OCT1, and OCT2: A Machine-Learning Approach." *J Pharmacol Exp Ther* 359 (1): 215-29. https://doi.org/10.1124/jpet.116.232660.

Liu, K., and Kokubo, H. 2017. "Exploring the Stability of Ligand Binding Modes to Proteins by Molecular Dynamics Simulations: A Cross-docking Study." *Journal of Chemical Information and Modeling* 57 (10): 2514-2522. https://doi.org/10.1021/acs.jcim.7b00412.

Liu, L., and Liu, X. 2019. "Roles of drug transporters in blood-retinal barrier." *Drug Transporters in Drug Disposition, Effects and Toxicity*: 467-504.

Lomize, M. A., Lomize, A. L., Pogozheva, I. D., and Mosberg, H. I. 2006. "OPM: orientations of proteins in membranes database." *Bioinformatics* 22 (5): 623-625.

Ma, R., Li, G., Wang, X., Bi, Y., and Zhang, Y. 2021. "Inhibitory effect of sixteen pharmaceutical excipients on six major organic cation and anion uptake transporters." *Xenobiotica* 51 (1): 95-104.

Mahmood, T., and Yang, P. C. 2012. "Western blot: technique, theory, and trouble shooting." *N Am J Med Sci* 4 (9): 429-34. https://doi.org/10.4103/1947-2714.100998.

Malani, M., Hiremath, M. S., Sharma, S., Jhunjhunwala, M., Gayen, S., Hota, C., and Nirmal, J. 2023. "Interaction of systemic drugs causing ocular toxicity with organic cation transporter: an artificial intelligence prediction." *J Biomol Struct Dyn*: 1-12. https://doi.org/10.1080/07391102.2023.2226717.

Malani, M., and Nirmal, J. 2022. "Retinal Pathophysiological Evaluation in a Rat Model." *JoVE (Journal of Visualized Experiments)* (183): e63111.

Malekian, A., and Chitsaz, N. 2021. "Chapter 4 - Concepts, procedures, and applications of artificial neural network models in streamflow forecasting." In *Advances in Streamflow Forecasting*, edited by Sharma, P. and Machiwal, D., 115-147. Elsevier.

Manisha, N. 2023. Systemic Drug causing Ocular Toxicity. Hyderabad.

Mannermaa, E., Vellonen, K.-S., and Urtti, A. 2006. "Drug transport in corneal epithelium and blood–retina barrier: emerging role of transporters in ocular pharmacokinetics." *Advanced drug delivery reviews* 58 (11): 1136-1163.

Martin, X., and Brennan, M. 1993. "Dopamine and its metabolites in human tears." *European journal of ophthalmology* 3 (2): 83-88.

---. 1994. "Serotonin in human tears." *European journal of ophthalmology* 4 (3): 159-165.

Mason, C. G. 1977. "Ocular accumulation and toxicity of certain systemically administered drugs." *J Toxicol Environ Health* 2 (5): 977-95. https://doi.org/10.1080/15287397709529497.

Melles, R. B., and Marmor, M. F. 2014. "The risk of toxic retinopathy in patients on long-term hydroxychloroquine therapy." *JAMA Ophthalmol* 132 (12): 1453-60. https://doi.org/10.1001/jamaophthalmol.2014.3459.

Bibliography

Meyer, M. J., and Tzvetkov, M. V. 2021. "OCT1 Polyspecificity—Friend or Foe?" *Frontiers in Pharmacology* 12: 698153.

Michelson, M., Chow, T., Martin, N. A., Ross, M., Ying, A. T. Q., and Minton, S. 2020. "Artificial Intelligence for Rapid Meta-Analysis: Case Study on Ocular Toxicity of Hydroxychloroquine." *Journal of Medical Internet Research* 22 (8): e20007.

Misaka, S., Knop, J., Singer, K., Hoier, E., Keiser, M., Müller, F., Glaeser, H., König, J. r., and Fromm, M. F. 2016. "The nonmetabolized β-blocker nadolol is a substrate of OCT1, OCT2, MATE1, MATE2-K, and P-glycoprotein, but not of OATP1B1 and OATP1B3." *Molecular Pharmaceutics* 13 (2): 512-519.

Moaddel, R., Ravichandran, S., Bighi, F., Yamaguchi, R., and Wainer, I. 2007. "Pharmacophore modelling of stereoselective binding to the human organic cation transporter (hOCT1)." *British journal of pharmacology* 151 (8): 1305-1314.

Moorthy, R. S., and Valluri, S. 1999. "Ocular toxicity associated with systemic drug therapy." *Current Opinion in Ophthalmology* 10 (6): 438-446.

Muderrisoglu, A. E., Becher, K. F., Madersbacher, S., and Michel, M. C. 2019. "Cognitive and mood side effects of lower urinary tract medication." *Expert Opin Drug Saf* 18 (10): 915-923. https://doi.org/10.1080/14740338.2019.1652269.

Mukhtar, S., and Jhanji, V. 2022. "Effects of systemic targeted immunosuppressive therapy on ocular surface." *Current opinion in ophthalmology* 33 (4): 311-317.

Nagy, T., Tóth, Á., Telbisz, Á., Sarkadi, B., Tordai, H., Tordai, A., and Hegedűs, T. 2021. "The transport pathway in the ABCG2 protein and its regulation revealed by molecular dynamics simulations." *Cellular and Molecular Life Sciences* 78 (5): 2329-2339. https://doi.org/10.1007/s00018-020-03651-3.

Neuhoff, S., Ungell, A.-L., Zamora, I., and Artursson, P. 2003. "pH-dependent bidirectional transport of weakly basic drugs across Caco-2 monolayers: implications for drug–drug interactions." *Pharmaceutical research* 20 (8): 1141-1148.

Nigam, S. K. 2015. "What do drug transporters really do?" *Nature reviews Drug discovery* 14 (1): 29-44.

Nirmal, J., Singh, S., Biswas, N., Thavaraj, V., Azad, R., and Velpandian, T. 2013a. "Potential pharmacokinetic role of organic cation transporters in modulating the transcorneal penetration of its substrates administered topically." *Eye* 27 (10): 1196-1203.

Nirmal, J., Singh, S. B., Biswas, N. R., Thavaraj, V., Azad, R. V., and Velpandian, T. 2013b. "Potential pharmacokinetic role of organic cation transporters in modulating the transcorneal penetration of its substrates administered topically." *Eye (Lond)* 27 (10): 1196-203. https://doi.org/10.1038/eye.2013.146.

Bibliography

Nirmal, J., Sirohiwal, A., Singh, S. B., Biswas, N. R., Thavaraj, V., Azad, R. V., and Velpandian, T. 2013a. "Role of organic cation transporters in the ocular disposition of its intravenously injected substrate in rabbits: implications for ocular drug therapy." *Exp Eye Res* 116: 27-35. https://doi.org/10.1016/j.exer.2013.07.004.

Nirmal, J., Sirohiwal, A., Singh, S. B., Biswas, N. R., Thavaraj, V., Azad, R. V., and Velpandian, T. 2013b. "Role of organic cation transporters in the ocular disposition of its intravenously injected substrate in rabbits: Implications for ocular drug therapy." *Experimental Eye Research* 116: 27-35. https://doi.org/https://doi.org/10.1016/j.exer.2013.07.004.

Nirmal, J., Velpandian, T., Biswas, N., Azad, R., Vasantha, T., Bhatnagar, A., and Ghose, S. 2010. "Evaluation of the relevance of OCT blockade on the transcorneal kinetics of topically applied substrates using rabbits." FIP 2010 World Congress in Association with AAPS, New Orleans, USA.

Nirmal, J., Velpandian, T., Singh, S. B., Ranjan Biswas, N., Azad, R., Thavaraj, V., Mittal, G., Bhatnagar, A., and Ghose, S. 2012. "Evaluation of the functional importance of organic cation transporters on the ocular disposition of its intravitreally injected substrate in rabbits." *Current eye research* 37 (12): 1127-1135.

Nirmal J, V. T., Biswas NR, Azad RV, Vasantha T, Bhatnagar A, Ghose S. 2010. "Evaluation of the relevance of OCT blockade on the transcorneal kinetics of topically applied substrates using rabbits." *FIP 2010 World Congress in association with AAPS, New Orleans, USA, Nov*.

Noureddin, B. N., Seoud, M., Bashshur, Z., Salem, Z., Shamseddin, A., and Khalil, A. 1999. "Ocular toxicity in low-dose tamoxifen: a prospective study." *Eye* 13 (6): 729-733.

OECD. 2020. Overview of Concepts and Available Guidance related to Integrated Approaches to Testing and Assessment (IATA). In *Series on Testing and Assesment No. 329*, edited by OECD: Environment, Health and Safety, Environment Directorate, OECD.

---. 2021. "The OECD QSAR Toolbox." https://www.oecd.org/chemicalsafety/risk-assessment/oecd-qsar-toolbox.html. OECD. Accessed 07/10/2022.

OECD. 1994. *OECD Guidelines for the Testing of Chemicals*. Organization for Economic.

"Organisation for Economic Co-operation and Development, About OECD iLibrary." *https://www.oecd-ilibrary.org/oecd/about*.

Otter, M., Oswald, S., Siegmund, W., and Keiser, M. 2017. "Effects of frequently used pharmaceutical excipients on the organic cation transporters 1–3 and peptide transporters 1/2 stably expressed in MDCKII cells." *European Journal of Pharmaceutics and Biopharmaceutics* 112: 187-195. https://doi.org/https://doi.org/10.1016/j.ejpb.2016.11.028.

Ozdemir, S., and Susarla, D. 2018. *Feature Engineering Made Easy: Identify unique features from your dataset in order to build powerful machine learning systems*. Packt Publishing Ltd.

Bibliography

Pan, X., Wang, L., Gründemann, D., and Sweet, D. H. 2013. "Interaction of ethambutol with human organic cation transporters of the SLC22 family indicates potential for drug-drug interactions during antituberculosis therapy." *Antimicrobial agents and chemotherapy* 57 (10): 5053-5059.

Peng, Y., Chen, L., Ye, S., Kang, Y., Liu, J., Zeng, S., and Yu, L. 2020. "Research and development of drug delivery systems based on drug transporter and nano-formulation." *Asian J Pharm Sci* 15 (2): 220-236. https://doi.org/10.1016/j.ajps.2020.02.004.

Pérez Santín, E., Rodríguez Solana, R., González García, M., García Suárez, M. D. M., Blanco Díaz, G. D., Cima Cabal, M. D., Moreno Rojas, J. M., and López Sánchez, J. I. 2021. "Toxicity prediction based on artificial intelligence: A multidisciplinary overview." *Wiley Interdisciplinary Reviews: Computational Molecular Science*: e1516.

Police, A., Shankar, V. K., and Murthy, S. N. 2020a. "Role of taurine transporter in the retinal uptake of vigabatrin." *AAPS PharmSciTech* 21: 1-9.

---. 2020b. "Role of Taurine Transporter in the Retinal Uptake of Vigabatrin." *AAPS PharmSciTech* 21 (5): 1-9.

Pope, B., and Kent, H. M. 1996. "High Efficiency 5 Min Transformation of Escherichia Coli." *Nucleic Acids Research* 24 (3): 536-537. https://doi.org/10.1093/nar/24.3.536.

Popp, C., Gorboulev, V., Müller, T. D., Gorbunov, D., Shatskaya, N., and Koepsell, H. 2005. "Amino acids critical for substrate affinity of rat organic cation transporter 1 line the substrate binding region in a model derived from the tertiary structure of lactose permease." *Molecular pharmacology* 67 (5): 1600-1611.

Prakash, B., Kumar, H. M., Palaniswami, S., and Lakshman, B. H. 2019. "Ocular side effects of systemic drugs used in dermatology." *Indian journal of dermatology* 64 (6): 423.

Prevention, C. f. D. C. a. 2022. "About Chronic Diseases." Centers for Disease Control and Prevention. Last Modified 21 July 2022. Accessed 25 November. https://www.cdc.gov/chronicdisease/about/index.htm.

Pu, L., Naderi, M., Liu, T., Wu, H.-C., Mukhopadhyay, S., and Brylinski, M. 2019. "e toxpred: A machine learning-based approach to estimate the toxicity of drug candidates." *BMC Pharmacology and Toxicology* 20 (1): 1-15.

Raies, A. B., and Bajic, V. B. 2016. "In silico toxicology: computational methods for the prediction of chemical toxicity." *Wiley Interdisciplinary Reviews: Computational Molecular Science* 6 (2): 147-172.

Ramachandran, G. t., and Sasisekharan, V. 1968. "Conformation of polypeptides and proteins." *Advances in protein chemistry* 23: 283-437.

Redeker, K.-E. M., Jensen, O., Gebauer, L., Meyer-Tönnies, M. J., and Brockmöller, J. 2022. "Atypical substrates of the organic cation transporter 1." *Biomolecules* 12 (11): 1664.

Bibliography

Richa, S., and Yazbek, J.-C. 2010. "Ocular adverse effects of common psychotropic agents." *CNS drugs* 24 (6): 501-526.

Rolando, M., and Zierhut, M. 2001. "The Ocular Surface and Tear Film and Their Dysfunction in Dry Eye Disease." *Survey of Ophthalmology* 45: S203-S210. https://doi.org/https://doi.org/10.1016/S0039-6257(00)00203-4.

Sadee, W., and Dai, Z. 2005. "Pharmacogenetics/genomics and personalized medicine." *Human molecular genetics* 14 (suppl_2): R207-R214.

Sahoo, S., Aurich, M., Jonsson, J., and Thiele, I. 2014. "Membrane transporters in a human genome-scale metabolic knowledgebase and their implications for disease." *Frontiers in Physiology* 5. https://doi.org/10.3389/fphys.2014.00091.

Santaella, R. M., and Fraunfelder, F. W. 2007. "Ocular adverse effects associated with systemic medications." *Drugs* 67 (1): 75-93.

Sarker, I. H. 2021. "Machine Learning: Algorithms, Real-World Applications and Research Directions." *SN Computer Science* 2 (3): 160. https://doi.org/10.1007/s42979-021-00592-x.

Saxena, R., Singh, D., Phuljhele, S., Kalaiselvan, V., Karna, S., Gandhi, R., Prakash, A., Lodha, R., Mohan, A., Menon, V., and Garg, R. 2021. "Ethambutol toxicity: Expert panel consensus for the primary prevention, diagnosis and management of ethambutol-induced optic neuropathy." *Indian J Ophthalmol* 69 (12): 3734-3739. https://doi.org/10.4103/ijo.IJO_3746_20.

Schechter, J. E., Warren, D. W., and Mircheff, A. K. 2010a. "A lacrimal gland is a lacrimal gland, but rodent's and rabbit's are not human." *The ocular surface* 8 (3): 111-134.

Schechter, J. E., Warren, D. W., and Mircheff, A. K. 2010b. "A lacrimal gland is a lacrimal gland, but rodent's and rabbit's are not human." *Ocul Surf* 8 (3): 111-34. https://doi.org/10.1016/s1542-0124(12)70222-7.

Schirmer, P. O. 1903. "Studien zur Physiologie und Pathologie der Tränenabsonderung und Tränenabfuhr." *Albrecht von Graefes Archiv für Ophthalmologie* 56: 197-291.

Schlessinger, A., Welch, M. A., van Vlijmen, H., Korzekwa, K., Swaan, P. W., and Matsson, P. 2018. "Molecular Modeling of Drug-Transporter Interactions-An International Transporter Consortium Perspective." *Clin Pharmacol Ther* 104 (5): 818-835. https://doi.org/10.1002/cpt.1174.

Sharma, H. P., Halder, N., Singh, S. B., and Velpandian, T. 2021. "Evaluation of the Presence and Functional Importance of Nucleoside Transporters in Lacrimal Gland for Tear Disposition of Intravenously Injected Substrate in Rabbits." *Curr Eye Res* 46 (11): 1659-1665. https://doi.org/10.1080/02713683.2021.1925698.

Bibliography

Shimizu, T., Masuo, Y., Takahashi, S., Nakamichi, N., and Kato, Y. 2015. "Organic cation transporter Octn1-mediated uptake of food-derived antioxidant ergothioneine into infiltrating macrophages during intestinal inflammation in mice." *Drug metabolism and pharmacokinetics* 30 (3): 231-239.

Shin, E., Lim, D. H., Han, J., Nam, D.-H., Park, K., Ahn, M.-J., Kang, W. K., Lee, J., Ahn, J. S., Lee, S.-H., Sun, J.-M., Jung, H. A., and Chung, T.-Y. 2020. "Markedly increased ocular side effect causing severe vision deterioration after chemotherapy using new or investigational epidermal or fibroblast growth factor receptor inhibitors." *BMC Ophthalmology* 20 (1): 19. https://doi.org/10.1186/s12886-019-1285-9.

Shoichet, B. K., Leach, A. R., and Kuntz, I. D. 1999. "Ligand solvation in molecular docking." *Proteins: Structure, Function, and Bioinformatics* 34 (1): 4-16.

Shu, Y., Leabman, M. K., Feng, B., Mangravite, L. M., Huang, C. C., Stryke, D., Kawamoto, M., Johns, S. J., DeYoung, J., Carlson, E., Ferrin, T. E., Herskowitz, I., and Giacomini, K. M. 2003. "Evolutionary conservation predicts function of variants of the human organic cation transporter, OCT1." *Proc Natl Acad Sci U S A* 100 (10): 5902-7. https://doi.org/10.1073/pnas.0730858100.

Silva, A. C., Borba, J. V., Alves, V. M., Hall, S. U., Furnham, N., Kleinstreuer, N., Muratov, E., Tropsha, A., and Andrade, C. H. 2021. "Novel computational models offer alternatives to animal testing for assessing eye irritation and corrosion potential of chemicals." *Artificial Intelligence in the Life Sciences* 1: 100028.

Soodvilai, S., Soodvilai, S., Chatsudthipong, V., Ngawhirunpat, T., Rojanarata, T., and Opanasopit, P. 2017a. "Interaction of pharmaceutical excipients with organic cation transporters." *Int J Pharm* 520 (1-2): 14-20. https://doi.org/10.1016/j.ijpharm.2017.01.042.

Soodvilai, S., Soodvilai, S., Chatsudthipong, V., Ngawhirunpat, T., Rojanarata, T., and Opanasopit, P. 2017b. "Interaction of pharmaceutical excipients with organic cation transporters." *International journal of pharmaceutics* 520 (1-2): 14-20.

Stevens, A., and Spooner, D. 2001. "Lacrimal Duct Stenosis and Other Ocular Toxicity Associated with Adjuvant Cyclophosphamide, Methotrexate and 5-Fluorouracil Combination Chemotherapy for Early Stage Breast Cancer." *Clinical Oncology* 13 (6): 438-440. https://doi.org/https://doi.org/10.1053/clon.2001.9308.

SUGAI, S., MURATA, K., KITAGAKI, T., and TOMITA, I. 1991. "STUDIES ON EYE IRRITATION CAUSED BY CHEMICALS IN RABBITS: II. STRUCTURE-ACTIVITY RELATIONSHIPS AND IN VITRO APPROACH TO PRIMARY EYE IRRITATION OF SALICYLATES IN RABBITS." *The Journal of toxicological sciences* 16 (3): 111-130.

Bibliography

Taylor-Wells, J., and Meredith, D. 2014. "The Signature Sequence Region of the Human Drug Transporter Organic Anion Transporting Polypeptide 1B1 Is Important for Protein Surface Expression." *J Drug Deliv* 2014: 129849. https://doi.org/10.1155/2014/129849.

Tehrani, R., Ostrowski, R. A., Hariman, R., and Jay, W. M. 2008. "Ocular toxicity of hydroxychloroquine." Seminars in ophthalmology.

Thakkar, P. H. 2015. "Influence of excipients on drug absorption via modulation of intestinal transporters activity." *Asian Journal of Pharmaceutics (AJP): Free full text articles from Asian J Pharm* 9 (2): 69-82.

Trope, G. E., and Rumley, A. G. 1984. "Catecholamine concentrations in tears." *Exp Eye Res* 39 (3): 247-50. https://doi.org/10.1016/0014-4835(84)90012-5.

Ubels, J. L., Hoffman, H. M., Srikanth, S., Resau, J. H., and Webb, C. P. 2006. "Gene Expression in Rat Lacrimal Gland Duct Cells Collected Using Laser Capture Microdissection: Evidence for K+ Secretion by Duct Cells." *Investigative Ophthalmology & Visual Science* 47 (5): 1876-1885. https://doi.org/10.1167/iovs.05-0363.

Ueda, H., Horibe, Y., Kim, K.-J., and Lee, V. H. L. 2000. "Functional Characterization of Organic Cation Drug Transport in the Pigmented Rabbit Conjunctiva." *Investigative Ophthalmology & Visual Science* 41 (3): 870-876.

Unni, E. 2023. Medicine Use in Chronic Diseases. MDPI.

V Kleandrova, V., Luan, F., Speck-Planche, A., and Cordeiro, N. D. 2015. "In silico assessment of the acute toxicity of chemicals: recent advances and new model for multitasking prediction of toxic effect." *Mini reviews in medicinal chemistry* 15 (8): 677-686.

Valsson, O., Tiwary, P., and Parrinello, M. 2016. "Enhancing important fluctuations: Rare events and metadynamics from a conceptual viewpoint." *Annu. Rev. Phys. Chem* 67 (1): 159-184.

Vamathevan, J., Clark, D., Czodrowski, P., Dunham, I., Ferran, E., Lee, G., Li, B., Madabhushi, A., Shah, P., Spitzer, M., and Zhao, S. 2019. "Applications of machine learning in drug discovery and development." *Nat Rev Drug Discov* 18 (6): 463-477. https://doi.org/10.1038/s41573-019-0024-5.

Van Haeringen, N. J. 1981a. "Clinical biochemistry of tears." *Survey of ophthalmology* 26 (2): 84-96.

Van Haeringen, N. J. 1981b. "Clinical biochemistry of tears." *Surv Ophthalmol* 26 (2): 84-96. https://doi.org/10.1016/0039-6257(81)90145-4.

Velpandian, T., Nirmal, J., Arora, B., Ravi, A. K., and Kotnala, A. 2012. "Understanding the charge issues in mono and di-quaternary ammonium compounds for their determination by LC/ESI-MS/MS." *Analytical letters* 45 (16): 2367-2376.

Bibliography

Velpandian, T., Nirmal, J., Sirohiwal, A., Singh, S. B., Vasantha, T., Azad, R. V., and Ghose, S. 2012. "Evaluation of the modulation of Organic Cation Transporter (OCT) in the Tear Disposition of its Substrates in Rabbits." *Investigative Ophthalmology & Visual Science* 53 (14): 5333-5333.

Venter, J. C., Adams, M. D., Myers, E. W., Li, P. W., Mural, R. J., Sutton, G. G., Smith, H. O., Yandell, M., Evans, C. A., and Holt, R. A. 2001. "The sequence of the human genome." *science* 291 (5507): 1304-1351.

Vijayakumar, A., Velpandian, T., and Saxena, R. 2011. "Ocular adverse effects of systemically administered drugs." *Essential of Ocular Pharmacology. Malaysia, Shah Alam*: 343-364.

Vishnevskia-Dai, V., Rozner, L., Berger, R., Jaron, Z., Elyashiv, S., Markel, G., and Zloto, O. 2021. "Ocular side effects of novel anti-cancer biological therapies." *Sci Rep* 11 (1): 787. https://doi.org/10.1038/s41598-020-80898-7.

Wang, Q., Li, X., Yang, H., Cai, Y., Wang, Y., Wang, Z., Li, W., Tang, Y., and Liu, G. 2017. "In silico prediction of serious eye irritation or corrosion potential of chemicals." *RSC advances* 7 (11): 6697-6703.

Weiss, S. L., and Kramer, W. G. 2019. "Ocular distribution of cyclosporine following topical administration of OTX-101 in New Zealand white rabbits." *Journal of Ocular Pharmacology and Therapeutics* 35 (7): 395-402.

Weng, Y. L., Naik, S. R., Dingelstad, N., Lugo, M. R., Kalyaanamoorthy, S., and Ganesan, A. 2021. "Molecular dynamics and in silico mutagenesis on the reversible inhibitor-bound SARS-CoV-2 main protease complexes reveal the role of lateral pocket in enhancing the ligand affinity." *Sci Rep* 11 (1): 7429. https://doi.org/10.1038/s41598-021-86471-0.

Wenge, B., Geyer, J., and Bönisch, H. 2011. "Oxybutynin and trospium are substrates of the human organic cation transporters." *Naunyn-Schmiedeberg's archives of pharmacology* 383 (2): 203-208.

Wu, Y., and Wang, G. 2018. "Machine learning based toxicity prediction: from chemical structural description to transcriptome analysis." *International journal of molecular sciences* 19 (8): 2358.

Yamagata, T., Kusuhara, H., Morishita, M., Takayama, K., Benameur, H., and Sugiyama, Y. 2007. "Effect of excipients on breast cancer resistance protein substrate uptake activity." *Journal of controlled release* 124 (1-2): 1-5.

Yasujima, T., Ohta, K., Inoue, K., and Yuasa, H. 2011. "Characterization of human OCT1-mediated transport of DAPI as a fluorescent probe substrate." *Journal of pharmaceutical sciences* 100 (9): 4006-4012.

Yuan, X., Feng, Y., Li, D., and Li, M. 2019. "Unilateral visual impairment in a patient undergoing chemotherapy: a case report and clinical findings." *BMC Ophthalmology* 19 (1): 236. https://doi.org/10.1186/s12886-019-1246-3.

Bibliography

Yusuf, I., Sharma, S., Luqmani, R., and Downes, S. 2017. "Hydroxychloroquine retinopathy." *Eye* 31 (6): 828-845.

Zeino, M., Saeed, M. E., Kadioglu, O., and Efferth, T. 2014. "The ability of molecular docking to unravel the controversy and challenges related to P-glycoprotein—a well-known, yet poorly understood drug transporter." *Investigational new drugs* 32 (4): 618-625.

Zhang, H., Yao, M., Morrison, R. A., and Chong, S. 2003. "Commonly used surfactant, Tween 80, improves absorption of P-glycoprotein substrate, digoxin, in rats." *Archives of Pharmacal Research* 26: 768-772.

Zhang, L., Dresser, M. J., Gray, A. T., Yost, S. C., Terashita, S., and Giacomini, K. M. 1997. "Cloning and functional expression of a human liver organic cation transporter." *Mol Pharmacol* 51 (6): 913-21. https://doi.org/10.1124/mol.51.6.913.

Zhang, T., Xiang, C. D., Gale, D., Carreiro, S., Wu, E. Y., and Zhang, E. Y. 2008. "Drug transporter and cytochrome P450 mRNA expression in human ocular barriers: implications for ocular drug disposition." *Drug Metabolism and Disposition* 36 (7): 1300-1307.

Appendix

Appendix

A. Publications and Presentations (Thesis work)

Publications

1. **Manisha Malani**, Manthan S. Hiremath, Surbhi Sharma, Manisha Jhunjhunwala, Shovanlal Gayen, Chittaranjan Hota, and Jayabalan Nirmal. Interaction of systemic drugs causing ocular toxicity with organic cation transporter: an artificial intelligence prediction. Journal of Biomolecular Structure and Dynamics (2023): 1-13.

2. **Manisha Malani**, Anirudh Kasturi, Md Moinul, Shovanlal Gayen, Chittaranjan Hota, and Jayabalan Nirmal. Role of Artificial Intelligence in the Toxicity Prediction of Drugs. In Biomedical Applications and Toxicity of Nanomaterials, pp. 589-636. Singapore: Springer Nature Singapore, 2023.

3. **Manisha Malani,** Mansi Shah, Niharika P, Nirmal J. Functional role of organic cation transporter in lacrimal gland: Carrier of ocular toxic drugs (Manuscript under preparation).

4. **Manisha Malani,** Suraj Paulkar, Nirmal J. Expression of transporters and its role in lacrimal gland secretion (Manuscript under preparation).

Presentations

1. **Manisha Malani**, Surbhi Sharma, Manisha Jhunjhunwala, Manthan S Hiremath, Shovanlan Gayen, Chittaranjan Hota, Jayabalan Nirmal. Artificial intelligence and experimental studies to understand the role of transporters in ocular toxicity of systemic drugs. ARVO-USA, May 2022 held at Denver, Colorado, USA.

Appendix

2. **Manisha Malani**, Manthan S Hiremath, Jayabalan Nirmal. Functional role of Organic Cation Transporter 1 in systemic drug induced ocular toxicity. ARVO-India, 29th Annual meeting of Indian Eye Research Group, July 2023, held at Aravind Medical Research Foundation (AMRF), Madurai, Tamil Nadu, India.

3. Suraj Paulkar, **Manisha Malani**, Jayabalan Nirmal. Transporter profiling of the lacrimal gland to decipher their role in ocular toxicity. ARVO-India, 29th Annual meeting of Indian Eye Research Group, July 2023, held at Aravind Medical Research Foundation (AMRF), Madurai, Tamil Nadu, India.

4. **Manisha Malani**, Manthan S Hiremath, Surbhi Sharma, Chittaranjan Hota, Shovanlal Gayen, Jayabalan Nirmal. In-silico models to comprehend the drug-transporter interaction. ARVO-India, 28th Annual meeting of Indian Eye Research Group, September 2022, held at L V Prasad Eye Institute, Hyderabad, Telangana, India.

5. Manthan Hiremath, **Manisha Malani**, Surbhi Sharma, Chittaranjan Hota, Jayabalan Nirmal. Artificial intelligence and biophysical simulation delineates the potential role of organic anion transporter-1 in systemic drug induced ocular toxicity. ARVO-India, 28th Annual meeting of Indian Eye Research Group, September 2022, held at L V Prasad Eye Institute, Hyderabad, Telangana, India.

6. **Manisha Malani**, Jayabalan Nirmal. Membrane Transporters in Lacrimal Gland: Portal for Systemic Drugs to Enter Eye. 3rd National Biomedical Research Competition (NBRCOM), India, December 2021, held by Society of Young Biomedical Scientists, India.

7. **Manisha Malani**, Surbhi Sharma, Manisha Jhunjhunwala, Shovanlal Gayen, Chittaranjan Hota, Jayabalan Nirmal. Artificial Intelligence in Predicting the Drug Transporter Interaction: Understanding the Entry of Systemic Drugs into Eye. ARVO-India, 27th Annual meeting of Indian Eye Research Group, October 2021, held at L V Prasad Eye Institute, Hyderabad, Telangana, India.

8. Manthan Hiremath, **Manisha Malani**, Surbhi Sharma, Manisha Jhunjhunwala, Shovanlan Gayen, Chittaranjan Hota, Jayabalan Nirmal. In silico methods to predict interaction between systemic drugs causing ocular toxicity and organic cation transporter. APOGEE-2022, April 2022, held at BITS-Pilani, Pilani Campus.

B. Publications and Presentations (Others)

<u>**Publications**</u>

1. **Manisha Malani**, Aiswarya Thattaru Thodikayil, Sampa Saha, and Jayabalan Nirmal. Carboxylated nanofibrillated cellulose empowers moxifloxacin to overcome Staphylococcus aureus biofilm in bacterial keratitis. Carbohydrate Polymers (2023): 121558.

2. **Manisha Malani**, and Jayabalan Nirmal. Retinal Pathophysiological Evaluation in a Rat Model. JoVE (Journal of Visualized Experiments) 183 (2022): e63111.

3. Velmurugan Kailasam, Sai Shreya Cheruvu, **Manisha Malani**, Srujana Mosalikanti Sai Kameswari, Prashant Kesharwani, and Jayabalan Nirmal. Recent advances in novel

formulation approaches for tacrolimus delivery in treatment of various ocular diseases. Journal of Drug Delivery Science and Technology (2022): 103945.

4. **Manisha Malani**, Prerana Salunke, Shraddha Kulkarni, Gaurav K. Jain, Afsana Sheikh, Prashant Kesharwani, and Jayabalan Nirmal. Repurposing pharmaceutical excipients as an antiviral agent against SARS-CoV-2. Journal of Biomaterials Science, Polymer Edition 33, no. 1 (2022): 110-136.

Presentations

1. Raj Girish Savla, **Manisha Malani**, Aiswarya Thattaru Thodikayil, Sampa Saha, Jayabalan Nirmal. Moxifloxacin loaded carboxylated cellulose particles to treat corneal infections. ARVO-India, 29th Annual meeting of Indian Eye Research Group, July 2023, held at Aravind Medical Research Foundation (AMRF), Madurai, Tamil Nadu, India.

2. Sai Shreya Cheruvu, Velmurugan Kailasam, **Manisha Malani**, Soumyava Basu, Jayabalan Nirmal. Efficacy of phosphodiesterase-4 inhibitor to treat anterior uveitis in in vivo model. ARVO-India, 28th Annual meeting of Indian Eye Research Group, September 2022, held at L V Prasad Eye Institute, Hyderabad, Telangana, India.

3. Vemuri Durga Srishti, **Manisha Malani**, Aiswarya Thattaru Thodikayil, Velmurugan Kailasam, Sampa Saha, Jayabalan Nirmal. Nanofibrillated cellulose carrier for treating bacterial keratitis. ARVO-India, 28th Annual meeting of Indian Eye Research Group, September 2022, held at L V Prasad Eye Institute, Hyderabad, Telangana, India.

Appendix

C. Awards and Fellowships

1. Awarded **Travel Fellowship** from ARVO-India to attend the 29th Annual meeting of the Indian Eye Research Group, July 2023, held at Aravind Medical Research Foundation, Madurai, India.

2. Received **best paper presentation** award for presenting Artificial Intelligence in Predicting the Drug Transporter Interaction: Understanding the Entry of Systemic Drugs into Eye at ARVO-India, 27th Annual meeting of Indian Eye Research Group, October 2021, held at L V Prasad Eye Institute, Hyderabad, Telangana, India.

3. Recipient of **Junior Research Fellowship** (September 2019 to September 2022) and **Senior Research Fellowship** (October 2022 to Present) from the University Grants Commission, India.

Appendix

Biography of the candidate (Manisha Malani)

Ms. Manisha Malani obtained her Bachelor of Science (2016) and Master of Science (2018) in Microbiology from Osmania University, Hyderabad. After post-graduation, she worked as a trainee executive at Incillia Therapeutic Pvt Ltd from 2018-2019. Later, she qualified for the joint CSIR-UGC NET examination with an all-India rank of 47 and was awarded the prestigious research fellowship (Junior Research Fellowship and Senior Research Fellowship) from the University Grants Commission (UGC). In 2019, she Joined BITS-Pilani, Hyderabad campus, to pursue her doctoral degree under the supervision of Dr. Nirmal. Her doctoral research revolves around understanding the role of membrane transporters in systemic drug-induced ocular toxicity. To date, she has published six peer-reviewed articles in reputed international journals. She was awarded an International travel grant by the Department of Biotechnology (DBT) in May 2022 and a National travel grant by the Association for Research in Vision and Ophthalmology Association (ARVO), India, in August 2023 for presenting her doctoral research at the international and national conference. She received the best paper presentation award from ARVO India in October 2021 for her thesis work.

Appendix

Biography of the supervisor (Prof. Nirmal J)

Prof. Nirmal J is an Associate Professor in the Department of Pharmacy, Birla Institute of Technology and Sciences (BITS)-Pilani, Hyderabad campus. He has completed his Bachelor of Pharmacy and Master of Pharmacy (Pharmaceutics) from Dr. M.G.R. Medical University, Tamil Nadu, and PhD in ocular pharmacology and pharmacy from All India Institute of Medical Sciences (AIIMS), New Delhi. He carried out his postdoctoral research at Oakland University William Beaumont School of Medicine (Beaumont Health System), Michigan, USA (2011-2013) and Nanyang Technological University, Singapore (2015-2017). Before joining BITS, he worked as an assistant professor at Dr. Harisingh Gour Central University, Sagar, Madhya Pradesh (2013-2015) and the National Institute of Pharmaceutical Education and Research (NIPER), Kolkata (2017). He has received several prestigious awards for his scientific work including Research Scholars Award from the Urology Care Foundation, USA, sponsored by Allergan Pharmaceuticals. He is member of Journal Editorial Board of International Urology and Nephrology, Springer Nature. Also, he is reviewer for various reputed international journals such as Scientific Reports, Journal of Controlled Release, International Journal of Pharmaceutics, Colloids Surface B, and many more. His research interest lies in ocular drug delivery, pharmacokinetics, drug transporters, and toxicity. His research group (Translational Pharmaceutics Research Laboratory) works on ophthalmic formulation development and pre-clinical evaluation of the developed formulations. His research work has been published in several reputed journals and led to the generation of many intellectual property rights. He has authored 54 publications, 87 conference papers, 08 patents and 15 book chapters. Currently, he is guiding 12 PhD scholars to carry out their research work in the field of ocular therapeutics.